

# Advanced In Vitro Lung Models for Drug and Toxicity Screening: The Promising Role of Induced Pluripotent Stem Cells

Anabela Moreira, Michelle Müller, Pedro F. Costa,\* and Yvonne Kohl\*

The substantial socioeconomic burden of lung diseases, recently highlighted by the disastrous impact of the coronavirus disease 2019 (COVID-19) pandemic, accentuates the need for interventional treatments capable of decelerating disease progression, limiting organ damage, and contributing to a functional tissue recovery. However, this is hampered by the lack of accurate human lung research models, which currently fail to reproduce the human pulmonary architecture and biochemical environment. Induced pluripotent stem cells (iPSCs) and organ-on-chip (OOC) technologies possess suitable characteristics for the generation of physiologically relevant in vitro lung models, allowing for developmental studies, disease modeling, and toxicological screening. Importantly, these platforms represent potential alternatives for animal testing, according to the 3Rs (replace, reduce, refine) principle, and hold promise for the identification and approval of new chemicals under the European REACH (registration, evaluation, authorization and restriction of chemicals) framework. As such, this review aims to summarize recent progress made in human iPSC- and OOC-based in vitro lung models. A general overview of the present applications of in vitro lung models is presented, followed by a summary of currently used protocols to generate different lung cell types from iPSCs. Lastly, recently developed iPSC-based lung models are discussed.

## 1. Introduction

Respiratory diseases are among the global leading causes of morbidity and mortality. Acute conditions arising from infection, such as pneumonia and tuberculosis, affect millions of people worldwide, the latter being the most common lethal infectious disease with 1.4 million annual deaths.<sup>[1]</sup> Upon infection, the severe acute respiratory syndrome-coronavirus-2 (SARS-CoV-2), which caused a worldwide pandemic, leads to the clinical picture of the coronavirus disease-2019 (COVID-19) with possibly severe and life-threatening progression. Lung cancer is the most frequently diagnosed malignancy and the main cause of cancer-related death,<sup>[2]</sup> with markedly low survival rates especially when the diagnosis is performed at an advanced state of the disease.<sup>[3]</sup> Moreover, chronic respiratory diseases (CRDs), including chronic obstructive pulmonary disease (COPD), asthma, and interstitial lung disease (ILD), have consistently received less

attention in comparison to other non-communicable diseases, continuing to exert a considerable socioeconomic impact.<sup>[4,5]</sup> Risk factors for the development of respiratory diseases include, for example, tobacco use and second-hand smoke, as well as exposure to air-pollutants, which has been accentuated with the widespread use of fossil fuels.<sup>[4]</sup> It is clear that a great number of these risks can be mitigated by lifestyle changes, promoted by anti-tobacco campaigns already in place at a global scale and by the use of renewable, clean energy sources, and two recent studies indicate that the age-standardized incidence and prevalence of CRDs has decreased from 1990 to 2017.<sup>[4,5]</sup> However, the risk of developing CRDs, particularly COPD, appears to increase steeply with age,<sup>[4,5]</sup> most strikingly, these diseases were the third leading cause of death in 2017<sup>[4]</sup> and potentially in 2020.<sup>[6]</sup>

In addition to microbial, environmental, and lifestyle-related factors, a large number of lung diseases have a genetic origin.<sup>[7]</sup> Cystic fibrosis (CF), for example, is an incurable hereditary disorder known to originate from different mutations in the gene coding for the CF transmembrane conductance regulator (CFTR), an ion transporter, resulting in severe alterations in pulmonary physiology that culminate in impaired lung function, respiratory distress and, ultimately, death.<sup>[8,9]</sup>

A. Moreira, P. F. Costa  
BIOFABICS  
Rua Alfredo Allen 455, Porto 4200-135, Portugal  
E-mail: pedro.costa@biofabics.com

M. Müller, Y. Kohl  
Department of Bioprocessing and Bioanalytics  
Fraunhofer Institute for Biomedical Engineering IBMT  
Joseph-von-Fraunhofer-Weg 1, 66280 Sulzbach, Germany  
E-mail: yvonne.kohl@ibmt.fraunhofer.de

Y. Kohl  
Postgraduate Course for Toxicology and Environmental Toxicology  
Medical Faculty  
University of Leipzig  
Johannisallee 28, 04103 Leipzig, Germany

 The ORCID identification number(s) for the author(s) of this article can be found under <https://doi.org/10.1002/adbi.202101139>.

© 2021 The Authors. Advanced Biology published by Wiley-VCH GmbH. This is an open access article under the terms of the Creative Commons Attribution-NonCommercial-NoDerivs License, which permits use and distribution in any medium, provided the original work is properly cited, the use is non-commercial and no modifications or adaptations are made.

DOI: 10.1002/adbi.202101139

In order to tackle pulmonary disease, particularly CRDs, and to assess potential toxic effects of pollutant exposure, it is necessary to focus on the development of novel lung organotypic models that accurately represent the pulmonary anatomy and physiology under homeostasis and pathological conditions. In the case of genetic diseases, lung models effectively representing the individual genetic background of each patient could allow for personalized therapy approaches and, thus, the identification of effective treatments tailored to each specific clinical situation. Despite the extensive research routinely performed using animal models, the translation between *in vivo* and clinical results has been very limited, owing to the inherent disparity between the normal lung function and tissue organization in animals and humans.<sup>[10]</sup> Accordingly, the generation of *in vitro* human lung models can be a valuable tool to facilitate the extrapolation of results to the clinic and, simultaneously, help decrease the number of animals used in *in vivo* experiments.<sup>[11–14]</sup> In addition, such organotypic platforms may also be used for large-scale pharmacological and toxicological screening, where the potential toxicity of new therapeutic compounds can be addressed and the effects of pollutant or chemical agent exposure and inhalation can be evaluated.<sup>[15,16]</sup>

Nevertheless, the reproduction of lungs “on a dish” is far from straightforward, as the pulmonary architectural complexity and cell heterogeneity are difficult to replicate *in vitro*. In spite of the wide use of 2D, homogeneous cultures, these hardly represent the intricate relationship among different kinds of cells, as well as their interaction with the surrounding extracellular matrix (ECM) and the influence of systemic responses. In fact, numerous cell types are in close collaboration in the respiratory system: the pulmonary epithelium is surrounded by secretory, endothelial, mesenchymal, immune, and nerve cells, all of which help maintain lung homeostasis and function.<sup>[10,15]</sup> Besides this cellular diversity and the associated biochemical elements, such as immune mediators (cytokines, chemokines) and growth factors, the lungs are also under dynamic mechanical stress during the respiratory process.<sup>[17]</sup> Therefore, it should be clear that typical, static 2D monoculture systems do not accurately mimic this microenvironment, and thus are not ideal models for toxicological and therapeutic screening.<sup>[16]</sup>

Additionally, the generation of *in vitro* models requires an appropriate cell source, capable of providing not only an accurate representation of the pulmonary cell biology and function, but also sufficient numbers and proliferation rates for high-throughput research. As such, cell sources with easy accessibility, scalability, and capability of maintaining a differentiated phenotype over culture time and passaging are needed. Induced pluripotent stem cells (iPSCs) have grown steadily as a viable option, due to their embryonic-like state but somatic origin that circumvents the ethical hurdles associated with embryonic stem cells (ESCs). This review provides a critical analysis of the different *in vitro* lung modeling tools currently under development and testing, focusing on the promise of iPSCs on the generation of multicellular models that can closely mimic the natural anatomy and physiology of the human pulmonary system. Special focus will be given to 3D methods (spheroids, organoids, and scaffold-based models) and microfluidic (lung-on-chip) devices. The potential applications of these platforms are also explored, and the respective shortcomings and possible solutions are discussed. Thus, the main aim of this article is

to highlight encouraging progress made in this field and determine the missing steps for the generalized use and, where applicable, clinical translation of the presented lung models.

## 2. In Vitro Modeling of the Human Lung

### 2.1. Pulmonary Anatomy and Physiology

The lung is a specialized organ that performs several crucial physiological functions, such as the gas exchange between the blood and the atmosphere and the metabolism of endogenous and xenobiotic agents. Importantly, the lung maintains a functional barrier between the atmosphere and fluid-containing tissues – the so-called air-liquid interface (ALI). This ALI enables the delivery of oxygen to the blood, from which carbon dioxide produced by cellular metabolic activity is also eliminated. For the adequate performance of this process, a large surface area is provided by the complex structure of branched airways and blood vessels uniting at the most distal part of the lung, the alveoli.<sup>[18]</sup> The lungs consist of three right and two left lobes enveloped by a membrane known as pleura, resting with their ends over a concave-shaped diaphragm. The trachea, the most proximal part of the airways, bifurcates into right and left main stem bronchi, which branch out further into increasingly thinner bronchioles, until finally the narrowest airways connect to the alveoli (Figure 1A).<sup>[19]</sup> Thus, inhaled air flows through the conducting airways until it reaches the alveoli, the sites of gas exchange.

The air-exposed surfaces of the respiratory system are covered with epithelial cells, which play a central role in lung function (Figure 1B). In a recent single-cell ribonucleic acid (RNA) sequencing analysis, 58 different cell populations were identified in the human lung, encompassing epithelial and endothelial cells (ECs), immune cells, such as alveolar macrophages (AMs), and mesenchymal elements, including airway and vasculature smooth muscle, pericytes, and fibroblasts.<sup>[20]</sup> Pulmonary epithelial cells are distinguished between airway (tracheal and bronchial) and alveolar cell types. The upper (tracheobronchial) airways are lined by a pseudostratified epithelium, where each cell has direct contact with the basement membrane.<sup>[18,19]</sup> The majority of the airway epithelium consists of mucus-secreting and ciliated cells, which act together as a mucociliary escalator, removing particles or other irritants out of the airways. Submucosal glands contain duct, serous, and goblet cells, also contributing to the fluid balance, which is critically controlled by ion channels present in epithelial cell membranes. Additionally, airways contain a pool of multipotent progenitor cells (basal cells) located within the epithelial layer, acting as stem cells that self-renew and differentiate into secretory and ciliated cells during homeostasis and repair.<sup>[18,19]</sup>

The terminal airways are covered by the alveolar epithelium, encompassing two different types of alveolar epithelial cells, surrounded by blood vessels and fibroblasts. Alveolar epithelial cells type 1 (AT1) are squamous, flat, terminally differentiated cells that cover the majority of the alveolar area, providing the surface needed for gas exchange and participating in ion and protein transport.<sup>[21]</sup> Alveolar type 2 cells (AT2) are cuboidal, twice as frequent as AT1, and specialized in the production and secretion of pulmonary surfactant, that decreases surface tension during breathing (Figure 1B). They also act as a type of alveolar stem cell, owing to the ability to self-renew and differentiate into AT1 cells. Moreover,

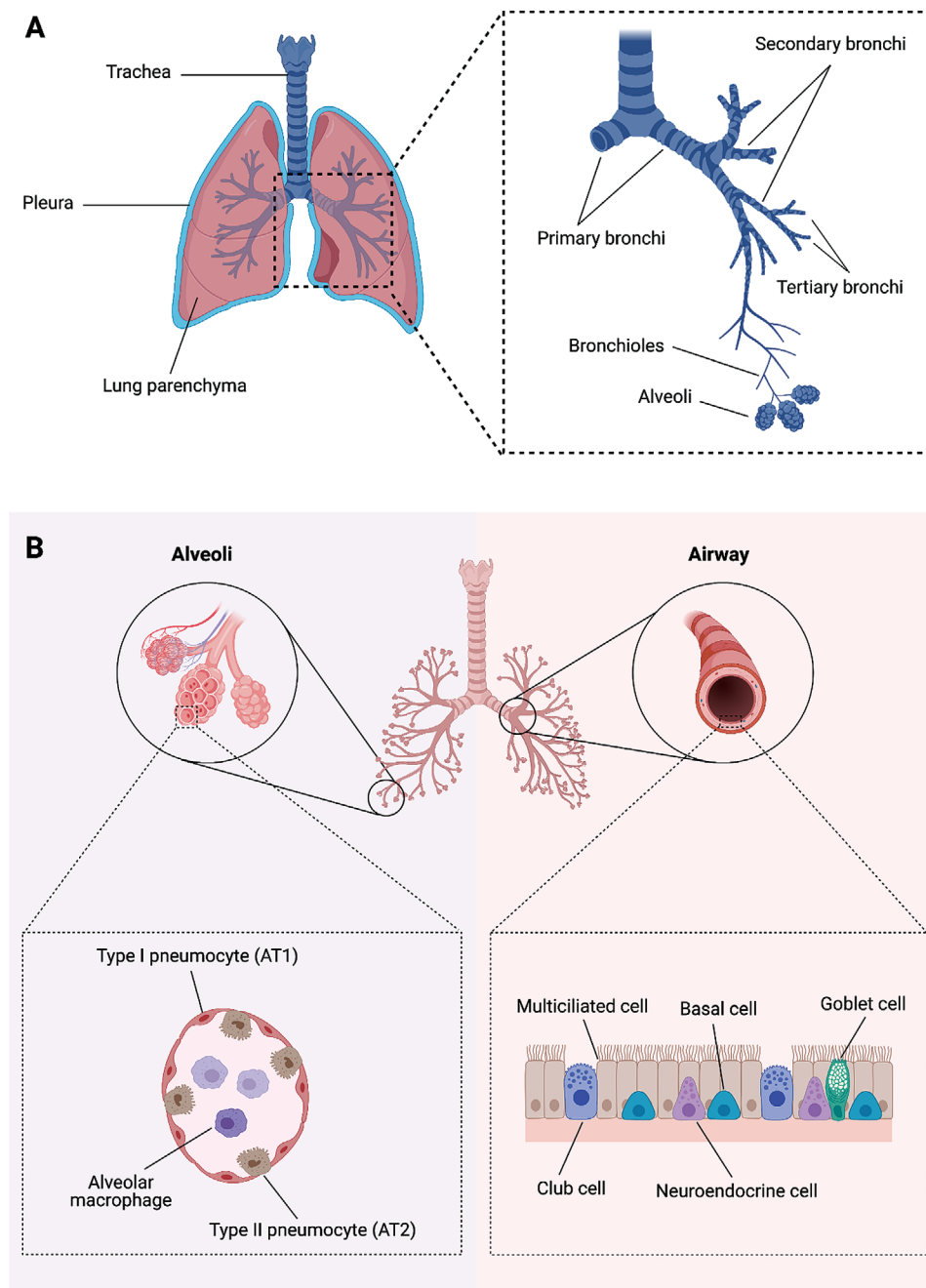


**Figure 1.** Pulmonary anatomy and cellular organization. A) Schematic representation of the hierarchical branching organization of the human airways and alveoli. B) Overview of the main cell types present in the proximal airway and alveolar epithelia. Created with BioRender.com.

the pulmonary surfactant secreted by AT2 cells contains collectins, which, together with the lung-resident population of immune cells, the AMs, function to promote host defense and clear the alveoli from bacteria and other pathogens.<sup>[18,19]</sup> AMs are the first cells contacting inhaled antigens, including infectious agents, allergens and particulate debris. Thus, AMs are the most abundant antigen-presenting cells in the airways and alveoli, playing a critical role in regulating immune responses and inflammation in the lung. The AM population self-renews from a progenitor population in the lung parenchyma and has a slow turnover rate, with an estimated half-life of 30–60 days, and their growth

and survival partially depends on locally produced cytokines, such as colony-stimulating factor (CSF).<sup>[22]</sup> In addition, the respiratory epithelium is known to be a rich source of granulocyte-macrophage CSF (GM-CSF).<sup>[22]</sup> Lastly, together with pericytes, fibroblasts constitute 10–20% of all lung cells, and both differentiate into myofibroblasts. Their function is not yet well defined, but it is assumed that they might play a role in lung and vasculature regeneration upon injury.<sup>[23]</sup>

Although the epithelial cells of the respiratory system show a great functional diversity, they all share common features, collectively contributing to the formation and preservation of

an ALI barrier that regulates the fluid composition of the airspaces and protects them from environmental pollution. This is achieved by the generation of cellular apical-basolateral polarity, which specifically contributes to the orientation of ion channels and transporters, enabling the lung epithelium to function and facilitating respiration.<sup>[18]</sup> To study such dynamic processes in the respiratory system, it is necessary to have suitable models capable of representing the properties of the human lung and providing an appropriate platform for toxicological screening.

## 2.2. Current In Vitro Human Lung Models

### 2.2.1. In Vitro Versus In Vivo Research: Is It Time to Change the Paradigm?

The development, clinical evaluation, and introduction to the market of novel therapeutic candidates are a complex, time-consuming process that incurs in an enormous financial impact in pharmaceutical companies. A 2020 report analyzing new therapeutic agents approved by the U.S. Food and Drug Administration (FDA) between 2009 and 2018 indicates that the median investment necessary for a new drug to reach the market is US\$985.3 million.<sup>[24]</sup> These costs arise not only from the typically lengthy preclinical and clinical investigation stages, as well as regulatory barriers enforced by the FDA or European Medicines Agency (EMA), but also from severely high attrition rates. In particular, drugs targeting respiratory disorders are amongst the most expensive therapeutics to develop, due to both long development times and very limited clinical success.<sup>[25]</sup> Although, in the past, the most frequent causes of clinical drug failure were related to inadequate pharmacokinetics and bioavailability, currently these unsatisfactory results appear to be connected to lack of effectiveness or manifestation of toxicity.<sup>[26,27]</sup>

Many factors are likely to contribute for these issues, including a poor understanding of the pathological mechanisms involved in pulmonary disease, inefficient formulation, and lack of investment in respiratory research, but a determinant aspect seems to concern the scarcity of preclinical models capable of recapitulating human biology and physiology.<sup>[12,26,27]</sup> Specifically, animal models of pulmonary physiology and disease present substantial limitations. The human and animal (particularly rodent) respiratory systems differ in terms of airway architecture and geometry, mucus and cellular composition, and metabolism, which highly affect the response to therapeutic molecules.<sup>[20,28]</sup> In addition, unlike humans, rodents are obligatory nose breathers.<sup>[28,29]</sup> Naturally, other animals, such as rabbits, dogs, sheep, pigs, and nonhuman primates can be used to overcome these problems, but larger animal models usually imply higher housing and maintenance costs, specialized handling, and further ethical considerations.<sup>[29]</sup> Besides physiological interspecies differences, pulmonary disease animal models frequently rely on the administration of exogenous agents (e.g., elastase, bleomycin, allergens, irritant gas) to induce damage and emulate pathological mechanisms observed in the human lung, not being able to entirely reproduce the features of human disease or exposure to disease-inducing agents.<sup>[26]</sup> As an example, both acute lung infections characterized by acute respiratory distress syndrome (ARDS) and chronic conditions such as CF are associated with a strong influx of inflammatory cells, such as neutrophil

granulocytes, into the lungs, leading to life-threatening lung damage.<sup>[30,31]</sup> Experimental sepsis and pneumonia rodent models used in basic research and drug development include cecal ligation and puncture (CLP) and systemic and pulmonary administration of bacteria and endotoxins.<sup>[30,31]</sup> However, these animal models are not a reliable representation of human lung disease due to important disparities in inflammatory response: for instance, the chemokine interleukin-8 (IL-8), which recruits and activates neutrophil granulocytes in humans, is not present in mice.<sup>[31]</sup> Animal models are also limited in their ability to mimic the extremely complex physiology and progression of human carcinogenesis, resulting in a rate of successful translation from preclinical to clinical studies of under 8%.<sup>[32]</sup>

Consequently, over the last decades, it has been shown that results from animal studies often do not agree with those obtained from human subjects in clinical trials. In fact, a study from 2007 found that human and animal results were consistent in only half of the cases studied.<sup>[33,34]</sup> As such, substances that are harmless in mice or monkeys can have harmful consequences for humans, possibly resulting in unexpected and severe side effects, and vice-versa, where the abandonment of a drug or treatment due to toxicity in animal models might cause safe and effective therapies to go to waste. A highly mediatic case that set a precedent for tighter regulation and evaluation of preclinical animal studies is that of thalidomide, a drug originally marketed as a hypnotic sedative and soon made extremely popular due to its antiemetic effects during gestation.<sup>[35]</sup> Four years after its commercialization and widespread therapeutic use, in 1961, thalidomide was linked to teratogenicity and withdrawn from the market, having caused the birth of more than 10 000 children with severe congenital malformations.<sup>[35,36]</sup> The rodent animal models used during preclinical investigation were shown to be much less sensitive to the toxic effects of thalidomide compared to other non-human mammals, such as rabbits and primates, thus having failed to predict any teratogenic effects and leading to one of the most substantial medical catastrophes in history.<sup>[36]</sup> Only almost 40 years later, in 1998, did thalidomide reenter the market after an FDA approval for the treatment of erythema nodosum leprosum, and it has been shown to be an effective therapeutic strategy in a wide variety of other conditions.<sup>[35]</sup> Further examples where animal studies failed to predict toxicity in humans include the anti-inflammatory drug rofecoxib (Vioxx), which increased the risk of developing severe cardiovascular problems; the hepatitis B drug Fialuridine, associated with serious liver toxicity and the death of five human volunteers; and TGN1412, a CD28 superagonist monoclonal antibody that caused human volunteers to suffer permanent and life-threatening damage from multiorgan failure within two hours after administration.<sup>[37–39]</sup> In the case of TGN1412, differences in the human and non-human primate CD28 receptor may have contributed for the different effects observed in preclinical and clinical trials, along with further disparities between the human and macaque immune systems,<sup>[40]</sup> highlighting the fact that, even with the use of complex animal models presenting increasing similarities to humans, unpredictable and devastating effects can occur.

Even though it is still not possible, in present days, to replace animal studies entirely with ex vivo/in vitro research, the latter has been evolving continuously toward increasingly complex and representative models of human biology, thus emerging as attractive alternatives to in vivo investigation. The use of human

**Table 1.** Advantages and disadvantages of the different in vitro lung models presented in this work.

In vitro model	Advantages	Disadvantages	References
2D ALI culture	<ul style="list-style-type: none"> <li>• Simple and easy handling</li> <li>• Mimic lung ALI</li> <li>• Relatively low cost</li> <li>• Unlimited cell supply</li> <li>• Scalability (high-throughput)</li> <li>• Suitable for drug/particle permeability and transport studies</li> </ul>	<ul style="list-style-type: none"> <li>• Limited physiological relevance: immortalized/tumoral phenotypes, inability to recapitulate the native 3D pulmonary microenvironment</li> </ul>	[56,62,183,184]
Spheroids/organoids	<ul style="list-style-type: none"> <li>• Representation of multiple cell types</li> <li>• Strong cell-cell and cell-ECM communication (3D environment)</li> <li>• Emulation of native physiological processes in lung organoids (e.g., surfactant secretion, particle clearance)</li> <li>• Suitable for biobanking</li> </ul>	<ul style="list-style-type: none"> <li>• High cost</li> <li>• Complex protocols for spheroid/organoid development and maintenance</li> <li>• Usually associated with poorly characterized, animal-derived products (e.g., Matrigel)</li> <li>• Lack of vascularization and interorgan communication</li> <li>• Difficulty in achieving fully differentiated phenotypes</li> <li>• Lack of mechanical stimulation</li> <li>• Lack of size uniformity</li> </ul>	[56,86,183]
Scaffold-based cell culture	<ul style="list-style-type: none"> <li>• 3D matrices with variable/tunable chemical composition and geometry</li> <li>• Abundance of natural and synthetic materials for biofabrication</li> <li>• Use of cell-instructive materials to guide cellular responses</li> </ul>	<ul style="list-style-type: none"> <li>• Difficulties in replicating the intricate pulmonary 3D architecture artificially</li> <li>• Frequent use of organic solvents may compromise scaffold biocompatibility</li> <li>• May involve complex and expensive manufacturing technologies</li> </ul>	[62,86]
Decellularized extracellular matrix (ECM)	<ul style="list-style-type: none"> <li>• 3D lung architecture with vascular network is preserved</li> <li>• Cell-guiding properties</li> </ul>	<ul style="list-style-type: none"> <li>• Shortage of human lung tissue</li> <li>• Complex decellularization protocols</li> <li>• Loss of ECM components during decellularization process and alteration of mechanical properties of the tissue</li> </ul>	[104,188,189]
Lung-on-chip devices	<ul style="list-style-type: none"> <li>• Representation of multiple lung tissue compartments (epithelium, mesenchymal tissue, blood vessels)</li> <li>• Efficient emulation of the lung microenvironment (ALI, shear flow, biochemical gradients, mechanical breathing motions)</li> <li>• Possibility for interconnected multiorgan devices (interorgan communication)</li> <li>• Possibility for automation</li> <li>• Incorporation of sensors for monitoring of biological parameters</li> </ul>	<ul style="list-style-type: none"> <li>• Early stage of development</li> <li>• High complexity</li> <li>• Frequent lack of an immune compartment</li> <li>• Challenges in the co-culture of multiple cell types (particularly from different tissue compartments or organs)</li> <li>• Relatively low throughput</li> </ul>	[13,62,183]

cells and tissue for disease modeling and therapeutic development may help improve the predictability of preclinical models and, consequently, the clinical success of new pharmaceutical agents.<sup>[15]</sup> The European Centre for the Validation of Alternative Methods (ECVAM) data base of non-animal models for respiratory disease research of the European Commissions (EC) Joint Research Centre (JRC) provides a comprehensive overview of all the models currently available for studying respiratory diseases, distributing them over different categories that cover model structures (2D, 3D, spheroids, co-cultures, microfluidic systems, bioreactors), cell types, target diseases, and applications, to name just a few.<sup>[41]</sup> In the next sections, a short overview of the main types of in vitro lung models with their advantages and disadvantages (**Table 1**) will be presented.

### 2.2.2. 2D Cell Culture

Traditional cell culture methods usually rely on the use of 2D surfaces from tissue culture flasks, plates, or Transwell

inserts, in which mono- or co-cultures of lung cells are grown and maintained under submerged conditions.<sup>[42,43]</sup> However, because the lung epithelium is in direct and constant contact with atmospheric air, it fails to properly and fully differentiate into a functional, physiological-like barrier when submerged, an aspect that has been illustrated by the inability to generate differentiated ciliated cells in a liquid culture environment.<sup>[44,45]</sup> As an alternative, a simple way of effectively mimicking the pulmonary environment is to seed epithelial cells in Transwell inserts or specialized devices and remove cell medium from the apical compartment, thus exposing the cell monolayer to air and recreating the ALI barrier in vitro.<sup>[46–48]</sup> Commercially available ALI platforms, such as EpiAirway (MatTek, Ashland, Massachusetts)<sup>[49,50]</sup> and MucilAir (Epithelix Sàrl, Geneva, Switzerland),<sup>[51,52]</sup> have also been widely explored. In this type of setup, cells have access to culture medium from the basolateral side of the insert membrane and are able to develop apical-basolateral polarity.<sup>[53,54]</sup> Importantly, these 2D systems can easily be used for the evaluation of important processes involved in disease pathogenesis and drug absorption, transport, and permeability

under controlled experimental conditions and well-defined environmental parameters.<sup>[21]</sup>

In the context of model development for *in vitro* representation of highly complex organs such as the lung, in which the intercellular communication and mechanosensing processes are very challenging to replicate artificially, conventional 2D cell culture is naturally linked with clear shortcomings. Considerable research on the comparison between cellular responses in 2D versus 3D environments has demonstrated that cells in 2D surfaces tend to display physiologically irrelevant behavior, favoring cell-substrate interactions over cell-cell and cell-ECM communication, assuming altered morphologies, and presenting aberrant proliferation rates and distinct gene and protein expression profiles compared to those observed *in vivo*.<sup>[55,56]</sup> Particularly in lung cells, marked differences have been observed regarding the maturation and functionality of the epithelial barrier and innate immune response in 2D and 3D lower (transepithelial electrical resistance (TEER), minimal expression of tight junction proteins, and higher susceptibility to bacterial infection were observed under 2D conditions).<sup>[57,58]</sup> Yet, 2D culture is associated with a few practical and logistical advantages that represent significant difficulties when handling 3D culture models, namely in terms of suitability for cell imaging and large-scale studies, due to its scalability, low cost, and simpler experimental data interpretation.<sup>[55,56]</sup> As a solution, 2D culture methods can be enhanced with a few modifications that better simulate the native tissue microenvironment, such as the introduction of dynamic culture conditions<sup>[59]</sup> or surface modifications to include appropriate physical micropatterns capable of cellular recognition and mechanosensing.<sup>[60]</sup> Such micropatterned surfaces, where specialized structures like micro-/nanogrooves, pillars, or pits are used, have extensively shown the ability to influence cell morphology, attachment, and migration, giving rise to the so-called 2.5D cell culture.<sup>[56]</sup> Thus, 2.5D cell culture may represent an important compromise between scalability/reproducibility and representativeness of the *in vivo* cell microenvironment, serving as relatively simple approaches to achieve consistent and physiologically relevant cellular responses. Of note, 3D ALI multi-layered cell culture models have also been established: Klein et al. developed a 3D tetraculture system composed of the alveolar type-II cell line A549, differentiated macrophage-like cells (THP-1), mast cells (HMC-1), and endothelial cells (EA.hy 926) to mimic the cellular organization at the alveolar barrier.<sup>[61]</sup> Like the other ALI models, this 3D tetraculture system is also based on cell culture inserts.<sup>[61]</sup>

### 2.2.3. Lung Spheroids and Organoids

Moving forward to increasingly complex structures and *in vivo*-like environments, 3D multicellular models, such as spheroids and organoids, serve as biomimetic platforms that enable the investigation of intercellular communications, cell-ECM interactions, and overall organ development and function.<sup>[62,63]</sup> Of note, although the terms “spheroid” and “organoid” are often used interchangeably, they actually differ in a few key aspects: spheroids are usually considered simpler structures capable of self-assembly without requiring a scaffold or 3D matrix to

guide the self-organization process.<sup>[64]</sup> They are commonly used as tumor models, due to their hierarchical structure of external layers composed of active and proliferative cells and an internal necrotic core that arises from nutrient and oxygen deprivation, as well as waste accumulation in this area.<sup>[65–69]</sup> However, as spheroids are most commonly derived from cell lines<sup>[66–68]</sup> or primary, patient-derived cells,<sup>[69,70]</sup> they frequently lack the presence of stem or progenitor cells capable of self-renewal and endowed with differentiation potential, resulting in a greater difficulty in sustaining the 3D culture and generating complex, multicellular structures.<sup>[63]</sup>

These limitations can be addressed with the use of organoids, which, as the name implies, consist of self-assembled “miniaturized organs” with multiple cell types, self-renewal and differentiation potential, and some level of function and organization that mimic those of the native target organ.<sup>[71]</sup> Lung organoids should be able to perform organ-specific functions such as surfactant secretion, particle clearance, or protection against microbial infections.<sup>[72]</sup> These can be obtained from patient-derived adult stem cells (ASCs),<sup>[73–77]</sup> from both healthy tissue (organoids) and malignant tissue (tumoroids), or multipotent/pluripotent stem cells (PSCs), such as ESCs,<sup>[78–81]</sup> which form 3D cell aggregates when embedded in a 3D ECM and can be directed toward specific differentiation paths with the use of exogenous biochemical cues (e.g., growth factors and small molecules).<sup>[63,82]</sup> PSC-derived organoids are established through the recapitulation of specific mechanisms that take place during embryonic development: by emulating the signaling cascades and other processes that occur during organogenesis, it is, therefore, possible to reproduce these events *in vitro* and obtain “mini-organs” in different developmental stages and originating from multiple germ layers, with varying cellular composition and degree of differentiation.<sup>[63,82,83]</sup> Conversely, ASC-derived organoids are representative of adult tissue repair and predominantly of epithelial nature, without stromal, nerve, or vascular elements in their composition. Thus, ASC-derived organoids can only be obtained from adult tissues with inherent regenerative capacity, whereas those derived from PSCs may be a valuable tool to study organs with limited regeneration potential.<sup>[83]</sup>

Importantly, the high expansion capability and genomic stability characteristic of organoids and tumoroids make them appropriate for biobanking and high-throughput drug screening studies.<sup>[72]</sup> Moreover, because they can be established from patient-derived stem cells, organoids pave the way for personalized disease modeling and toxicological screening, as several reports have demonstrated that organoids generated from patients with genetic disorders are capable of replicating the disease phenotypes *in vitro*.<sup>[83,84]</sup> Nevertheless, even though organoids have great potential to revolutionize basic research and *in vitro* disease modeling, there are various limitations to address before these models can live up to the excitement by which they have been surrounded.<sup>[84]</sup> First, the lack of protocol standardization for organoid development, the frequent use of animal-derived ECM as 3D supporting matrix, often Matrigel (Corning) or basement membrane extract (Cultrex, R&D Systems), and supplementation of culture media with non-chemically defined elements such as fetal bovine serum (FBS) are associated with high variability among different research groups and production batches, hindering study reproducibility

and consistency.<sup>[83–85]</sup> Second, organoid culture is more expensive than 2D cell culture, owing not only to these animal-derived materials, but also to the differentiation/growth factor cocktails used for organoid establishment and maintenance.<sup>[83]</sup> In the context of *in vitro* lung modeling, it is also challenging to attain a representation of all pulmonary tissue elements within lung organoids, particularly of the vascular compartment.<sup>[84,86]</sup> In addition, both lung spheroids and organoids lack interorgan communication and, therefore, can only provide restricted predictions of drug safety and efficacy, excluding potential effects arising from drug metabolism and systemic circulation.<sup>[83,84]</sup> Hence, these should be faced as models in continuous and progressive development, toward versatile platforms highly representative of human biology for basic research and personalized disease modeling and therapeutics.

#### 2.2.4. Decellularized ECM and Scaffold-Based Models

*In vitro* lung models can also rely on natural or artificially produced 3D scaffolds, which may guide and support cell organization, proliferation, and differentiation and contribute to an overall physiological-like microenvironment. In order to achieve pulmonary models with native architecture and incorporated vascular channels, extensive research has been dedicated to the use of decellularized lung ECM as a possible solution. Human or animal-derived decellularized lung ECM can be obtained from whole lungs<sup>[87,88]</sup> and lung resections or fragments,<sup>[89]</sup> which are usually submitted to a detergent-based protocol that strips these tissues of any cellular component, whilst maintaining the 3D branched airway and alveolar structure and vascular organization. Afterwards, the decellularized matrices can be recellularized with endothelial, epithelial, and/or stromal cells and dynamically cultured in specialized bioreactors, which recapitulate important pulmonary physiological processes such as vascular perfusion, liquid ventilation, and mechanical stimulation (**Figure 2**).<sup>[90]</sup> These approaches provide unmatched pulmonary biomimetic geometry and an active ECM endowed with cellular responsiveness, thus being capable of guiding cell attachment and behavior, as well as supporting progenitor cell differentiation.<sup>[91,92]</sup> Decellularized lung ECM may also be further processed into other scaffold forms, such as hydrogels,<sup>[93,94]</sup> which can similarly be used to study lung cell-ECM interactions *in vitro*, or small 3D-fragments with preserved vasculature and airway structure, suitable for high-throughput analysis.<sup>[95]</sup> Relevantly, a number of reports have demonstrated that healthy and aged or diseased lungs respond to decellularization protocols differently and result in disparate cellular behaviors,<sup>[96–99]</sup> representing potentially useful models to study lung pathophysiology.

Nonetheless, it should be noted that, although the pulmonary macro- and microarchitecture are generally preserved after the decellularization process, the ECM chemical composition can be altered, resulting in the loss of components, such as elastin and glycosaminoglycans,<sup>[100,101]</sup> that are essential to maintain the native structural integrity and mechanical properties of the organ. Interestingly, lungs isolated from different species react differently to the same decellularization protocol, showing variation in their chemical composition post-processing and eliciting distinct responses

in human cells upon recellularization.<sup>[102]</sup> Additionally, decellularization protocols are complex and time-consuming, and incomplete antigenic removal may give rise to immunological responses and compromise the clinical translation of the models. Importantly, the availability of human lung material for tissue engineering studies is also very limited. On one hand, this is because healthy donor lungs are always used for transplantation and only those deemed unsuitable to be transplanted can be used for generating decellularized lung ECM. On the other hand, in lung surgeries, hardly any healthy tissue is removed in addition to the diseased tissue. For this reason, the use of animal material remains necessary. Porcine lungs, which are much more widely available, are a particularly promising ECM alternative to human lungs for research purposes, since they effectively mimic the complex architecture, biomechanics, and topological specificity of the human lung.<sup>[103–105]</sup> However, utilizing xenogeneic material inevitably raises concerns about the potential influence of anatomical and physicochemical interspecies differences on cellular behavior, which may limit the physiological relevance of these models. To mimic the complex architecture and biomechanics of the human lung, there is a need for alternatives. Synthetic hydrogels, which get more and more established in tissue engineering, represent an alternative approach as they are able to reproduce the mechanical properties of the lung due to their viscoelasticity and can further be used for 3D bio-printing (examples of applications are described in Sections 4.2 and 4.3).<sup>[94]</sup>

As potential alternatives for *in vitro* lung modeling, a few research groups have focused on other natural materials, such as collagen<sup>[106]</sup> and gelatin,<sup>[107,108]</sup> as well as synthetic polymers, frequently poly( $\epsilon$ -caprolactone) (PCL)<sup>[107]</sup> and poly(lactide-co-glycolic acid) (PLGA),<sup>[109]</sup> to fabricate artificial 3D scaffolds in which lung cells can be cultured, differentiated, and maintained. Natural materials are advantageous due to the presence of cell adhesion properties that promote cell attachment, which synthetically produced scaffolds lack. However, biomaterials of natural origin are often associated with interindividual variability and poor biomechanical properties, shortcomings that are not present in synthetic constructs. In addition, synthetic polymers frequently allow for fine tuning of a scaffold's porosity, surface modifications, and degradation rate adjustments. These complementary advantages and limitations have encouraged the generation of hybrid tissue-engineered scaffolds, that is, blends or composites of both natural and synthetic materials capable of delivering adequate cell adhesion and suitable mechanical properties and reproducibility.<sup>[110]</sup>

Two of the most popular techniques for the production of scaffolds for tissue engineering are electrospinning and additive manufacturing (3D printing). Electrospinning is an electrohydrodynamic technique that relies on the controlled extrusion of a polymeric solution, emulsion, or melt through a conductive spinneret or orifice under a strong electric field. The application of this electric field causes the polymer solution to form a jet, which gradually solidifies along with solvent evaporation and deposits onto a grounded or oppositely charged collector, such as a metal plate or rotating mandrel, forming solid, continuous polymer fibers.<sup>[111]</sup> Electrospun scaffolds are well-known for their high surface area-to-volume ratios, interconnected porosity, and

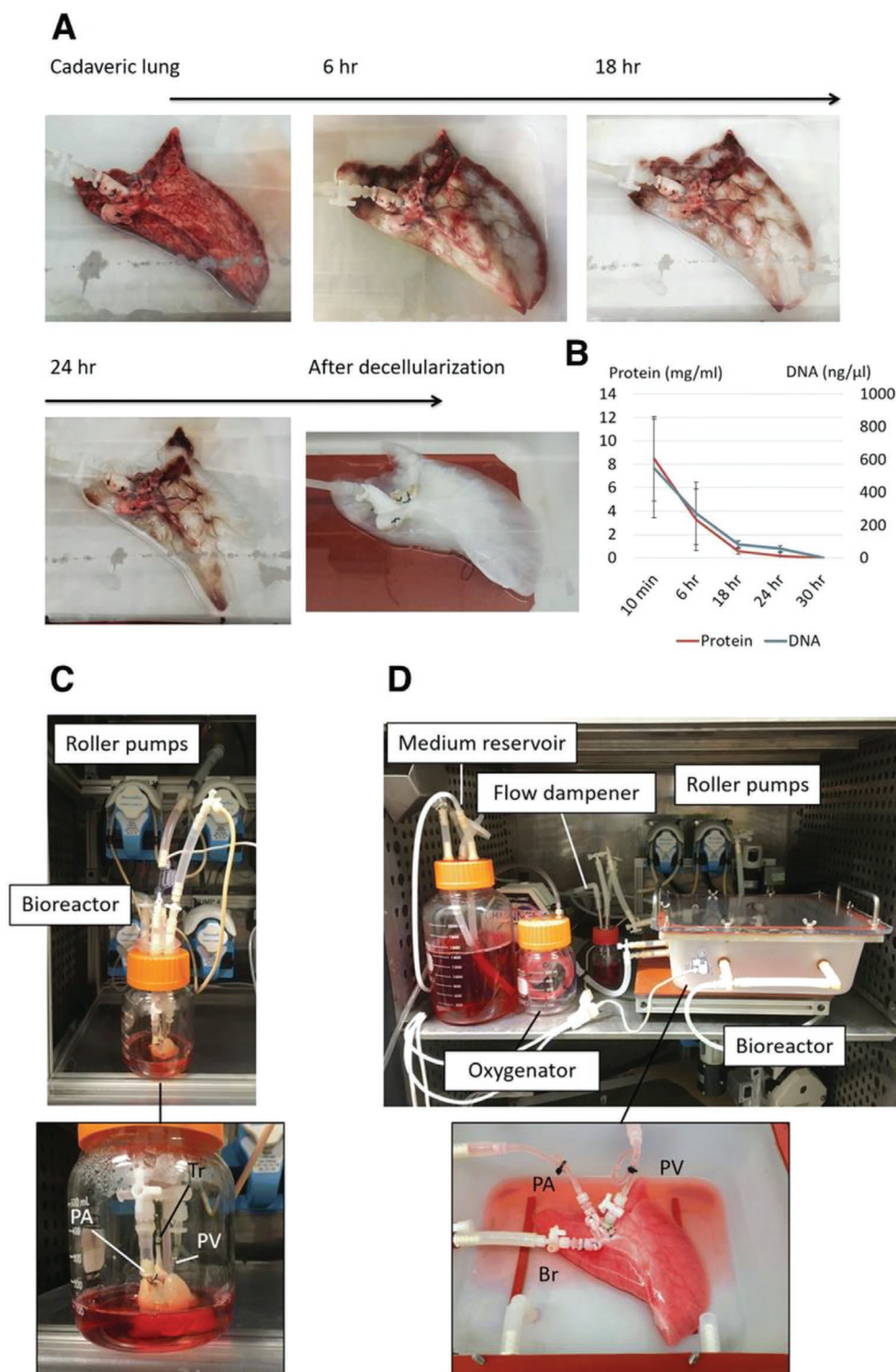


**Figure 2.** Lung matrix decellularization and culture procedure. Gradual loss of A) cellular components and B) protein and DNA content with the decellularization protocol in porcine lungs. C, D) Bioreactor apparatus for the culture of recellularized C) rat and D) human lungs. PA – pulmonary artery; PV – pulmonary vein; Br – left bronchus; Tr – trachea. Adapted with permission.<sup>[90]</sup> Copyright 2020, Springer.

micro-/nanofiber-based structure, emulating the ECM organization in vivo.<sup>[112]</sup> Importantly, several reports have demonstrated the potential of electrospun meshes for the development of lung biomimetic platforms, showing suitability for mono-

or co-culture of airway/alveolar epithelial cells,<sup>[113–115]</sup> airway smooth muscle,<sup>[116,117]</sup> and lung fibroblasts.<sup>[113,114]</sup> In turn, 3D printing is indicated for the development of constructs with controlled, pre-determined geometry, making use of

computer-aided design software and layer-by-layer deposition to model and create the intended scaffold structures.<sup>[118]</sup> A number of 3D lung scaffolds have been recently developed by seeding lung cells onto 3D-printed matrices<sup>[119]</sup> or by employing bioprinting technology, in which cells can be directly incorporated within a bioink and distributed into a pre-defined 3D array in a one-step procedure. This latter methodology has allowed the engineering of in vitro models with notable potential for the investigation of lung influenza A infection<sup>[120]</sup> and cancer.<sup>[121,122]</sup>

Such biomanufacturing techniques unquestionably serve as versatile platforms for lung tissue and organ modeling, effectively mimicking, albeit to a limited extent, their characteristic 3D architecture. In fact, to the present day, it is still not possible to replicate the entire intricate geometry of native lungs with any biofabrication method. To name just a few obstacles, the production of 3D structures using electrospinning is quite challenging, and the low fabrication speed and resolution of most additive manufacturing techniques is generally prohibitive for large-scale production and generation of submicron structures, respectively.<sup>[123]</sup> High-resolution technology will be necessary to develop biomimetic lung models with a complex and self-supporting geometry, composed of both large and small caliber airway branches and blood vessels, as well as thin and interconnected alveolar structures with a functional blood-air barrier. Of note, a lot of research has already been directed to the development of 3D electrospinning<sup>[124,125]</sup> and high-resolution 3D printing techniques,<sup>[126,127]</sup> even though these are still not necessarily biocompatible, due to the frequent use of toxic solvents and/or materials and high processing temperatures.<sup>[128]</sup> Technological advances will hopefully result in a wider range of both biofabrication methods endowed with the necessary resolution, biocompatibility, and speed and biomaterials capable of supporting cell attachment, proliferation, and delivering physicochemical cues to achieve wholly functional lung tissue models for in vitro research.

### 2.2.5. Lung-on-Chip Models

In recent years, remarkable progress has been made not only in the field of cell-based, in vitro model development, but also in that of microfabrication technology. By combining physiologically relevant cellular models and microfluidic systems, the drawbacks that come along with standard static in vitro systems can be overcome, in order to better mimic the microstructure, dynamic mechanical properties, and biochemical functionalities of living organs. So-called organ-on-chip (OOC) systems have recently evolved from a conceptual idea to a strong potential surrogate for animal models. These biohybrid devices combine the unique features of classical cell assays and animal models with 3D tissue organization and fluid circulation and, therefore, have the potential to revolutionize drug development and toxicological testing in the context of chemical approval according to the registration, evaluation, authorization and restriction of chemicals (REACH) regulation.<sup>[129,130]</sup> Indeed, the OOC principle is now well recognized by the pharmaceutical and chemical industries, as well as governmental authorities, as an alternative to

animal testing that complies perfectly with the 3Rs principle (replace, reduce, refine). These devices promise to improve the transferability of preclinical results to the clinical phases of drug development, making the entire process more cost-effective, faster, and safer. They constitute an experimental in vitro platform to assess drug efficacy and toxicity profiles in human cell and tissue models. Thus, they may be better predictors of therapeutic effectiveness and safety in the clinic compared to animal studies.

OOC models have already been developed for numerous organs,<sup>[131]</sup> generating an ever-growing portfolio that includes gut-on-chip,<sup>[132,133]</sup> liver-on-chip,<sup>[134–137]</sup> muscle-on-chip,<sup>[138]</sup> blood brain barrier (BBB)-on-chip,<sup>[139,140]</sup> kidney-on-chip,<sup>[141–144]</sup> and skin-on-chip systems.<sup>[145]</sup> Even though lung-on-chip devices have equally been described in several reports, this field is still in its infancy, presumably owing to the complex geometry and heterogeneous cell composition of the lung microenvironment, which, unlike the liver, kidney, BBB, or gastrointestinal tract, is located at an ALI. Currently existing lung-on-chip systems are discussed below in detail.

*From the 1st to the 2nd to the Next Generation of Lung-on-Chip Systems:* While earlier OOC microsystems were silicon-based, entailing complex and expensive microfabrication processes, current microfluidic devices are most commonly generated by poly(dimethylsiloxane) (PDMS) soft lithography, as the physicochemical characteristics of this polymer make it particularly suitable for cell and tissue culture purposes. PDMS has high gas permeability, which ensures oxygen supply to the cells inside the microchannels, and it enables the visualization of living cells thanks to its optical transparency. Furthermore, PDMS is very flexible and can be deformed locally, which allows the application of mechanical actions, such as membrane stretching. Its inherent hydrophobicity is not favorable for cell attachment, but can be counteracted by numerous surface modification strategies, such as plasma treatment or coating with ECM-derived proteins.<sup>[146]</sup> With such technological advancements and the generation of increasingly complex research platforms, it has become evident that the appropriate choice of representative cell models and biochemical signaling are not sufficient to entirely emulate the anatomy and physiology of the lung: important mechanical factors must come into play, particularly the air flowing through these organs during the breathing process, in a cyclic mechanism that causes the continuous expansion and relaxation of the lungs. The possibility of creating both microenvironmental biomolecular gradients and relevant mechanical stimulation (e.g., shear stress, strain) is a major advantage of OOC systems that distinguishes them from conventional, static cell cultures.<sup>[147]</sup>

In the first-ever OOC report, Huh et al. developed a device mimicking the alveolar-endothelial interface through which gas exchanges occur.<sup>[148]</sup> To this end, human alveolar epithelial cells and microvascular ECs were cultured on opposite sides of a flexible and porous PDMS membrane located between two parallel microchannels (**Figure 3A,B**) with a width similar to the average diameter of human alveoli, thereby proving the suitability of this device for studying pulmonary biology and toxicology.<sup>[149–151]</sup> The chamber containing epithelial cells was filled with air, in order to reproduce the pulmonary ALI, and the controlled introduction of vacuum into the device enabled

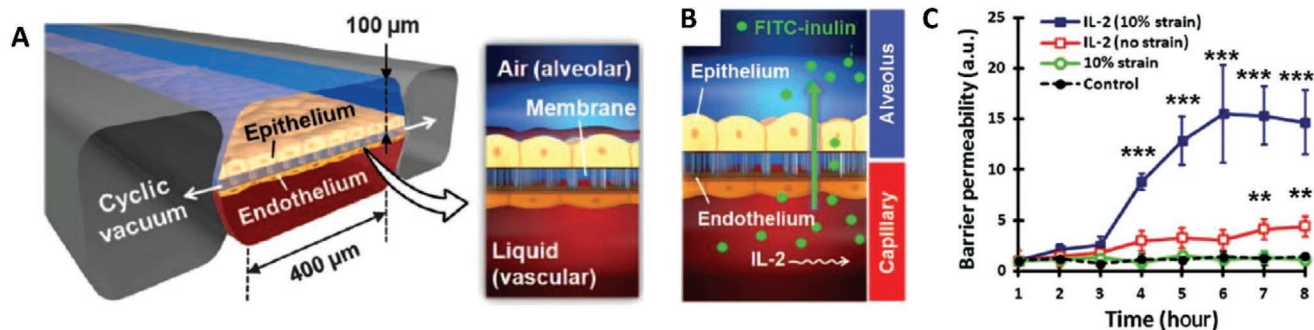


**Figure 3.** The first breathing lung-on-chip, a microengineered chip system to mimic the architecture and breathing function of the lung. A) Schematic structure of the lung-on-a-chip model imitating the alveolar-capillary interface. The epithelium side on the top presents the alveolar side (with air flow), the endothelium side on the bottom presents the vascular side (with liquid flow). B) Interleukin-2 (IL-2) administration to the microvascular channel induced an increase in endothelial permeability and allowed the recapitulation of pulmonary edema on-chip. Alterations of the lung barrier function could be quantified by measuring, for example, the permeability of fluorescein isothiocyanate (FITC)-inulin from the vascular to the alveolar side. C) The combination of IL-2 exposure and cyclic strain significantly increased barrier permeability compared to IL-2 without cyclic strain. This shows how important it is to use realistic *in vitro* models for toxicological studies and drug analyses. Adapted with permission.<sup>[151]</sup> Copyright 2012, American Association for the Advancement of Science.

a pressure-driven cyclic stretching of the PDMS membrane and adhered cells, thereby resembling the alveolar expansion during the respiratory process. This integration of physical stimulation and investigation on the influence of mechanical strain on pulmonary toxicity brings the lung-on-chip systems to a next level of complexity, which is close to the *in vivo* microenvironment. In fact, increased reactive oxygen species (ROS) production by alveolar epithelial cells was detected upon exposure to ultrafine silica nanoparticles in conjunction with 10% cyclic strain, whereas the nanoparticles or mechanical strain alone had no such effect.<sup>[148]</sup> Moreover, the translocation of nanoparticles across the air–blood interface was significantly increased in the presence of this mechanical stimulus.<sup>[148,150]</sup> Thus, this pioneering study unmistakably exposed the limitations of static cultures in which mechanical stimulation is not incorporated.

Although most of the OOC systems described to date are PDMS-based, it should be noted that, given its hydrophobicity, this material tends to adsorb small molecules on its surface, possibly altering the chemical profile of the cellular microenvironment.<sup>[152]</sup> For this reason, other synthetic and natural polymers are becoming increasingly important as candidates for stretchable and porous membranes. Both their physical (thickness, pore size, porosity) and mechanical (elasticity, elongation) properties qualify substances such as PCL,<sup>[153,154]</sup> poly(L-lactic acid-*co*- $\epsilon$ -caprolactone) (P(LLA-CL)),<sup>[155–157]</sup> polyethylene terephthalate (PET),<sup>[158]</sup> silk,<sup>[159]</sup> collagen,<sup>[160]</sup> fibrinogen,<sup>[161,162]</sup> and Bionate<sup>[163]</sup> as suitable materials for the production of flexible and porous membranes to mimic biological tissue barriers. Some approaches have already been described for this purpose.<sup>[164–169]</sup> For example, Yang et al. used a PLGA nanofibrous membrane to co-culture A549 cells, HFL1 fibroblasts, and human umbilical vein endothelial cells (HUVECs) in their lung-on-chip system.<sup>[170]</sup> In addition to pure polymer fiber-based membranes, ECM-derived materials also display interesting properties, such as semipermeability, optical transparency, and cost-effectiveness.<sup>[171]</sup> In addition to new materials, innovative technologies for scaffold production are also finding their way into the field of OOC systems, including solution, emulsion, and

melt electrospinning, casting and freeze drying, to name just a few.<sup>[153–163]</sup> Importantly, even though a recent critical summary on currently available *in vitro* cell-stretching devices reveals most are used in combination with cell lines,<sup>[6]</sup> OOC are also compatible with primary cell culture. This was demonstrated by Sellgren and colleagues, who developed a double membrane-based microchip in which triple co-culture of primary human airway epithelial cells, lung microvascular endothelial cells, and lung fibroblasts was successfully established.<sup>[172]</sup>

By experimenting with first-generation lung-on-chip systems and coupling different tissues in microfluidic devices, increasingly more complex systems with higher similarity to the physiology of human organs can be created (e.g., a microfluidic cell culture array with varying oxygen tensions,<sup>[173]</sup> engineered artificial alveolar-capillary membranes,<sup>[174]</sup> vascularized OOC<sup>[175]</sup>), with the attainment of more detailed structures and the possible choice from a wider range of suitable materials. A next-generation lung-on-chip with an array of stretchable alveoli made with a biological membrane has been recently described by Zamprogno et al.<sup>[176]</sup> Instead of PDMS, this research group used a collagen-elastin (CE) membrane integrated in a hexagonal mesh (Figure 4). Additionally, poly(methyl methacrylate) (PMMA) has also been used to fabricate lung-on-chip devices. By means of a solvent-assisted thermal bonding technique, a PMMA-based airway-on-chip model was developed, containing airway epithelial cells and SMCs in co-culture separated by a suspended ECM-derived hydrogel layer, mimicking the native structure of the respiratory branch interface.<sup>[177]</sup>

Even though, in most studies describing breathing lung-on-chip devices, membrane stretching is unidirectional, it is also possible to achieve 3D stretching, so as to better replicate the actual alveolar dilation. Stucki and colleagues imitated the physiological action of the diaphragm in the cyclic expansion of the lungs, making use of a biomimetic microdiaphragm that, controlled by electropneumatic mechanisms, oscillated periodically and caused the cyclic 3D extension of a cell-seeded PDMS membrane (Figure 5).<sup>[179,180]</sup> Such “breathing” *in vitro* lung devices represent precious technological advancements that

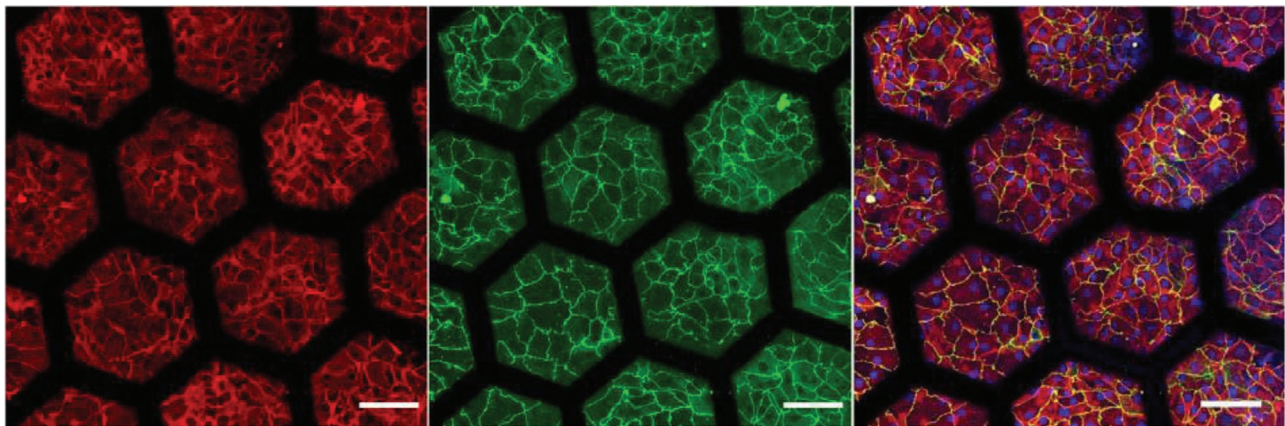


**Figure 4.** Immunostaining of primary human lung alveolar epithelial cells cultured on a hexagonal structured mesh. After 4 days of culture an air lift was performed. Following 2 days of culture at the ALI, cells expressed adherence junctions (E-Cadherin, red) and tight junction (zonula occludens-1 (ZO-1), green). In the right image the markers are merged (Hoechst, blue; E-Cadherin, red; ZO-1, green). Scale bar: 100  $\mu\text{m}$ . Adapted with permission.<sup>[178]</sup> Copyright 2021, Springer Nature.

enable the artificial reproduction not only of the anatomical structure and cellular composition of the lung, but also of the dynamic physiological and mechanical processes taking place in the respiratory interface, allowing for increasingly complex and accurate replications of the pulmonary microenvironment. Relevantly, this technology can be easily adapted to develop other human OOC, offering the methodology for the artificial, in vitro recapitulation of other biomechanical motions, such as gastrointestinal peristalsis within a gut-on-chip device.<sup>[181]</sup> In addition, by integrating specific sensors, such as impedance sensors for monitoring cell activity, barrier function, and membrane movements,<sup>[182]</sup> the quality of these devices as screening tools in drug development and preclinical toxicity assessment can be enhanced.

### 2.3. Current Applications of In Vitro Lung Models

Given the wide applicability of in vitro lung models across varied fields of basic research, disease modeling, pharmacological research, and toxicology, this section does not aim to be an exhaustive list of all applications of these tools, but rather a general overview of a few relevant examples from recent literature. Accordingly, a broad summary of applications in the areas of developmental biology and lung disease pathophysiology, drug design, and toxicological testing is provided. For more extensive reviews on the subject, the EC JRC ECVAM database<sup>[41]</sup> can be consulted, along with other review articles previously published.<sup>[15,83,183,184]</sup>

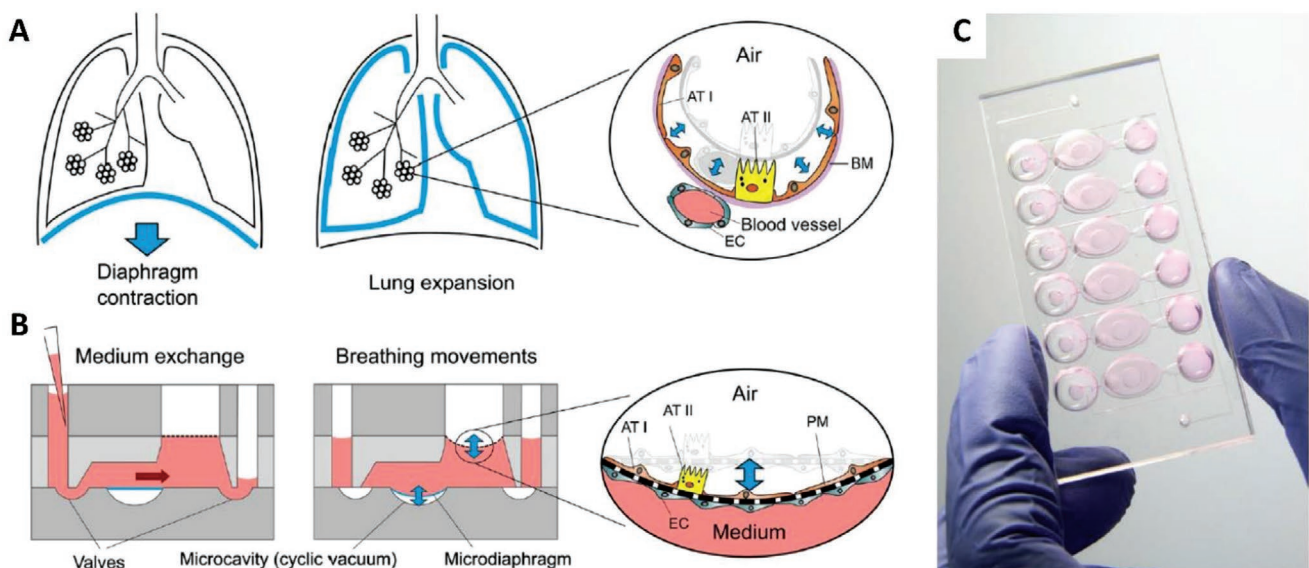


**Figure 5.** Breathing-on-chip model. A) The breathing motions of the lung in vivo and especially the barrier function of the alveoli are replicated on the microfluidic chip. B) Hydrostatic and surface tension forces transport the medium through the fluidic channels. A bio-inspired microdiaphragm reproduces the breathing motions on chip. C) Six independent alveolar barrier systems could be used in parallel as a high-throughput lung breathing model. AT I: alveolar epithelial cells type 1, AT II: alveolar epithelial cells type 2, EC: endothelial cells. Adapted with permission.<sup>[179]</sup> Copyright 2018, Springer Nature.

### 2.3.1. Analysis of Developmental, Homeostatic, and Pathological Processes

The comprehension of the cellular and molecular mechanisms that lead to lung formation and maturation during embryonic and early post-natal development may enable their recapitulation in *in vitro* organ models and tissue-engineered constructs, in which progenitor cells can be guided toward regenerative responses by mimicking developmental signaling cascades, biochemical, and biomechanical stimuli. Moreover, a considerable number of human diseases have a developmental origin, may it be due to mutational mechanisms, exposure to toxins, or nutritional deficits during gestation.<sup>[185]</sup> As such, significant effort has been directed at utilizing human lung models to emulate the processes involved in lung development.<sup>[186]</sup> Organoids and other types of lung models, such as lung-on-chip devices, have been designed to investigate, for example, cellular dynamics during airway branching,<sup>[187]</sup> interactions between epithelial and smooth muscle cells,<sup>[177]</sup> and cell–cell communication between epithelial and endothelial cells (ECs).<sup>[187]</sup> Developmental gene expression analyses have also been carried using human and murine embryonic lungs, as well as organoids derived from human lung tip epithelium, which allowed for comparative studies with murine lung development.<sup>[78]</sup> This helped establish a series of parallelisms and discrepancies between the processes of lung morphogenesis in humans and mice, therefore contributing for a better understanding of the suitability of these animals as models for lung therapy and disease. Relevantly, these organoids had self-renewal capability and the potential for differentiation into both bronchiolar and alveolar fates *in vitro*, posing as promising candidates for further use in modeling lung development and physiology.<sup>[78]</sup>

The relative simplicity of several common models and the presence of only one or two cell types can be an important asset to study specific cell–cell interactions and evaluate the role of individual cell populations in the maintenance of lung homeostasis or pathological mechanisms. Nevertheless, these still do not quite replicate the complexity of the lung cellular niche, which may be required when performing toxicological screenings or reproducing the conditions of a pulmonary disease. Chen and co-workers have generated lung bud organoids from ESCs, which were then cultured in Matrigel *in vitro* and ectopically, as a xenotransplant, in mouse kidney capsules.<sup>[190]</sup> These organoid structures could successfully reproduce the formation of branching airways and early alveoli occurring during lung morphogenesis, presenting important similarities to the second trimester of human gestation in terms of structural organization and gene expression after six months of Matrigel culture. More recently, bronchioalveolar lung organoids (BALOs) have also been created from murine bronchioalveolar stem cells (BASCs), where multiple lung cell specific markers, including alveolar epithelial cells, basal, ciliated, and secretory cells, were expressed, a mesenchymal component was observed, and successful co-culture with lung-resident immune cells, namely tissue-resident macrophages, was established.<sup>[191]</sup> BALOs self-organized into extensively branched structures over 21 days, mimicking the bronchiolar and alveolar architecture *in vivo*. With this increased cellular complexity, the role of mesenchymal cells in organoid formation and maturation could be

unraveled, possibly shedding some light on the existing epithelial-mesenchymal communication in the lung.<sup>[191]</sup> Likewise, immune cells are a fundamental component of the pulmonary cellular niche and represent a crucial line of defense against invading pathogens, therefore implying that the inclusion of tissue-resident macrophages in this organotypic model may represent a valuable tool for studying lung infection and immune response.<sup>[191]</sup> *In vitro* lung biomimetic platforms have also been used for disease modeling, which is fundamental not only to understand the pathogenic mechanisms leading to the target condition, but also to provide the respective drug screening and testing platforms (Section 2.3.2). Characteristics of pulmonary edema,<sup>[151]</sup> intravascular thrombosis,<sup>[192]</sup> lung cancer,<sup>[193,194]</sup> and even rare genetic diseases like Hermansky–Pudlak Syndrome (HPS) Type 2<sup>[195]</sup> have already been reproduced and investigated using *in vitro* lung models. Sachs and co-workers have recently developed human airway organoids derived from CF and non-small cell lung cancer patients which recapitulate several features of these diseases.<sup>[76]</sup> In addition, pulmonary infectious diseases caused by, for example, influenza A,<sup>[191]</sup> parainfluenza,<sup>[196]</sup> and respiratory syncytial virus<sup>[76,190,196]</sup> can also be modeled and studied using such biomimetic tools. Importantly, in light of the recent COVID-19 pandemic, caused by the SARS-CoV-2, numerous *in vitro/ex vivo* preliminary platforms have been created to emulate and investigate the pathogenesis of this infectious condition.<sup>[197–199]</sup>

Lung-on-chip devices have the unique advantage of incorporating mechanical biomimetic components into *in vitro* models, resulting in dynamic tools that can be used to investigate the influence of biomechanical stimulation on cellular behavior and disease pathogenesis. For instance, Novak et al. developed an OOC consisting of two perfused microfluidic channels separated by a permeable elastomeric membrane, in which parenchymal cells and microvascular endothelium were cultured in opposite sides to study lung-specific mechanical cues, such as breathing motions.<sup>[200]</sup> Another lung-on-chip array with an integrated bio-inspired respiration mechanism was used to assess how cyclic stretching affects the permeability properties of epithelial cell layers.<sup>[180]</sup> To this end, an alveolar barrier was formed by coculturing lung epithelial (16HBE) and endothelial (HUVEC) cells on each side of a thin, porous, and stretchable membrane. Felder et al. developed a lung chip to study the role of mechanical motions and recombinant human hepatocyte growth factor (rhHGF) administration in wound healing, proving that cyclic mechanical stretching has a significant influence on this process.<sup>[201]</sup> In addition, lung-on-chip devices have been widely applied in cancer research, serving as platforms to study invadopodia formation<sup>[202]</sup> and stromal-cancer cell communication<sup>[170,203]</sup> during lung tumor growth and invasion processes, as well as resistance mechanisms to chemotherapeutics.<sup>[170,204]</sup> Hassell et al. cultured human lung cancer cells within an OOC device mimicking lung structure and function to study tumor growth, dormancy, and response to therapy.<sup>[205]</sup> Of note, the establishment of biochemical gradients within lung-on-chip devices has also allowed for investigation on the effects of cytokine and chemotactic gradients on mucin expression by lung epithelial cells<sup>[206]</sup> and immune cell migration.<sup>[207]</sup> Hence, “tumor-on-chip” devices represent invaluable platforms to study cancer development and progression and potentially

perform personalized drug screening under physiologically relevant conditions.

With focus on inflammatory diseases, small airway-on-chip devices that can be used to unravel pathological mechanisms involved in lung inflammation, discover new disease biomarkers, and evaluate tissue response to therapeutic molecules have been recently developed.<sup>[208–211]</sup> Pathophysiological characteristics of CRDs, such as asthma and COPD, were efficiently emulated in these systems by exposure of the lung epithelium to IL-13 and use of COPD patient-derived epithelial cells, respectively, providing a versatile *in vitro* model platform of complex and dynamic pulmonary inflammatory responses under homeostatic and pathological conditions. In addition, real-time analysis of immune cell recruitment by the reconstituted endothelium could also be modeled in such devices by circulating neutrophils through the microvascular compartment,<sup>[208,209]</sup> as previously demonstrated in earlier reports.<sup>[148]</sup> Likewise, Punde et al. focused on circulating cell recruitment in the context of lung inflammation, studying the effects of eosinophil cationic protein (ECP)-mediated CXCL-12 secretion on fibrocyte migration under flow conditions.<sup>[212]</sup> The chemotactic and pro-inflammatory profile of the lung epithelium in response to microbial infection has also been recently assessed in a microfluidic system encompassing human airway bronchial cells, microvascular ECs, and normal lung fibroblasts, representing a polyvalent, biologically relevant model of host-pathogen interactions.<sup>[213]</sup> Immune cells, such as macrophages, can also be included and co-cultured with lung epithelium in these models, providing important information on pulmonary pathogen recognition and defense and representing innovative platforms for drug screening and toxicological testing.<sup>[214]</sup> To investigate epithelium damage and protection during reopening of occluded airways in a physiological context, a microfluidic pulmonary airway model with separated air and liquid inlets was combined with A549 alveolar epithelial cells by Tavana and coworkers.<sup>[215]</sup>

Therefore, it is clear that human lung biomimetic models may become helpful tools in understanding pulmonary physiology and pathogenesis, providing versatile, scalable, and biologically relevant devices that tackle the limitations of classic 2D monoculture systems.

### 2.3.2. Drug Design and Testing

The availability of *in vitro* lung models can also be advantageous for preliminary efficacy testing of newly developed drugs or other therapeutic candidates in pre-clinical studies, simultaneously allowing for more accurate predictions of the treatment effects in human tissues and minimizing the number of animals required during *in vivo* research. Due to the very poor prognosis and high mortality rates of lung cancer, considerable effort has been directed either at finding new antitumoral agents or repurposing well-known drugs for use in distinct pathologies or novel therapeutic strategies. For example, the anti-proliferative effect of Paclitaxel, a widely used chemotherapeutic agent, was shown to be enhanced by co-administration with a tumor-penetrating peptide, iRGD, in air-grown spheroids derived from the A549 lung adenocarcinoma cell line.<sup>[216]</sup> A549 cell-derived microphysiologic 3D tumor models have also been used to test

the efficacy of cell-based anticancer therapies, namely chimeric antigen receptor (CAR) T cells targeting the receptor tyrosine kinase-like orphan receptor 1 (ROR1), of which the high expression in malignant cells and scarce presence in healthy cells provides a base for tumor cell-targeted treatment.<sup>[217]</sup>

Furthermore, because numerous lung models are compatible with the use of autologous cells, it is possible to achieve patient-specific screening platforms that pave the way for the implementation of precision medicine, enabling the selection of the most suitable therapeutic option according to the individual cellular and tissue response. Accordingly, lung cancer organoids can be derived and established from surgical tumor resections or biopsies, representing several cancer types (small cell and non-small cell lung cancer, including adenocarcinoma, squamous cell carcinoma, and neuroendocrine carcinoma) and maintaining a high fidelity to the parental tumor genetic and molecular profiles and histopathological features, even after long-term *in vitro* culture.<sup>[73–76,218,219]</sup> Such research models allow for individual pharmacogenomic analyses and high-throughput screening of antitumoral drugs, providing specialized, robust, and time-efficient pharmaceutical testing platforms. Interestingly, these patient-derived organoids have unquestionably demonstrated that patient-specific tumor signatures dictate the respective sensitivity to chemotherapeutic or molecularly targeted drugs, due to the inherent heterogeneity of lung cancer, thus emphasizing the importance of personalized models and therapeutic regimens.

In the field of OOC, a lung chip containing an electrospun nanofiber membrane for the co-culture of A549 lung cancer cells, HFL-1 fetal lung fibroblasts, and HUVECs was built to evaluate the effectiveness of gefitinib, an anti-tumor drug targeting epidermal growth factor receptor (EGFR).<sup>[170]</sup> In another study, microfluidic 3D-co-culture systems of stromal and cancer cells (both SPCA-1 and patient-derived cells) were used to assess tumor responsiveness to varying concentrations and combination regimens of anti-tumor drugs, making use of concentration gradients for a fast dosage and efficacy screening.<sup>[220]</sup> As a final example, Huh and colleagues demonstrated the beneficial effects of two agents, angiopoietin-1 and GSK2193874, on ameliorating interleukin (IL)-2-induced pulmonary edema using their previously developed “breathing” lung-on-chip device.<sup>[151]</sup>

### 2.3.3. Toxicological Studies

With the constantly increasing industrialization of the modern world and persistent social behaviors such as tobacco and electronic-cigarette (e-cigarette) smoking, the exposure to particulate matter, air pollutants, engine exhaust fumes, and other nefarious chemicals is nearly ubiquitous. Assessing the toxic effects of inhaled pollutants is essential to understand the pathogenesis of several pulmonary diseases, design new strategies for recovery, and establish environmental guidelines for public health protection.<sup>[221,222]</sup>

In fact, tobacco smoking is the main risk factor for the development of COPD and it highly increases the probability of developing other pulmonary diseases, including cancer, potentially causing deleterious effects even after passive (environmental) exposure.<sup>[223]</sup> Accordingly, many researchers have been applying

lung biomimetic models to studying the toxicological response to tobacco-related products. Cadmium (Cd), for instance, is a highly toxic heavy metal found in high concentrations in tobacco smoke that has been associated with severe lung damage after both short-term and long-term/chronic exposure.<sup>[224]</sup> In an ALI model derived from human primary bronchial epithelial cells, cadmium treatment was shown to interfere with the cellular function of both secretory and ciliated cells, resulting in oxidative stress and secretion of pro-inflammatory cytokines (e.g., Interleukin-1beta, Interleukin-6, tumor necrosis factor  $\alpha$  (TNF- $\alpha$ ) and enzymes involved in tissue remodeling, namely matrix metalloproteinases (MMPs)).<sup>[225]</sup> Similarly, in a recent paper, ALI models derived from healthy individuals and COPD patients were used to evaluate the effects of whole cigarette smoke exposure. It was demonstrated that cigarette smoke affected cell differentiation and function, compromising the epithelial barrier integrity and decreasing the cilia beat frequency in ciliated cells, as well as the area covered by actively moving cilia.<sup>[226]</sup> The impairment of ciliary function caused by cigarette smoke was also observed when tested in human small airway organotypic cultures.<sup>[227]</sup> Moreover, the effects of whole smoke from both conventional tobacco and electronic cigarettes were assessed using a micro-fabricated “breathing” small airway-on-chip device, in which the pathophysiological responses induced by smoking in bronchiolar epithelium derived from healthy individuals and COPD patients were compared.<sup>[228]</sup> Interestingly, analyses carried in in vitro lung models have shown that tobacco substitutes, such as e-(cigarettes)<sup>[229]</sup> and modified-risk tobacco products,<sup>[227]</sup> may be a safer alternative to traditional cigarettes, as the toxic effects they exert in small airway cells are less pronounced.

Additionally, with the exponential advancement of nanotechnology and its growing use in the fields of medicine, cosmetics, and food industry, concerns have been arising regarding local and potentially systemic effects of nanoparticle uptake, in this context, by inhalation.<sup>[230]</sup> Exposure of ALI co-cultures of primary bronchial epithelial cells and MRC-5 fibroblasts to aerosolized palladium (Pd) nanoparticles caused the secretion of higher IL-8 amounts, particularly in IL-13-conditioned chronic bronchitis-like cultures, indicating a potential exacerbation of an inflammatory response, although cell viability was not affected.<sup>[231]</sup> In turn, silica nanoparticles elicited different responses in two different lung cell lines, A549 (alveolar epithelial cells) and 16HBE (bronchial epithelial cells): A549 cells presented higher resistance to the toxicity exerted by the nanoparticles compared to 16HBE cells.<sup>[232]</sup> As an additional example, a co-culture model of bronchial epithelial (Calu-3), endothelial (EA.hy926), and macrophage-like (THP-1) cells was used to evaluate the effects of silver nanoparticle inhalation and the translocation of this particulate material through the epithelial and endothelial barriers.<sup>[233]</sup> In a recent study, ALI cultures of A549 cells were used to identify the safest nanosystems for the encapsulation and delivery of two antimicrobial peptides, AA139 and M33, to be used as aerosol formulations for the treatment of infectious respiratory diseases.<sup>[234]</sup>

Airway-on-chip platforms in which human bronchial epithelial cells could be cultured under ALI conditions were also recently developed to evaluate cytotoxic effects caused by aerosol inhalation exposure.<sup>[235]</sup> Alternatively, direct spraying at an ALI can be performed,<sup>[214,236–238]</sup> leading toward a new generation of advanced in vitro lung toolkits for human inhalation tox-

icity assays. Cei et al. developed a dynamic in vitro model of the alveolar interface with aerosol delivery,<sup>[239]</sup> in one of the very few systems combining ALI models with dynamic flow and stretch conditions. This moving ALI (MALI) is based on a modular bioreactor<sup>[240,241]</sup> composed of two chambers, between which a flexible porous membrane is positioned for cell cultivation, mimicking the alveolar air–blood interface. In a distinct study, a lung chip with a sandwich structure and three parallel channels was designed, which were individually perfused with human pulmonary epithelial cells (HPiC) alveolar epithelial cells, Matrigel, and HUVECs. The device was used to evaluate the effects of pulmonary nanoparticle exposure (titanium dioxide (TiO<sub>2</sub>) and zinc oxide (ZnO)) on cell morphology, connexin expression, ROS generation, and epithelial and endothelial cell apoptosis.<sup>[242]</sup> Inhaled particle dynamics and deposition in the lung could be further studied by a true-scale microfluidic pulmonary acinar model (“acinus-on-chip”) consisting of three PDMS layers stacked on top of a PDMS-covered glass slide.<sup>[243]</sup>

A very important aspect of in vitro pharmacological screening of new potential therapeutic candidates is the accurate prediction of their toxicological profiles in lung tissues in vivo. Sivars et al. showed that it was possible to assess drug epithelial toxicity in vitro, obtaining predictive results that reflected the respective effects after in vivo administration, using a human 3D airway epithelial model (MucilAir).<sup>[51]</sup> At last, but not least, environmental pollutants arising from industrial<sup>[244]</sup> and automobile<sup>[245]</sup> exhaust fumes can also be tested using in vitro lung models, so as to address the effects of the ever-growing worldwide industrialization. Detailed reviews on the subject of in vitro lung models for inhalation toxicity studies have been previously published<sup>[16,246,247]</sup> and are out of the scope of this article.

### 3. Induced Pluripotent Stem Cell (iPSC)-Based In Vitro Models

#### 3.1. The Promise of Human iPSC-Derived Lung Cells

To date, a great variety of cells has been used in in vitro lung models, including different pulmonary cell lines, primary cells, multipotent stem cells and PSCs, each presenting advantageous characteristics and shortcomings. Several commonly used lung epithelial cell lines have been obtained from tumor tissue, namely lung adenocarcinoma, including both bronchial (Calu-3<sup>[248,249]</sup>) and alveolar (NCI-H441<sup>[250]</sup> and A549<sup>[251]</sup>) epithelial cells. In addition, immortalized cell lines such as 16HBE,<sup>[252]</sup> BEAS-2B<sup>[253]</sup> (human bronchial epithelial cells), and hAELVi<sup>[254]</sup> (human alveolar epithelial cells) have also been widely used in in vitro lung models. Apart from the pulmonary epithelial compartment, human lung microvascular endothelial cell (EC) lines (e.g., HULEC cells) are equally available commercially and have been previously explored, for instance, in pulmonary infectious disease investigation.<sup>[255,256]</sup> Cell lines are frequently used in biological research due to their scalability, limitless supply, low cost, and easy accessibility. However, their immortalized or cancerous nature usually does not faithfully reproduce the phenotype of normal lung cells.<sup>[15,257]</sup> A common alternative are primary lung cells, derived from lung tissue biopsies or surgical resections, cadaveric lungs, and bronchoalveolar lavages, but

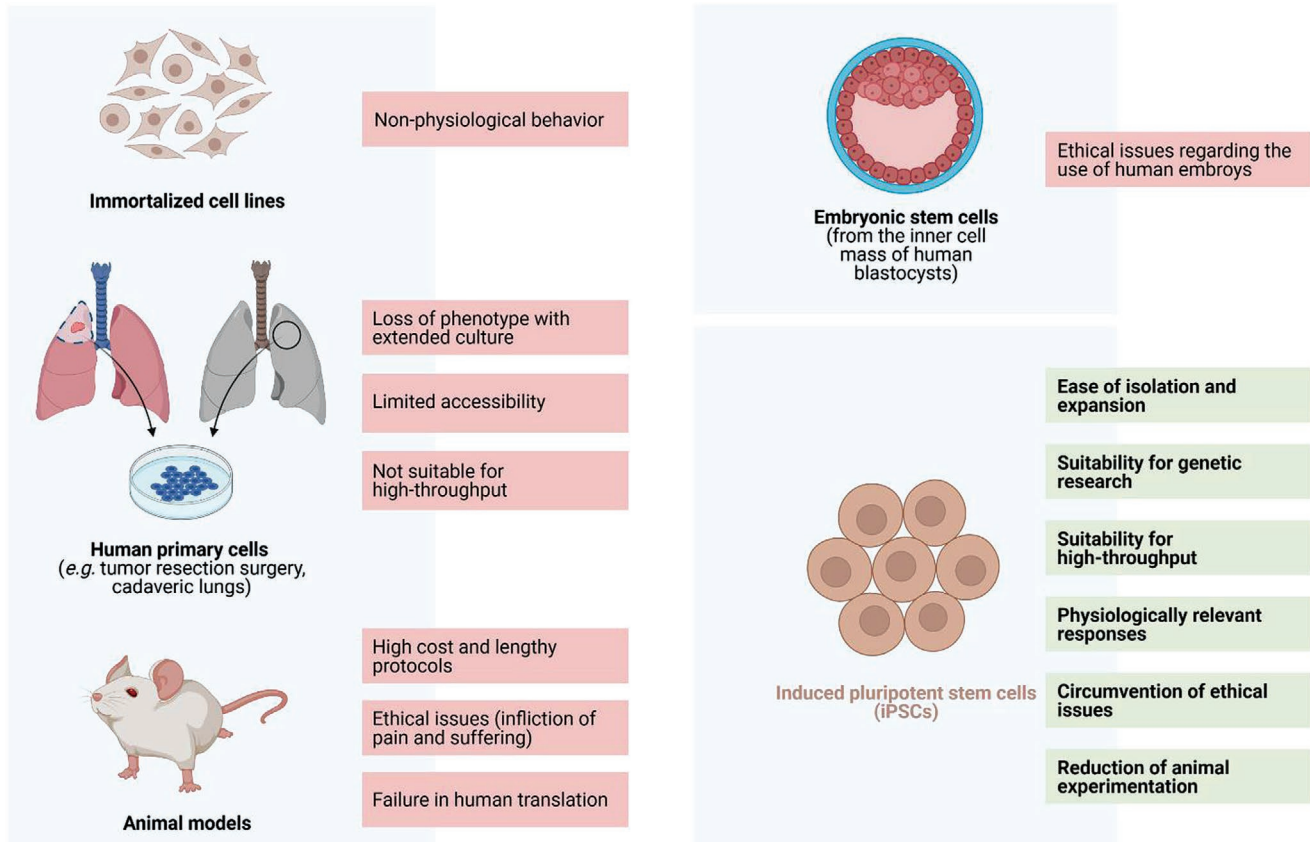


**Figure 6.** iPSCs as a promising cell source for in vitro modeling and toxicological screening. Created with BioRender.com.

these tend to lose their native characteristics with successive passaging and are hard to obtain in sufficient numbers, which is a significant limitation given the restricted access to healthy and diseased human lung tissue.<sup>[258–261]</sup> Moreover, unlike the homogeneity of single-donor cell lines, primary cells are highly heterogeneous, which, albeit more representative of the general population, may compromise study reproducibility.<sup>[21]</sup>

As such, the self-renewal and multilineage differentiation capability of stem cells can offer an answer to these issues. Stem cells endowed with pluripotency, such as ESCs, have the potential to generate all three germ layers of the developing embryo and, therefore, the capacity to differentiate into all somatic tissues in the human body, thus posing as promising candidates for the generation of lung models composed of multiple representative cell types. Nevertheless, the destruction of human embryos for ESC isolation inevitably raises ethical concerns tied to their use and the allogeneic origin of these cells may result in immunological rejection upon transplantation.<sup>[262–264]</sup> Hence, an autologous cell source with vast differentiation and self-renewal potential, easy accessibility, physiological representativeness, and long-term phenotypic stability is increasingly relevant in biomedical research.

The answer for this issue may rely on iPSCs, which can be obtained from somatic cells via reprogramming with four key factors (Oct4, Sox2, Klf4, c-Myc), first identified by Takahashi and Yamanaka in 2006.<sup>[265]</sup> These “induced” PSCs (iPSCs) are virtually indistinguishable from ESCs, displaying similar

transcriptional profiles, but hold distinct advantages (Figure 6), because they can be routinely generated from somatic adult cells without an invasive procedure while retaining the individual genome of the original donor.

Thus, the generation of iPSCs was an enormous breakthrough that paved the way for new therapeutic, cell-based approaches. In fact, the possible autologous extraction of iPSCs and their suitability for genetic manipulation have considerable potential for a new generation of cell-based and gene therapy, making use of gene editing technology such as the clustered regularly interspaced short palindromic repeats (CRISPR)/CRISPR-associated protein 9 (Cas9) system to insert, delete, or modify and correct genetic sequences associated with pathological phenotypes.<sup>[266–270]</sup>

Besides this therapeutic application, iPSCs hold a great promise in in vitro fundamental biology studies and disease modeling (Figure 7). In the context of this review, the possibility for iPSC genetic manipulation opens new windows for the investigation of individual roles of particular genes involved in lung development and disease pathogenesis.

Moreover, the embryonic-like nature of iPSCs implies that these cells may be used to study and model every stage from early to late lung development, and their high proliferative capacity facilitates their in vitro culture and maintenance in appropriate timeframes and provides a virtually limitless cell supply.<sup>[263,264]</sup> High-throughput drug screening and toxicological studies can also be carried out using iPSCs, allowing for

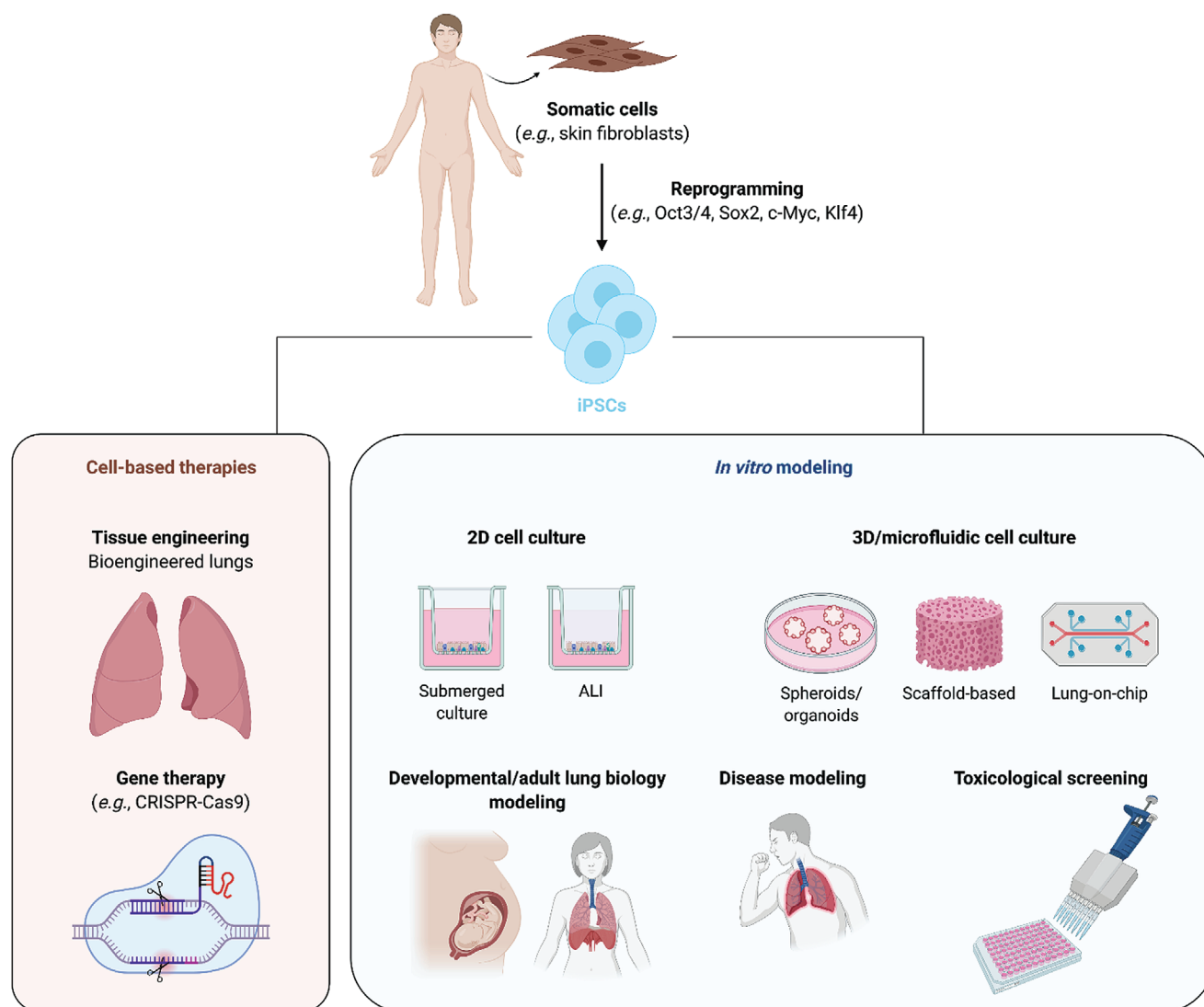


**Figure 7.** Applications of iPSCs in in vitro lung modeling and precision medicine. After isolation and reprogramming of somatic cells from a healthy donor or patient, the obtained iPSCs can be used for in vitro research, where both 2D and 3D lung models can be developed. iPSCs also have a strong potential for precision medicine, in the generation of bioengineered lung tissue or as suitable candidates for genetic manipulation (e.g., using CRISPR-Cas9 technology) and gene therapy. ALI: air-liquid interface. Created with BioRender.com.

the development of targeted testing platforms through directed differentiation to specific cell types, including those of limited accessibility, and isolation from healthy donors or patients afflicted with particular disorders, enabling the recapitulation of these pathological characteristics in vitro.<sup>[263,271,272]</sup>

In the field of lung research, iPSC technology has been a seminal step, due to the opportunity to obtain patient-specific cells from individuals with genetic and acquired lung diseases.<sup>[273]</sup> In 2010, the first 100 lung disease-specific iPSC lines were generated from patients, including the monogenic lung diseases CF,  $\alpha$ 1-antitrypsin deficiency, and hereditary pulmonary alveolar proteinosis (hPAP).<sup>[274]</sup> Wong et al. differentiated mature ciliated airway cells expressing functional CFTR protein, displaying the crucial factor in the pathogenesis of CF.<sup>[275]</sup> The characteristic accumulation of misfolded mutant  $\alpha$ 1-antitrypsin protein could be shown in iPSC-derived hepatocytes,<sup>[276]</sup> and

impaired GM-CSF signaling in iPSC-derived macrophages of hPAP-patients has also been demonstrated.<sup>[277]</sup> Therefore, iPSCs help model person-to-person differences in these diseases, providing the opportunity to identify the efficacy or evaluate toxicological profiles of new drugs toward personalized therapeutic approaches. The focus should be kept further on generating functional epithelial, endothelial, and interstitial lung cells, which remains a challenging task,<sup>[273]</sup> even though significant progress has been made during the past decade for the generation of lung cell types, especially of epithelial lineages.<sup>[269]</sup>

### 3.2. iPSC Differentiation to Lung-Specific Cell Types

For the differentiation of lung-specific cell types from iPSCs, key developmental pathways have to be reproduced in vitro.

This process is referred to as directed differentiation, typically achieved by a stepwise addition of signaling factors needed for the recapitulation of the embryonic lung development. It entails a series of steps, starting with generating definitive endoderm (DE) and directing it toward anterior foregut endoderm (AFE), followed by the induction of lung progenitor lineages, which finally undergo cell-type specific differentiation and maturation.<sup>[278]</sup> The key factors and pathways involved in these steps were identified in mouse organogenesis studies and this knowledge has already contributed to the development of differentiation protocols for ESCs.<sup>[269]</sup> For the right implementation of the directed differentiation approach, a good understanding of the embryonic lung development is required.

The lung arises from the endoderm, one of the three germ layers in a developing embryo. The endoderm participates mainly in the generation of the epithelial lining of the digestive tract, but also gives rise to the lung, liver, pancreas, and thyroid. The DE, a part of the endoderm, which forms inside of the embryo and does not contribute to extraembryonic structures, folds to make a gut tube and is patterned along an anterior-posterior and dorsal-ventral axis. A primitive lung bud is formed from the ventral side of the AFE surrounded by mesenchyme, soon starting to branch and generating the respiratory tree.<sup>[279]</sup> Endoderm-derived cells start to undergo differentiation into the respiratory and specialized epithelium, which lines the airways and the alveoli, respectively. These lung epithelial lineages developing from the foregut endoderm are first identified by the appearance of the key transcription factor NKX2.1. Soon after, the proximal-distal patterning starts to occur at the leading tips of the primary bud, denoted by the differential expression of SOX2. SOX2<sup>+</sup> progenitors differentiate into ciliated cells, secretory cells, and basal cells, thus forming the epithelial lining of the conducting airways. The most distal portion of the branching epithelium are multipotent SOX9<sup>+</sup>/ID2<sup>+</sup> cells, capable of regenerating both airway and alveolar epithelium. SOX9<sup>+</sup> are distal progenitors restricted to generate AT1 and AT2 cells.<sup>[280]</sup> The epithelial-mesenchymal interactions that control these stages of lung development entail a number of signaling pathways, including sonic hedgehog (SHH), WNT, fibroblast growth factor (FGF), bone morphogenetic proteins (BMP), and retinoic acid (RA).<sup>[269]</sup>

The two remaining germ layers are also involved in the development of the lung: the ectoderm plays a role in the innervation of the lung and the mesoderm gives rise to blood vessels, airway smooth muscles, pulmonary fibroblasts, cartilage, and other connective tissues in the trachea and lung.<sup>[279]</sup>

Contrarily to a long-term assumption, tissue-resident macrophage populations, such as lung AMs, hepatic Kupffer cells, and brain microglia, are not constantly replaced by monocytic precursors, but they derive from mesodermal yolk-sac progenitors during embryogenesis, completing their differentiation at the tissue site and self-maintaining under steady state conditions without the contribution of bone-marrow cells.<sup>[281–283]</sup> AM maintenance in the lung hence depends on a locally expanding population. Thus, AMs are not bone-marrow derived and proliferate independently from Myb and hematopoietic progenitors.<sup>[284]</sup> Erythromyeloid progenitors generated in the yolk-sac develop to fetal monocytes, emerging in the liver before the vascular system of the embryo is completed<sup>[285]</sup> and migrating

to embryonic tissues such as the lung, where they give rise to AMs. GM-CSF signaling is essential for their differentiation into immature AMs and their postnatal full maturation.<sup>[283]</sup>

### 3.2.1. Airway Epithelium

iPSC differentiation to airway epithelium, consisting of tracheal and bronchial cell types, can be achieved by reproducing the stages of lung development with the use of growth factors or small molecules that trigger the activation or inhibition of the decisive signaling pathways in vitro. The first step is to differentiate PSCs into a population of DE cells expressing the classic endoderm markers SOX17, CXCR4, and FOXA2. By addition of the Nodal agonist Activin A, a member of the transforming growth factor (TGF)- $\beta$  superfamily, the primitive streak formation can be mimicked.<sup>[286,287]</sup> In addition to Activin A, other small molecules have been shown to induce DE in vitro.<sup>[288]</sup> DE differentiation protocols are now well established and are the initial point for obtaining lung, intestine,<sup>[289]</sup> liver<sup>[290]</sup> pancreas,<sup>[291]</sup> and thyroid<sup>[292]</sup> cells, although these protocols vary significantly in terms of medium composition, growth factor combinations, and timing.<sup>[293]</sup>

Analogous to the anterior-posterior axis patterning in the primitive gut tube in vivo, FOXA2<sup>+</sup> definitive endodermal cells have to be directed into an AFE fate. For AFE patterning, different approaches were published.<sup>[294,295]</sup> Green et al. identified the dual inhibition of TGF- $\beta$  and BMP signaling by the combination of Noggin, a physiological inhibitor of BMP signaling, and SB-431542, a pharmacological inhibitor of Nodal and TGF- $\beta$  signaling, as the best condition to generate AFE cells. They are characterized by the expression of SOX2, a pluripotency marker that reemerges in this stage as a differentiation marker, while the expression of FOXA2 is maintained and the expression of the hindgut marker CDX2 is suppressed.<sup>[294]</sup> This dual inhibition approach was adopted by many others;<sup>[79,292,296,297]</sup> alternatively, a different method relying on SHH and FGF2 signaling can be used.<sup>[295]</sup> After AFE patterning, a lung-specific fate must be induced. In vivo, the lung primordium is formed along the ventral anterior foregut and expresses the lung fate marker NKX2.1. BMP signaling is important to inhibit SOX2 to prime the lung domain, whereas FGF10 secreted from the surrounding mesoderm as well as WNT ligands are necessary for NKX2.1 expression.<sup>[278]</sup> Since many more signaling pathways are involved in the process of lung specification and they are controlled in a very tight spatial and temporal manner in vivo, it has been challenging to translate them to in vitro conditions. Some groups use BMP, WNT, and RA activation to induce NKX2.1 expression with varying efficiencies.<sup>[292,297–300]</sup> A combination of TGF- $\beta$  and BMP inhibition plus SHH and WNT activation leading to a lung specification has been demonstrated by others.<sup>[79]</sup>

Within the proximal-distal patterning of the lung, NKX2.1<sup>+</sup> lung progenitors can give rise to SOX2<sup>+</sup> proximal airways or SOX9<sup>+</sup>/ID2<sup>+</sup> cells differentiating into alveolar cell types. The SOX2<sup>+</sup> airway progenitor population can generate ciliated, goblet, club, neuroendocrine, and basal cells. McCauley et al. identified WNT signaling as a key regulator in the proximal-distal patterning.<sup>[301]</sup> By activation of Notch signaling, SOX2<sup>+</sup> cells are

triggered to differentiate into secretory cell types, whereas the inhibition of Notch promotes the differentiation of neuroendocrine and ciliated cells.<sup>[278]</sup> In order to obtain proximal airway and reduce distal airway differentiation, a reduction of factors that promote distal specification, such as BMP4, and the administration of factors that result in proximal differentiation, such as FGF18, led to over 50 % of cells being positive for P63, a marker for basal cells, which function as progenitors for other airway cell types.<sup>[278]</sup> An additional maturation phase at ALI conditions resulted in an increase of mature airway cells and polarization of the epithelium. This cell population expressed markers for goblet, club, ciliated, and basal cells.<sup>[295]</sup>

Multicellular airway specification and differentiation can also be efficiently obtained by culturing and differentiating iPSCs in a 3D environment. Konishi et al. reported proximal airway progenitor spheroids generated from NKX2.1<sup>+</sup> cells, which could be induced to differentiate into multi-ciliated cells with motile cilia and other airway cells in the absence of alveolar cells via Notch signaling inhibition.<sup>[302]</sup> Similar spheroids grown in a 3D ECM (Matrigel) overlaid with medium containing high concentrations of FGF10 also formed a polarized airway epithelium surrounded by mesenchyme and containing basal and ciliated cells.<sup>[79]</sup> However, an efficient derivation of basal cells, evidenced by transcriptional profiling and demonstration of differentiation capacities into multi-ciliated and secretory cells, has not been convincingly achieved.<sup>[269]</sup> Due to the lack of in vitro or in vivo studies evaluating airway cellular physiological functionality, assessing parameters such as the transport function of chloride channels of iPSC-derived airway cells, the question remains whether these cells can be generated in a mature, functional status.<sup>[303]</sup>

### 3.2.2. Alveolar Epithelium

The alveolar epithelium consists of AT1 and AT2 cells, which develop from NKX2.1/SOX9<sup>+</sup> progenitors. The derivation of alveolar cell types in vitro has been attempted by the recapitulation of active signaling factors around the distal buds during branching in the developing embryo. To date, different approaches exist to generate AT1 and AT2 cells from human iPSCs (hiPSCs).<sup>[298,299,304]</sup> Huang et al. yielded AT1 and AT2 cells, besides a couple of other airway cell types, using a long-term differentiation approach.<sup>[183]</sup> After the generation of AFE cells, these were cultivated with CHIR99021 (CHIR), BMP4, FGF10, FGF7, and RA for 15 days, followed by CHIR, FGF10, and FGF7 for additional 25 days and, finally, treatment with dexamethasone, cyclic adenosine monophosphate (cAMP) and 3-isobutyl-1-methylxanthine (IBMX), a mixture that stimulates alveolar gene expression in vitro.<sup>[298]</sup> Others used WNT activation in AFE cells by CHIR along with BMP4 and RA, defined as the minimal factors required for lung specification. The resulting NKX2.1<sup>+</sup> population develops by cultivation with the factors CHIR, keratinocyte growth factor (KGF), IBMX, cAMP, and dexamethasone into AT2 populations expressing typical markers such as surfactant protein C (SFTPC), -B (SFTPB), -A (SFTPA), -D (SFTPD), and ABCA3.<sup>[299,300,304,305]</sup> Interestingly, dexamethasone is also administered to premature infants

to accelerate the maturation of the fetal lungs, resulting in enhanced surfactant secretion from AT2 cells.<sup>[278]</sup>

Through the identification of carboxypeptidase M (CPM) as a surface marker for NKX2.1<sup>+</sup> cells, a homogeneous progenitor population for generating AT2 cells in alveolar spheroids could be isolated by Gotoh et al.<sup>[299]</sup> The authors concluded that 3D co-culture differentiation with fetal lung fibroblasts enabled a more efficient differentiation into alveolar cell types than 2D differentiation.<sup>[299]</sup> The same group also developed a method for the expansion of AT2 cells in alveolar organoids involving human fetal lung fibroblasts.<sup>[304]</sup> More recently, Jacob et al. published a protocol for the generation and expansion of AT2 cells from a purified population of NKX2.1<sup>+</sup> progenitors seeded in Matrigel drops without fibroblasts.<sup>[305]</sup> Within 25–30 days of cultivation time along with the factors CHIR, KGF, IBMX, cAMP, and dexamethasone, cell populations positive for the AT2 marker SFTPC emerged in the cell aggregates. These “alveospheres” were capable of proliferation and suitable for passaging, making it possible to maintain the culture for several months.<sup>[305]</sup>

These protocols may help satisfy the need for human AT2 cells capable of long-term in vitro culture and expansion without spontaneously transdifferentiating into AT1 cells, as recurrently happens in cell cultures isolated from primary lung tissue.<sup>[300]</sup> Ghaedi et al. reported that NKX2.1<sup>+</sup> lung progenitor cultures on human lung ECM proteins promoted AT1 and AT2 cell differentiation, indicating that physical and chemical environments are important factors for alveolar differentiation as well.<sup>[306]</sup>

Since AT2 cells act as AT1 cell progenitors in the alveoli, the capability of transdifferentiation of AT2 into AT1 phenotypes is an important functional feature. In a recent study, a WNT-responsive AT2 cell subpopulation able to differentiate into AT1 cells was observed in alveolar organoids.<sup>[307]</sup> Transdifferentiation from hiPSC-AT2 cells into AT1 has also been achieved by inhibition of canonical WNT signaling via the addition of the rho-kinase inhibitor Y27623 for 5 days.<sup>[308]</sup> Additionally, the authors compared the generation of AT1 cells in fibroblast-dependent and fibroblast-free organoids generated from hiPSC-AT2 cells, concluding that AT1 phenotypes were mainly present in feeder-dependent organoids and their transcriptomes were comparable with their primary counterparts.<sup>[308]</sup> Another group exposed hiPSC-derived AT2-like cells to the small molecule IWR-1 for 7 days, resulting in a transition from an AT2 into an AT1 phenotype, evidenced by the expression of the AT1-specific markers AQP-5 and T1- $\alpha$ .<sup>[306,309]</sup>

Strategies for the directed differentiation of iPSCs into proximal and distal pulmonary epithelium are summarized in **Figure 8**.

### 3.2.3. Vasculature

To enable gas exchanges between the environment and the blood system, a fine capillary network surrounds the most distal part of the lung, the alveoli. Thus, vasculature is a critical aspect when developing lung models in vitro. During embryogenesis vasculature, bone, cartilage, adipose tissue, and blood cells are derived from the mesenchyme, leading to the development of

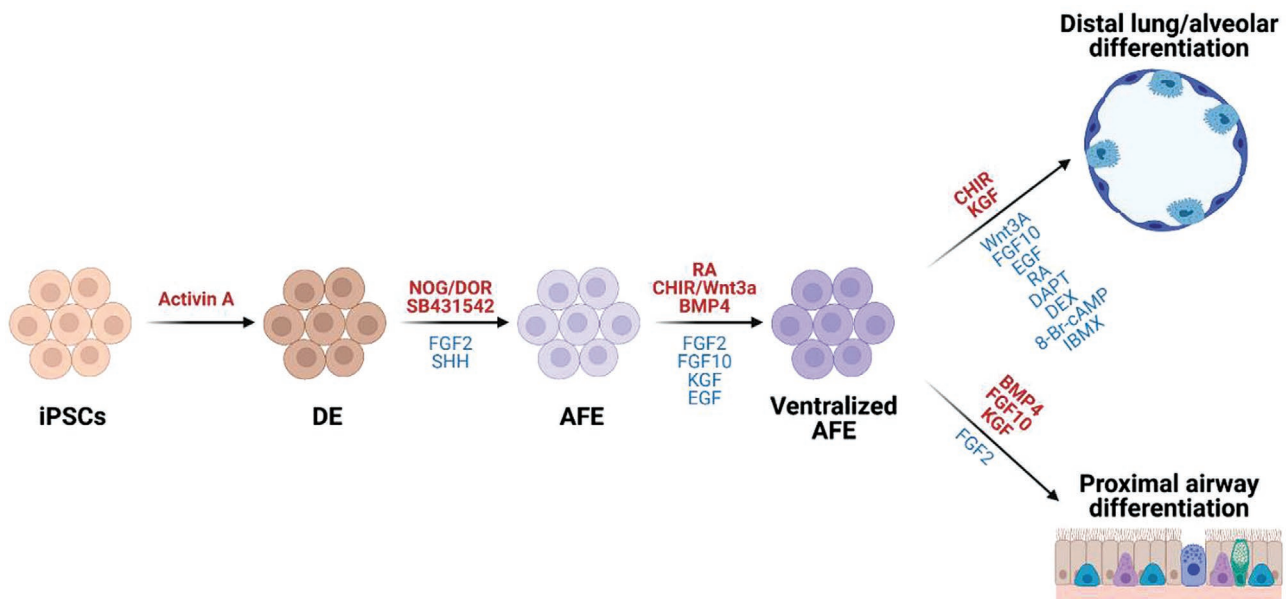


**Figure 8.** Directed differentiation of induced pluripotent stem cells (iPSCs) into proximal airway and distal epithelial fates. Growth/differentiation factors highlighted in red represent the most commonly used strategies throughout the literature, with alternative factors presented in blue. AFE: anterior foregut endoderm; BMP: bone morphogenetic protein; 8-Br-cAMP: 8-bromo-cyclic adenosine monophosphate; CHIR: CHIR99021; DAPT: *N*-[*N*-(3,5-difluorophenacetyl)-*L*-alanyl]-*S*-phenylglycine *t*-butyl ester; DE: definitive endoderm; DEX: dexamethasone; DOR: dorsomorphin; EGF: epithelial growth factor; FGF: fibroblast growth factor; IBMX: 3-isobutyl-1-methylxanthine; KGF: keratinocyte growth factor; NOG: noggin; RA: retinoic acid; SHH: sonic hedgehog. Created with BioRender.com.

cardiovascular, hematopoietic, skeletal, and soft tissues.<sup>[310]</sup> Such mesenchymal cells are comprised of functionally and developmentally diverse cell populations including mesenchymal stem/stromal cells (MSCs), pericytes, ECs, and smooth muscle cells (SMCs).<sup>[310]</sup> The differentiation of hiPSCs into mesenchymal cells has long been hampered by the lack of knowledge regarding the hierarchy of mesenchymal progenitors and markers that allow discriminating different mesenchymal cell populations.<sup>[310]</sup> An important milestone was the identification of a common mesodermal progenitor for mesenchymal cells and ECs, the mesenchymoangioblast (MB).<sup>[310]</sup> Directing hiPSCs toward a mesendodermal differentiation *in vitro*, hemangioblasts (HB), in analogy to MB, result, which can be further differentiated into endothelial and hematopoietic cells. The formation of MB colonies solely depends on the growth factor FGF2 and requires serum-free medium.<sup>[311]</sup> MB colonies have broad differentiation potential and generate different mesenchymal lineages including MSCs, pericytes, and SMCs.<sup>[310]</sup> However, the major components of blood vessels are ECs and SMCs, which are naturally required for vascular function. ECs arise from mesodermal progenitors under the stimulus of FGF2, BMP4, and vascular endothelial growth factor (VEGF) and organize into primitive tubular networks, a process called vasculogenesis.<sup>[312]</sup> Several studies described the differentiation of PSCs to vascular cells by inducing mesoderm differentiation via the activation of canonical WNT signaling with the GSK3 pathway inhibitors CHIR or BMP4, followed by treatment with VEGF, resulting in ECs, or platelet-derived growth factor (PDGF), resulting in SMCs.<sup>[313,314]</sup> The effect of VEGF, essential to induce EC differentiation, could be enhanced by cAMP.<sup>[315]</sup> hiPSC-derived ECs have already been extensively characterized under shear-stress

conditions in a microfluidic cell culture system.<sup>[316]</sup> Recently, the directed differentiation of PSC-derived blood vessel organoids was described. Starting from cell aggregation and mesoderm induction via WNT activation with CHIR and BMP signaling, followed by VEGF and FGF2 to induce vascular specification, the cell aggregates grew into a sprouting vasculature in an ECM matrix consisting of collagen and Matrigel.<sup>[317]</sup> Additionally, cocultures of separately differentiated ECs and pericytes in 2D, as well as culture with early vascular progenitor cells in 3D, has been used previously to generate vascular networks.<sup>[318,319]</sup> Alas, the appearance of ECs or vascular networks in lung organoids or in combination with hiPSC-derived airway or alveolar epithelial cells has not been demonstrated.

### 3.2.4. Alveolar Macrophages

Compromised or altered function of AMs is often associated with many chronic or acute lung diseases including hPAP, CF, COPD, and asthma. Although AMs differ from bone-marrow derived macrophages, recent studies suggest intratracheal delivery of bone-marrow or blood-derived macrophages to replace dysfunctional AMs in diseases like hPAP.<sup>[320,321]</sup> This hematopoietic differentiation approach of disease hiPSCs into macrophages and monocytes is described in recent studies.<sup>[277,322]</sup> However, other authors have proposed that alveolar-like macrophages could be best generated through yolk-sac hematopoiesis of hiPSCs or ESCs. Litvack et al. first described the generation of primitive yolk-sac macrophages from PSCs, which could be conditioned with GM-CSF to alveolar-like macrophages, representing the macrophage population of the

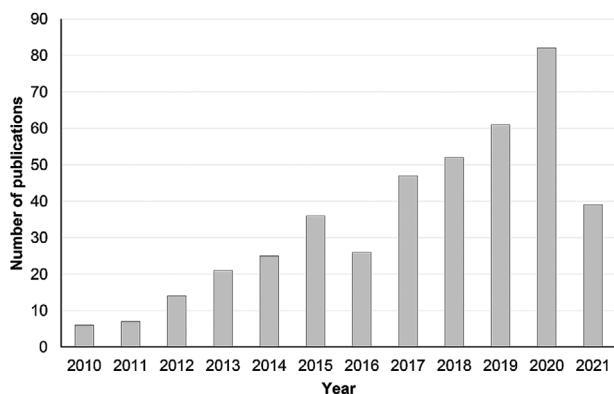


**Figure 9.** Number of publications per year between 2000 and 2021 (first half of 2021) retrieved using the search terms “iPSC” AND “lung” AND “model” in the PubMed database (date of consultation: 16/06/2021).

alveolus better than bone-marrow derived macrophages.<sup>[281]</sup> The Myb-independent yolk-sac macrophages could be generated by recapitulating the primitive hematopoiesis during embryogenesis, mimicking primitive streak formation followed by the stages of hemangioblasts and myeloid cells in a timely manner for a minimum of 21 days. This embryoid body-based protocol requires a series of growth factors and molecules including Activin A, vascular endothelial growth factor (VEGF), bone morphogenetic protein 4 (BMP4), IL-3, IL-6, stem cell factor (SCF), GM-CSF, and macrophage CSF (M-CSF). The resulting cells were examined for typical ligand markers CD45, CD11b, CD68, CD11c, the latter being only expressed by AMs.<sup>[281]</sup> Stem-cell derived AMs were then tested for therapeutic applications in vivo, being capable of survival and enhancing tissue repair without developing abnormal pathology and teratomas.<sup>[281]</sup>

Similar protocols have been used to obtain not only AMs,<sup>[283]</sup> but also other populations of tissue-resident immune cells, such as Kupffer cells<sup>[323]</sup> and microglia.<sup>[282]</sup> Macrophages from different tissue sites are uniquely adapted and it is clear that AMs, for instance, differ in their phenotype and function from microglia, the specialized macrophages of the brain. Tissue macrophage populations arise from different origins and sub-populations and differentiate into specialized cells under the influence of microenvironmental cues from the respective organ.<sup>[324]</sup> For more accurate hiPSC-derived tissue-resident macrophages, Lee et al. suggested a co-culture of primitive macrophages with hiPSC-derived isogenic tissue or organoids to mimic these microenvironmental niches.<sup>[324]</sup>

#### 4. iPSC-Based Lung Models

The potential of iPSCs in modeling lung development, homeostatic function, and pathogenesis has been drawing increasing attention over the last decade (Figure 9). Their induced pluripotency enables the generation of virtually every cell type that constitutes the lung and, therefore, iPSCs can be used as progenitors for the development of multicellular models or differentiated toward a single cell type for targeted studies.

iPSC-based lung models include 2D approaches, such as submerged or ALI monolayers, and 3D models, including

organoids, scaffold-based models, and lung-on-chip devices, which can all have a valuable application in understanding both the normal and diseased function of the lung. Each of these models will be explored in the following sections.

##### 4.1. 2D Models

Probably due to the limitations of 2D systems in modeling the pulmonary architecture and microenvironment presented previously, there are only a few studies that apply iPSC technology for the generation of 2D models to study lung biology. Nevertheless, these approaches may have important applications in the early stages of drug development or for the investigation and testing of individual types of cells, due to their ease of manipulation and high reproducibility, potential for high-throughput screening, and suitability for single-cell analysis.<sup>[60]</sup> Accordingly, a wide variety of protocols have described the generation of multicellular lung and airway epithelial 2D models from iPSC differentiation,<sup>[295,298,325]</sup> which contain virtually all the main types of airway and alveolar cells, including basal,<sup>[326]</sup> multi-ciliated,<sup>[296]</sup> and neuroendocrine<sup>[327]</sup> cells. The relative advantages of iPSC-derived lung cells compared to commonly used lung cell lines are evident in a report by Heo and coworkers:<sup>[328]</sup> while human iPSC-derived AT2 cells were shown to respond similarly to primary AT2 after treatment with Cadmium chloride (CdCl<sub>2</sub>), BEAS-2B cells, a human bronchial cell line, did not accurately represent these responses. Cadmium (Cd) exerted a more toxic response in BEAS-2B, with greater cell death and the expression of pro-inflammatory and pro-apoptotic genes in comparison to iPSC-AT2 and primary AT2 cells.<sup>[328]</sup> As such, iPSC-derived lung cells can be used for toxicological studies as a model that closely resembles the response of primary cells.

In the same line of thought, a “long-lasting” (LL) AT2 cell line was generated from iPSCs using a two-step differentiation protocol followed by transfection with two genes involved in stem cell self-renewal, human telomerase (hTERT), and hBmi-1.<sup>[329]</sup> iPSC-AT2 expressed SFTPC and presented lamellar bodies and microvilli, typical characteristics of AT2 cells. After viral transfection, LL-iPSC-AT2 expressed SFTPC and other epithelial markers such as cytokeratin and occludin, while no expression of AQP5, a marker for AT1 cells, was observed. LL-iPSC-AT2 could also be differentiated into AT1, replicating the in vivo behavior of these cells. It is important to note that this cell line is not immortalized despite the transfection procedure: it is reported to be suitable for use until passage 30, after which cell growth rate is reduced and epithelial marker expression is heterogeneous.<sup>[329]</sup>

Likewise, a model of alveolar repair under ALI was recently developed using iPSC-derived AT2 cells.<sup>[330]</sup> However, while these iPSC-AT2 cells presented lamellar bodies and expressed several surfactant proteins, the levels of SFTPB and SFTPD were markedly lower than those observed in human primary AT2 cells. TEER values and the proliferation rate of iPSC-AT2 were also distinctly reduced compared to those recorded in primary AT2 cells. Importantly, this study demonstrates that obtaining fully mature and functional cells from iPSCs can often be challenging and vary greatly among distinct differentiation protocols and culture conditions.

## 4.2. 3D Models

### 4.2.1. Self-Assembled Models: Spheroids and Organoids

Mishima's group has developed proximal airway epithelial spheroids<sup>[302]</sup> and alveolar (distal) epithelial spheroids<sup>[299]</sup> from human pluripotent stem cells (hPSCs), including both ESCs and iPSCs. In these studies, the surface marker carboxypeptidase M (CPM) was used to isolate NKX2.1<sup>+</sup> ventralized AFE cells. In the former model, proximal airway epithelial spheroids were derived from CPM<sup>+</sup> progenitor cells in a 3D environment without the presence of a feeder layer.<sup>[302]</sup> Differentiated proximal lung cell populations in these spheroids included FOXJ1<sup>+</sup> (multi-ciliated) cells, MUC5AC<sup>+</sup> (goblet) cells, KRT5<sup>+</sup> (basal) cells, SCGB1A1<sup>+</sup> (club) cells, and chromogranin (CHGA)<sup>+</sup>/synaptophysin (SYP)<sup>+</sup> (pulmonary neuroendocrine) cells (Figure 10A,B), while staining for distal lung markers such as AQP5 (AT1) and SFTPC (AT2) was almost completely absent. Importantly, hiPSC-derived multi-ciliated cells displayed ciliary beating function, as well as mucociliary clearance capability.<sup>[302]</sup>

Conversely, in the latter study, alveolar spheroids were developed from hiPSC-derived CPM<sup>+</sup> SFTPC-GFP reporter cells in 3D co-culture with fetal human lung fibroblasts, in which the expression of AT2-specific markers, namely surfactant proteins, was greater than that observed in 2D culture systems.<sup>[299]</sup> Lamellar body-like structures were also clearly observed in induced AT2 cells (Figure 10C,D).<sup>[299]</sup> More recently, another study from the same group reported the long-term maintenance of hiPSC-derived alveolar organoids containing SFTPC<sup>+</sup> AT2-like cells, both in the presence and in the absence of a fibroblast feeder component.<sup>[304]</sup> hiPSC-derived AT2 cells displayed gene expression profiles similar to those of adult lung AT2 cells, as well as lamellar bodies, and were able to uptake BODIPY-labeled phosphatidylcholine, a key component of pulmonary surfactant. Furthermore, the iPSC-derived alveolar organoids were able to recapitulate features of in vivo AT2 cell damage induced by two distinct drugs, amiodarone and GNE7915, revealing their applicability as platforms for toxicological screening. Interestingly, the presence of a fibroblast feeder layer in alveolar organoids appears to be paramount for the differentiation of hiPSC-derived AT2 to AT1 cells, demonstrating the importance of models incorporating multiple cellular types originating from distinct germ layers.

Accordingly, the generation and characterization of human lung organoids from hPSCs containing cell populations deriving from multiple germ layers, namely endoderm and mesoderm, have also been described.<sup>[79]</sup> After DE induction, hPSCs (hESCs and hiPSCs) were first self-assembled into anterior foregut spheroids, which were then embedded into Matrigel to provide a suitable 3D environment for the development of lung organoids (details on differentiation factors can be consulted in Table 2). After long-term culture (>2 months), both proximal airway and alveolar lung cell markers were identified in these organoids, together with a network of mesenchymal cells expressing myofibroblast (platelet-derived growth factor receptor  $\alpha$  (PDGFR $\alpha$ )<sup>+</sup>/vimentin (VIM)<sup>+</sup>), fibroblast (PDGFR $\alpha$ /VIM<sup>+</sup>), and smooth muscle cell (PDGFR $\alpha$ /smooth muscle actin (SMA)<sup>+</sup>) markers (Figure 11). The presence of cells in early stages of differentiation, such as FOXJ1<sup>+</sup> cells with no visible cilia, and RNA-sequencing data revealed

that these organoids were remarkably similar to human fetal lungs in terms of gene expression and developmental stage. Curiously, when plated onto acellular lung sections, anterior foregut spheroids gave rise to organoids with FOXJ1<sup>+</sup> cells displaying mature ACTTUB<sup>+</sup> cilia, suggesting that structures with a more advanced maturation stage could be obtained providing the appropriate biochemical and architectural environment.<sup>[79]</sup>

To further confirm this hypothesis, hPSC-derived lung organoids were suspended in Matrigel, seeded onto a poly(lactic-co-glycolic acid) (PLGA) microporous scaffold, and subsequently implanted into the epididymal fat pad of a mouse model.<sup>[331]</sup> Indeed, human lung organoids that had undergone in vivo differentiation resulted in more mature epithelial structures and enhanced cell differentiation, resembling adult lung epithelium more closely than organoids grown in vitro. The lumen of in vivo-grown human lung organoids was composed of multi-ciliated FOXJ1<sup>+</sup> cells, with beating ciliary function, and several basal-like cells staining positive for P63, KRT5, and NGFR. Other proximal airway cells were detected, such as MUC5AC<sup>+</sup> goblet-like cells and CC10<sup>+</sup>/PLUNC<sup>+</sup> club-like cells, whereas distal (alveolar) cell markers were not present in in vivo differentiated human lung organoids, therefore implying that, despite their presence during in vitro culture, these cells do not thrive in the conditions of this in vivo protocol. The network of mesenchymal cells observed in vitro, however, was still present after in vivo growth; several myofibroblast- and smooth muscle-like cells were present in this model, and organized cartilage deposition was also observed.<sup>[331]</sup> Of note, only hESC-derived organoids were studied in this report, implying that these results may not translate directly to hiPSC-derived organoids. Nevertheless, these two last studies demonstrate that in vitro hPSC differentiation protocols may be insufficient to achieve terminal cell differentiation, and that the attainment of fully mature organoids may be dependent on 3D bioengineered scaffolds and transplantation into a dynamic in vivo environment. Hence, investigation of human lung development and morphogenesis, encompassing not only the pulmonary epithelium, but also epithelial-mesenchymal cell communication, can be carried using these models. In later studies, the same protocol for the generation of hPSC-derived anterior foregut spheroids was then used to develop lung bud tip organoids.<sup>[332,333]</sup> After Matrigel embedding and culture in the presence of a minimum of three factors (fibroblast growth factor (FGF) 7, all-trans RA, and CHIR) these spheroids gave rise to "patterned lung organoids", in which separate proximal airway-like and bud tip-like branched domains could be distinctively observed, but no mesenchyme appeared to be generated. Moreover, needle passaging of patterned lung organoids produced NKX2.1<sup>+</sup> SOX2<sup>+</sup> SOX9<sup>+</sup> epithelial cysts (bud tip organoids), which displayed a greater proportion of highly proliferative, Ki67<sup>+</sup> SOX9<sup>+</sup> progenitor cells. The multilineage differentiation potential of hiPSC-derived bud tip organoids was first assessed in vitro, where culture in the presence of FGF7 only resulted in the expression of several proximal airway and alveolar cell markers, but no multi-ciliated cell phenotypes were detected. Interestingly, after intratracheal injection of hiPSC-derived bud tip organoids in injured mouse lungs, progenitor cells appeared to commit to an airway fate, as no alveolar expression markers were detected after in vivo growth, but multi-ciliated, neuroendocrine, and mucus-producing cells

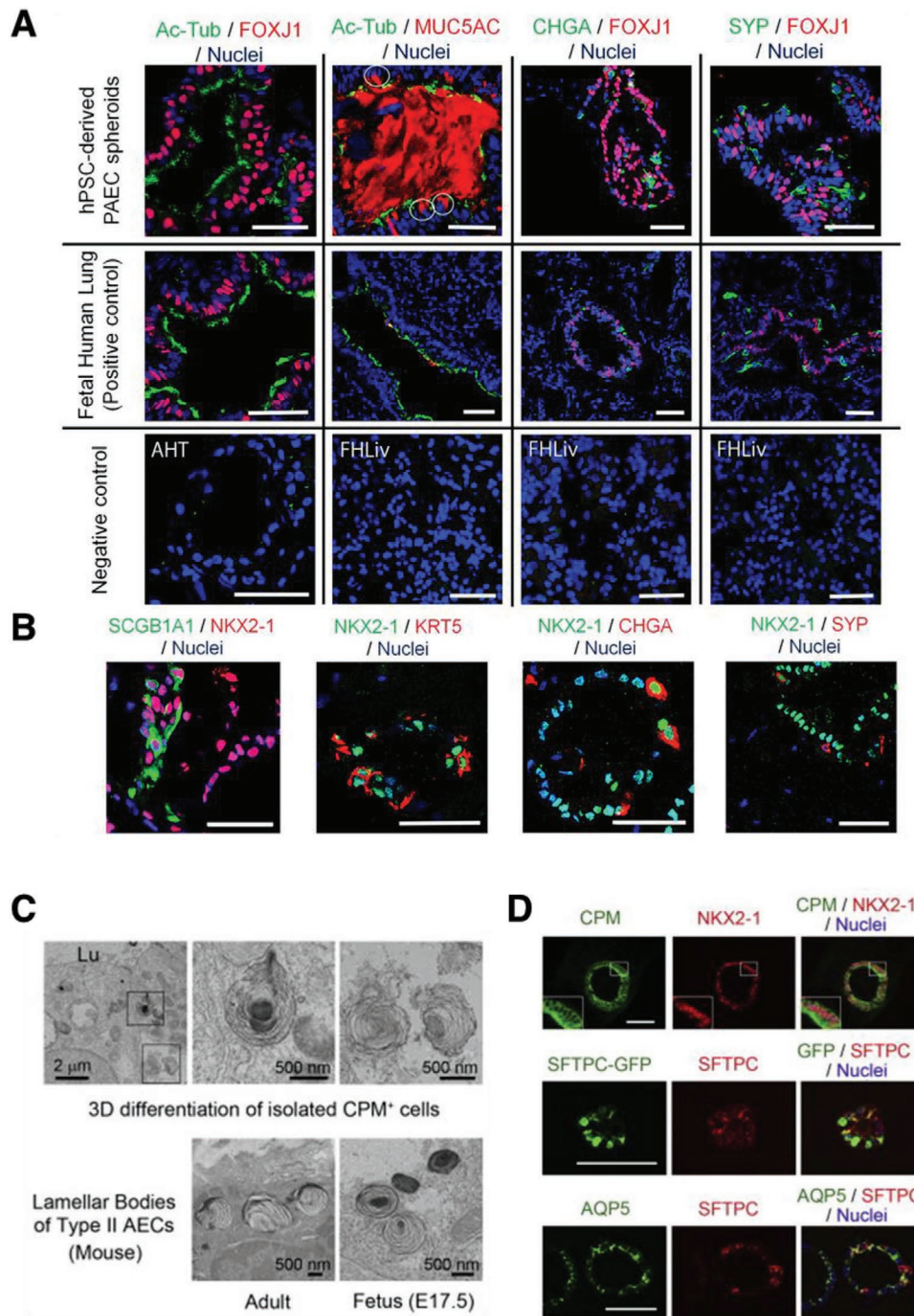


**Figure 10.** Generation of proximal airway (A,B) and alveolar (C,D) epithelial spheroids. A) Immunostaining of proximal airway epithelial spheroids, in which the markers for ciliated cells (FOXJ1<sup>+</sup>/Ac-Tub<sup>+</sup>), goblet cells (MUC5AC<sup>+</sup>), and neuroendocrine cells (CHGA<sup>+</sup>/SYP<sup>+</sup>) can be detected. Negative controls were adult human thyroid (AHT) and fetal human liver (FHLiv). The white circles indicate MUC5AC<sup>+</sup> cells. B) Positive signal for SCGB1A1 (club cell marker) and KRT5 (basal cell marker) was also detected. Scale bars: 50  $\mu$ m. (A) and (B) were adapted with permission.<sup>[302]</sup> Copyright 2016, Elsevier. C) Transmission electron microscopy (TEM) images of carboxypeptidase M (CPM)<sup>+</sup> cells derived from hPSCs in 3D co-culture with fetal human lung fibroblasts. Lamellar body-like structures can be observed in these cells, comparing to adult and fetal murine lung cells. D) Immunostaining of CPM<sup>+</sup> surfactant protein C (SFTPC)-green fluorescent protein (GFP) reporter hPSC-derived spheroids, which stained positively for NKX2.1 (early lung and thyroid development marker), SFTPC (AT2 marker) and AQP5 (AT1 marker). Scale bars: 100  $\mu$ m. (C) and (D) were adapted with permission.<sup>[299]</sup> Copyright 2014, Elsevier.

were present in the explants.<sup>[332]</sup> Such models in which lung epithelial progenitors are present can be used for the investigation of cell fate and differentiation during lung development.<sup>[333]</sup>

Of note, hPSC-derived lung bud tip organoids had also been generated in a previous report.<sup>[190]</sup> While double-positive SOX2<sup>+</sup> SOX9<sup>+</sup> cells were also observed, cellular components from both

**Table 2.** Human iPSC-based in vitro 2D and 3D lung models for basic research on pulmonary development, biology, and disease, as well as pharmacological screening for drug development and targeted therapy.

Model	Cell populations in vitro	Differentiation factors	Main findings	References
ALI	SFTPC <sup>+</sup> /SFTPB <sup>+</sup> /ABCA3 <sup>+</sup> (AT2-like) cells KRT5 <sup>+</sup> (basal-like) cells	DE specification Day 0–1: BMP4, Wnt3a, Y27632 Day 1–4: Activin A, BMP4, FGF2 AFE specification Day 4–5: Y27632, Noggin, SB431542 Day 5–6: SB431542, W/P-2 AFE ventralization and lung specification Day 6–14: CHIR99021, FGF10, KGF, BMP4, RA Day 14–24: CHIR99021, FGF10, KGF Distal lung specification Day 24 forward: CHIR99021 (except from days 35 to 42), FGF10, KGF, dexamethasone, 8-Br-cAMP, IBMX – Introduction of ALI at day 32	– This differentiation protocol yielded a AT2-like cell population, characterized by the expression of AT2-specific markers and the presence of lamellar bodies, with a few rare KRT5 <sup>+</sup> basal-like cells. – The administration of a pro-fibrotic cytokine cocktail mimicking the IPF biochemical microenvironment induced changes in the gene expression of iPSC-derived AT2-like cells. Genes involved in ECM remodeling were up-regulated, as well as proximal airway-specific genes, revealing some level of alveolar bronchiolization and loss of proximodistal specification, typical features of IPF.	[362]
Organoids	After long-term expansion: SFTPC <sup>+</sup> /DCLAMP (AT2-like) cells AQP5 <sup>+</sup> /PDPN <sup>+</sup> (ATI-like) cells	(Fibroblast-dependent cultures) DE specification Day 0–6: Activin A, CHIR99021, sodium butyrate, Y27632 (days 0–2 only) AFE specification Day 6–10: Noggin, SB431542 AFE ventralization Day 10–14: ATRA, BMP4, CHIR99021 Lung specification Day 14–21: CHIR99021, FGF10, KGF, DAPT Distal lung specification Day 21–35: Dexamethasone, 8-Br-cAMP, IBMX, KGF	– Alveolar organoids contained both ATI- and AT2-like cells. hiPSC-derived AT2-like (SFTPC <sup>+</sup> ) cells presented lamellar bodies and were able to uptake BODIPY-labeled phosphatidylcholine, demonstrating some level of AT2-specific cellular function. – These cells also possessed global gene expression profiles comparable to those of adult human AT2.	[304]
Lung organoids	FOXJ1 <sup>+</sup> /ACTTUB <sup>+</sup> (multi-ciliated-like) cells SCGB1A1 <sup>+</sup> (club-like) cells P63 <sup>+</sup> (basal-like) cells PDPN <sup>+</sup> /HOPX <sup>+</sup> (ATI-like) cells SFTPB <sup>+</sup> , SFTPC <sup>+</sup> (AT2-like) cells PDGFR $\alpha$ /VIM <sup>+</sup> (myofibroblast-like) cells PDGFR $\alpha$ /VIM <sup>+</sup> (fibroblast-like) cells PDGFR $\alpha$ /SMA <sup>+</sup> (smooth muscle-like) cells	DE specification Day 0–4: Activin A AFE specification and ventralization Day 4–10: Noggin, SB431542, FGF4, CHIR99021, SAG Lung lineage specification Day 10 forward: FGF10, FBS	– Organoids contained cell populations from both endodermal and mesodermal origin, providing a complex representation of the pulmonary epithelium and mesenchyme, respectively. – Organoids were immature in terms of cell differentiation: gene expression profiles were similar to those of fetal human lungs.	[79,333]
Patterned and bud tip organoids	Bud tip organoids: SOX2 <sup>+</sup> SOX9 <sup>+</sup> progenitor cells Patterned bud tip organoids, anterior (airway-like) zone: SOX2 <sup>+</sup> (airway progenitor) cells MUC5AC <sup>+</sup> (goblet-like) cells SCGB1A1 <sup>+</sup> cells Patterned bud tip organoids, bud tip zone, progenitor cells: Pro-SFTPC <sup>+</sup> cells SOX2 <sup>+</sup> SOX9 <sup>+</sup> cells SOX9 <sup>+</sup> (alveolar progenitor) cells	DE specification Day 0–4: Activin A AFE specification and ventralization Day 4–10: Noggin, SB431542, FGF4, CHIR99021, SAG Lung lineage specification and maintenance of bud tip organoids Day 10 forward: FGF7, CHIR99021, ATRA	– Bud tip organoids contained a large amount of proliferative (Klf6 <sup>+</sup> ) cells. Widespread SOX2 <sup>+</sup> SOX9 <sup>+</sup> double staining was observed, while the expression of both proximal airway and alveolar markers was scarce or absent. – Patterned bud tip organoids expressing both proximal and distal epithelial markers resulted from stochastic differentiation of bud tip organoids in the presence of FGF7 only.	[332,333]

**Table 2.** Continued.

Model	Cell populations in vitro	Differentiation factors	Main findings	References	
Decellularized lung ECM scaffolds	Whole rat lung/rat and human lung sections	iPSC-derived AT2 cell bioreactor culture in whole rat lungs: NKX2.1 <sup>+</sup> Pro-SFTPC <sup>+</sup> cells NKX2.1 <sup>-</sup> T1 $\alpha$ <sup>+</sup> (AT1-like) cells	In vitro differentiation (before ECM seeding) DE specification Day 0–6: Activin A AFE specification Day 6–8: Noggin, SB431542 Distal lung specification Day 8–21: EGF, KGF, FGF10, Wnt3a, RA In vitro ATI induced differentiation (with no ECM seeding) Day 21 forward: IWR-1	– A SFTPC <sup>+</sup> , SFTPA <sup>+</sup> , mucin-1 <sup>+</sup> AT2-like cell enriched population was obtained from two different iPSC lines. Spontaneous differentiation into AT1-like cells was observed and could be further enhanced by cell culture in the presence of IWR-1 (Wnt/ $\beta$ -catenin pathway inhibitor). – iPSC-derived AT2 cells were able to repopulate the alveolar regions of decellularized matrices. Most AT2 cells maintained their phenotype, but spontaneous differentiation into AT1 cells also occurred.	[306]
	iPSC-derived AT2 cell bioreactor culture in rat and human lung slices: NKX2.1 <sup>+</sup> SFTPC <sup>+</sup> cells NKX2.1 <sup>-</sup> T1 $\alpha$ <sup>+</sup> cells	Epithelial cell differentiation: DE specification Day 0–4: Activin A AFE specification Days 4–8: A-8301 AFE ventralization Day 8–12/15: BMP4, FGF2, CHIR99021 Endothelial cell differentiation: BMP-4, FGF2, VEGF for 6 days	– Ventralized AFE progenitors cultured onto decellularized human lung slices expressed both proximal airway and distal cell marker mRNA after 5 days of organotypic culture. – The vascular structure of decellularized whole rat lungs was successfully perfused with iPSC-derived ECs. iPSC-derived epithelial cells were seeded into the matrices and distributed heterogeneously, but were able to adhere, proliferate and differentiate.	[339]	
Human lung sections and whole rat lungs	Lung sections: NKX2.1 <sup>+</sup> cells ECAD <sup>+</sup> cells Ki67 <sup>+</sup> cells Whole lungs: CD31 <sup>+</sup> (endothelial-like) cells CCSP <sup>+</sup> (club-like) cells T1 $\alpha$ <sup>+</sup> cells	DE specification Days 0–2: Activin A Day 2–4 (cont.): Activin A, sodium butyrate AFE specification Day 5–6: dorsomorphin, SB431542 Day 6–7 (cont.): WWP-2, SB431542 AFE ventralization Day 7–15: FGF2, KGF, CHIR99021, BMP4 Distal lung specification: Day 15–24: FGF10, KGF, CHIR99021, EGF, RA Day 25 forward: FGF10, KGF, EGF, RA, dexamethasone, butyryl cGMP, IBMX Proximal airway specification: Day 15–32: KGF, BMP7, IWR-1, high RA, dexamethasone, butyryl cGMP, IBMX	– iPSC-derived lung cells are able to colonize rat and human lung decellularized ECM, proliferate, and express both proximal and distal epithelial markers. However, this expression is not site-specific. – Rat microvascular ECs perfused through the vasculature of decellularized whole rat lungs adhere to the ECM and colonize these structures, maintaining endothelial cell marker expression.	[340]	
	In whole rat lungs: FOXJ1 <sup>+</sup> cells CCSP <sup>+</sup> cells SFTPC <sup>+</sup> cells FOXJ1 <sup>+</sup> cells CCSP <sup>+</sup> cells P63 <sup>+</sup> cells SFTPC <sup>+</sup> /SFTPB <sup>+</sup> cells CD31 <sup>+</sup> /eNOS <sup>+</sup> (endothelial) cells (not iPSC-derived)				

Abbreviations: 8-Br-cAMP, 8-bromo-cyclic adenosine monophosphate; ALI, air-liquid interface; ATI, alveolar epithelial cell type I; AT2, alveolar epithelial cell type II; AFE, anterior ventral endoderm; ATRA, all-*trans* retinoic acid; BMP, bone morphogenetic protein; CCSP, Clara cell secretory protein; CD, cluster of differentiation; cGMP, cyclic guanosine monophosphate; DAPT, N-[1-(3-(5-difluorophenylacetyl)-L-alanyl]-S-phenylglycine *t*-butyl ester; DE, definitive endoderm; EGF, epithelial growth factor; eNOS, endothelial nitric oxide synthase; FBS, fetal bovine serum; FGF, fibroblast growth factor; IBMX, 3-isobutyl-1-methylxanthine; KGF, keratinocyte growth factor; RA, retinoic acid; SAC, smoothed agonist; VEGF, vascular endothelial growth factor; IPF, idiopathic pulmonary fibrosis; ECM: Extracellular matrix.

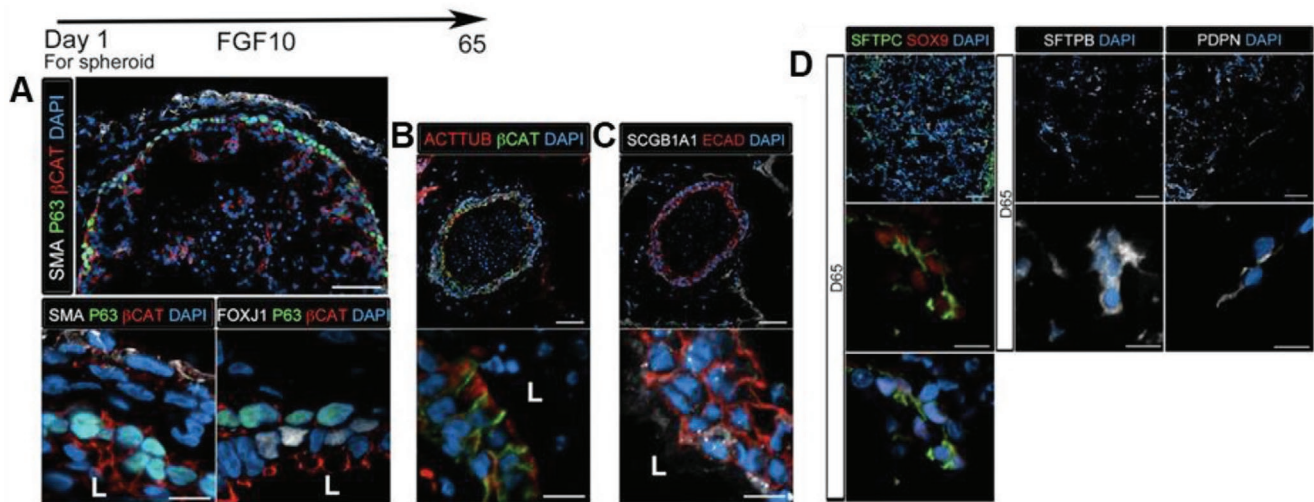


**Figure 11.** Generation of lung organoids from human pluripotent stem cells (hPSCs). A–D) Human lung organoids express proximal and distal lung markers. A) D65 human lung organoids displayed proximal epithelial ( $\beta$ CAT<sup>+</sup>) structures in which P63<sup>+</sup> and FOXJ1<sup>+</sup> cells were surrounded by smooth muscle actin positive (SMA<sup>+</sup>) mesenchymal tissue. Scale bars: 50  $\mu$ m (top) and 10  $\mu$ m (bottom). B,C) Proximal-airway-like epithelium also stained positive for ciliated cell marker ACTTUB and club cell marker SCGB1A1. DAPI: 4',6-diamidino-2-phenylindole (DNA marker). Scale bars: 50  $\mu$ m (top) and 10  $\mu$ m (bottom). D) Human lung organoids contained SFTPC<sup>+</sup>/SFTPB<sup>+</sup> (AT2 markers) and PDPN<sup>+</sup> (AT1 marker) cells. Adapted with permission.<sup>[79]</sup> Copyright 2015, eLife Sciences Publications Ltd.

mesodermal and endodermal origins were present in these 3D structures, and transplantation into a mouse kidney capsule resulted in a cell differentiation and specialization pattern similar to the proximodistal specification that occurs during lung branching morphogenesis. As such, both proximal airway (mucus-producing cells, multi-ciliated and neuroendocrine cells) and alveolar (AT1-like and AT2-like) cells, surrounded by a supporting mesenchymal tissue, were present in the explants after growth in an *in vivo* environment. Conversely, following *in vitro* culture, organoids were distinctively biased toward a distal fate, displaying mainly AT2-like cells with lamellar bodies and surfactant uptake function, but no mature proximal airway cell populations such as club cells, multi-ciliated cells, or basal cells.<sup>[190]</sup>

There is a tendency in the abovementioned studies for the attainment of organoid models that present immature differentiation profiles *in vitro*, of which full maturation can often only be achieved after *in vivo* engraftment and growth. While there are no definitive explanations for this phenomenon yet,<sup>[72]</sup> there are a few factors that may help explain this difficulty in generating organoid models with an accurate replication of adult lung cellular phenotypes and organization *in vitro*. Naturally, recapitulating the native pulmonary environment is highly challenging, due to the inherently complex architecture of the lung and ECM composition. Moreover, important lung cell types, such as immune cells, as well as the supporting pulmonary vasculature and smooth muscle cell network that enables gas and metabolite exchange are most frequently not represented in organoid models. It is, therefore, expected that the absence of these components in *in vitro* representations of the lung will affect the way cells self-assemble, differentiate, and function. Importantly, spheroids and organoids are usually spherical and possess an interior lumen filled with liquid, implying that the artificial lung epithelium is not exposed to air.<sup>[12,76,334–337]</sup> *In vivo*, however, epithelial cells of the respiratory tract stand in

direct interaction with air, representing a very important point for the future application of organoids in toxicological and pharmaceutical research, since toxicants or drugs reach the lung epithelium through air during breathing. A recent study by Lamers et al., in which a 2D ALI model consisting of lung cells grown from fetal lung bud organoids was presented for studying SARS-CoV-2 viral infection, shows the possibility to obtain the target lung cell types from organoids and adapting them afterwards to air-liquid conditions.<sup>[338]</sup>

These limitations may explain the consistent challenges in producing adult-like lung organoid models, unraveling new opportunities for the improvement and development of lung biomimetic models. Nevertheless, it should still be noted that the fetal-like state of the explored lung organoids provides excellent means for investigating both homeostatic mechanisms occurring during lung morphogenesis and developmental or early postnatal diseases.

#### 4.2.2. Decellularized ECM-Based Models and “Bioengineered Lungs”

Because current evidence seems to support that typical *in vitro* culture systems, even in the presence of a 3D hydrogel matrix such as Matrigel, may be insufficient to guide iPSC-derived cells and tissues toward full maturation, numerous reports have been dedicated to scaffold-based iPSC culture, with special attention to decellularized lung ECM. hiPSC-derived AT2 cells, for instance, have been cultured on rat and human decellularized lung sections and whole rat lungs.<sup>[306]</sup> AT2 cells diffusely repopulated the alveolar structures of the decellularized matrices, maintaining their proliferative capability and the expression of epithelial and AT2 markers such as NKX2.1 and SFTPC, respectively. Interestingly, spontaneous differentiation into an AT1 phenotype was also observed, represented by the expression of the AT1 marker

T1 $\alpha$  and loss of NKX2.1 expression, as well as changes from a cuboidal (AT2) to a squamous-like, flat morphology. Gilpin and co-workers opted to culture hiPSC-derived ECs and epithelial progenitors rather than differentiated epithelial cells in decellularized human lung slices and whole rat lungs.<sup>[339]</sup> In the latter model, hiPSC-derived ECs were first perfused through the pulmonary artery of the lungs, after which hiPSC-derived epithelial progenitors were delivered to the airway structure. Generally, cells could adhere and proliferate in both human and rat decellularized ECMs. CD31<sup>+</sup> ECs were observed in the vascular structure of the decellularized lungs, and proximal airway (FOXJ1, Clara cell secretory protein (CCSP)) and alveolar (Mucin-1, T1 $\alpha$ /PDPN) markers were equally identified (Table 2), indicating that these scaffold matrices were able to support cell growth and differentiation into relevant cell types. The use of both iPSC-derived endothelial and epithelial cells in this study should be specially highlighted, since a fundamental functional component of the lungs is precisely the vascular structure surrounding the airways and alveoli.

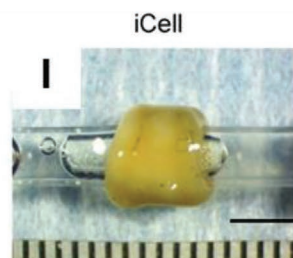
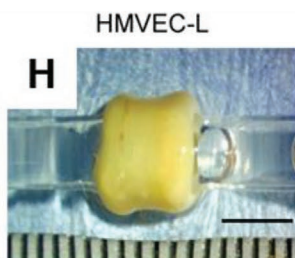
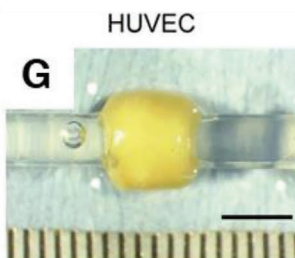
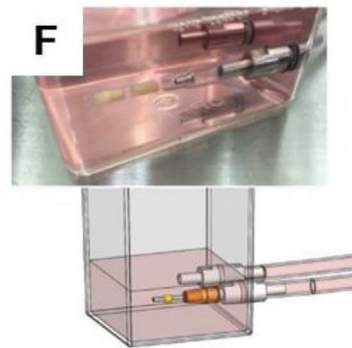
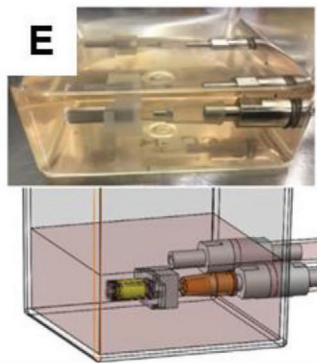
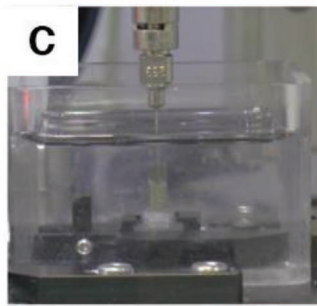
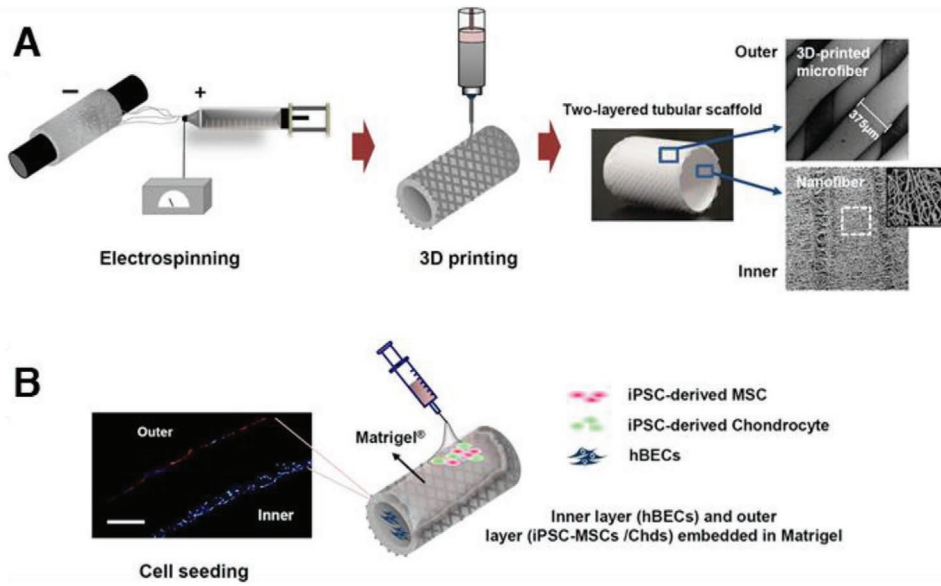
However, while the reports mentioned previously proved the potential of culturing iPSC-derived lung cells onto decellularized ECM, the cell populations obtained were still quite limited, representing only a small fraction of the cellular diversity characteristic of the human lung. To tackle this issue, Ghaedi et al. used hiPSCs to generate AT2 and proximal airway progenitor cells in vitro before transplantation into decellularized ECM.<sup>[340]</sup> hiPSC-derived epithelial cells were first cultured in decellularized human lung, diffusely repopulating both airway and alveolar structures in the matrix. The expression of several mature lung cell markers was subsequently detected, namely FOXJ1, CCSP, NKX2.1 and SFTPC. Nevertheless, such marker expression was not site-specific, that is, alveolar markers were observed in cells present in airway structures and vice versa. Similar results were observed after culturing hiPSC-derived epithelial cells in decellularized whole rat lungs, where the basal cell marker P63 was also expressed. These results suggest that the ECM itself is not sufficient to induce site-specific cell attachment, resulting in stochastic cell organization and mixed airway and alveolar cell populations throughout the lung matrix.<sup>[340]</sup>

Other work has instead been focused on the generation of a mature vascular structure in decellularized lung ECM, making use of the pluripotency of iPSCs to generate endothelial and perivascular (mesenchymal) cells.<sup>[341]</sup> Decellularized rat lungs were seeded with a mixture of both cell types, which formed an extensive vascular endothelial network in which perivascular spaces were occupied by perivascular cells. Apical-basolateral specification could be observed, generating a distinct endothelial lumen supported by mesenchymal cells, and a gradual improvement of the endothelial barrier function and a decrease in vascular resistance were registered with increasing culture time (up to 6 days). Notwithstanding, when this approach was upscaled to a decellularized human lung lobe, a very low EC coverage was observed after 6 days of culture, presumably due to the seeding of a much lower number of ECs (<10 %) than those present in native adult human lung.

Using decellularized lung ECM and iPSC-derived cells to achieve “bioengineered lungs” can, therefore, be challenging. There are significant difficulties in promoting site-specific cell homing and directed differentiation,<sup>[340]</sup> thus hindering the

generation of mature airway and alveolar structures. Likewise, obtaining mature vasculature is not straightforward, as it is difficult to attain homogeneous EC distribution throughout the scaffold and proper cell–cell and cell–ECM interactions needed for endothelial barrier formation and function.<sup>[341]</sup> As an alternative, it is possible to selectively remove the epithelial component of the pulmonary airways, which can then be reseeded with iPSC-derived epithelium, while preserving a viable vasculature and basement membrane.<sup>[342,343]</sup> While, to the best of our knowledge, the latter procedure has only been tested in a rodent lung model, such a chimeric approach could allow the maintenance of iPSC-derived epithelial cells in an in vivo-like environment and the occurrence of gas and nutrient exchange between alveolar and vascular compartments, thereby constituting a potentially valuable platform to study pulmonary physiology and disease. However, the ability to bioengineer whole lungs would have incredible applications not only in in vitro modelling, where, for instance, cell–ECM communication could be more accurately represented and investigated,<sup>[188]</sup> but especially in regenerative medicine, as the only solution for serious pulmonary damage and dysfunction is lung transplantation. The typical obstacles associated with organ transplantation, namely the shortage of donors, high rejection rates, and immunosuppressive regimens required,<sup>[128]</sup> could be overcome with the existence of tissue-engineered, iPSC-based (and, thus, patient-specific) lungs (Figure 7). In addition, if the decellularization process is completely effective, thereby removing all cells and antigenic elements, allogeneic and xenogeneic lung ECM (e.g., from porcine origin) could be used, improving the accessibility of suitable lung tissue.<sup>[90]</sup>

There is still a long way to go until fully functional bioengineered lung tissue is available: even if uniform and site-specific cell distribution are achieved, these pulmonary artificial units need to perform gas exchange efficiently after transplantation and maintain vascular patency and perfusion without the development of edema, thrombi or hemorrhages. In a pioneering study by Petersen and co-workers, decellularized rat lungs were recellularized with neonatal lung epithelial cells and microvascular ECs, resulting in location-specific expression of airway and alveolar markers and uniform distribution of the ECs throughout the construct.<sup>[100]</sup> Remarkably, after orthotopic transplantation in a rat model, the bioengineered lungs participated in gas exchange (implantation times between 45 and 120 min), thereby demonstrating some level of respiratory functionality. Promising results were also achieved by Gilpin et al., where decellularized rat lungs seeded with iPSC-derived endothelial and epithelial cells could be ventilated and perfused after in vivo transplantation.<sup>[339]</sup> Of note, permeation of red blood cells (RBCs) was observed in alveolar/airway structures in both studies, indicating that the endothelial barrier function was not completely established or the decellularization procedure may have compromised the lung structural integrity. A study by Ott et al. is equally noteworthy, in which decellularized rat lungs were seeded with fetal rat lung cells and human umbilical vein ECs (HUVECs) and subsequently transplanted orthotopically into a rat model.<sup>[344]</sup> The bioartificial lungs were successfully perfused and gas exchange was observed in vivo; such respiratory function was maintained even after extubation of the animals for 6 h after the operation. However, after



some time, pulmonary edema started to occur in the tissue-engineered constructs. Relevantly, a recent report has demonstrated that treatment with a small molecule cAMP analog (8-(*p*-chlorophenylthio)-2'-*O*-methyladenosine-3',5'-cAMP or 8CPT-2Me-cAMP) improves the barrier function of HUVECs and iPSC-derived ECs, and this effect was also observed after iPSC-EC culture in decellularized whole rat lungs, providing a potential solution for incomplete endothelial barrier formation or maturation.<sup>[345]</sup> As a final example, decellularized rat lungs co-seeded with HUVECs and MSCs were able to withstand perfusion for three days after orthotopic transplantation.<sup>[341]</sup> It should be taken into consideration that many of these results were obtained using primary cells or cell lines that are not, therefore, viable for clinical-grade, larger scale bioartificial lung manufacturing. Extensive studies focusing preferably on autologous and highly expandable cell sources, namely iPSCs, must be carried to make progress in this field toward clinical translation.

#### 4.2.3. Electrospinning and 3D Printing in iPSC-Based Lung Modeling

While several studies have focused on the application of electrospinning and 3D printing concomitantly with iPSC-based technology to other fields of regenerative medicine, such as cardiac repair and modeling,<sup>[346–348]</sup> blood-brain barrier modeling,<sup>[349]</sup> and neural tissue engineering,<sup>[350]</sup> there is a scarcity of reports that use such methods to generate lung biomimetics and study pulmonary physiology. Nevertheless, a few research groups have already described the use of iPSC culture on electrospun fibers and 3D-printed constructs in lung-related applications. Hoveizi and co-workers have proven that hiPSCs cultured on Matrigel-coated PLA/gelatin electrospun scaffolds are able to differentiate into FOXA2<sup>+</sup>/SOX17<sup>+</sup>/gooseoid (GSC)<sup>+</sup> DE progenitors upon treatment with activin A/Wnt3a or the small molecule inducer of DE 1 (IDE-1), although the differentiation efficiency is greater with the former.<sup>[351]</sup> DE is the precursor for several organs besides the lung, such as the intestine, liver, and pancreas, but the potential for further differentiation into any organ-specific cell type was not assessed. Electrospinning and 3D printing technology have also been used for the development of iPSC-based tracheal grafts. Tubular constructs with an inner layer of electrospun PCL fibers seeded with primary human bronchial epithelial cells and a 3D-printed PCL outer layer seeded with iPSC-derived MSCs or chondrocytes (in Matrigel) (**Figure 12A,B**) were cultured *in vitro* using a bioreactor system and subsequently implanted in a rabbit tracheal defect model.<sup>[352]</sup> Importantly, cells adhered to both scaffold layers and contributed to tracheal repair *in vivo*.

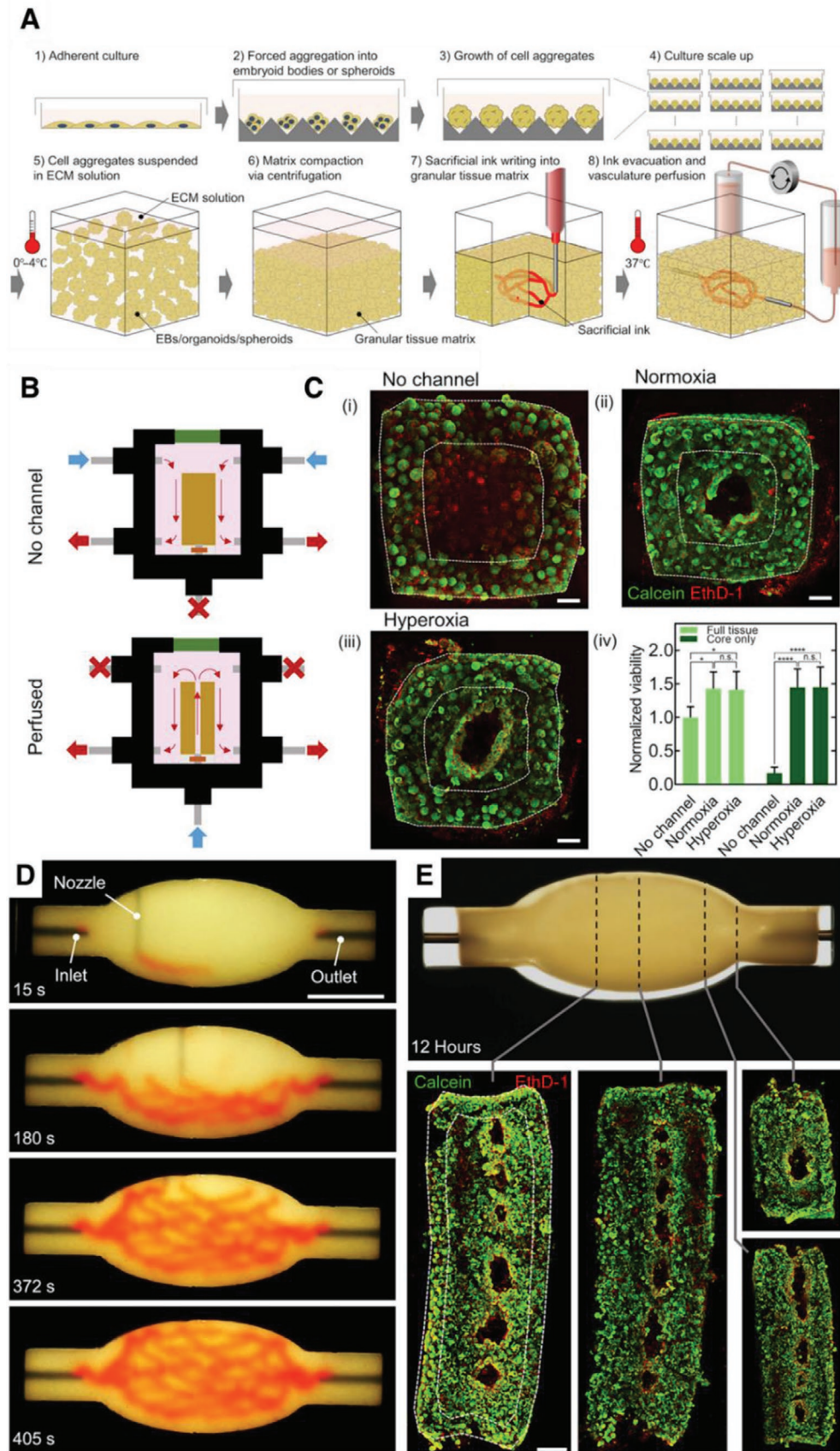
Furthermore, 3D bioprinting (3D printing of living cells) can be used for the fabrication of scaffold-free, cell-based constructs. Still in the field of tracheal restoration, scaffold-free tubular cell constructs, built from HUVEC-, human lung microvascular endothelial cell-, or hiPSC-derived endothelial cell spheroids, were developed using bioprinting (**Figure 12C–I**).<sup>[353]</sup>

Intriguingly, iPSC-derived endothelial cells generated ECM with lower contents of collagen and GAGs than that produced by HUVECs and microvascular endothelial cells, highlighting the difficulty in achieving fully functional and differentiated cells from PSCs. Notably, it was not possible to find any reports employing electrospinning/3D printing and iPSCs to model airway and distal lung structures, perhaps illustrating how hard artificial reproductions of the lung are to achieve.

Vascular tissue engineering is a field of expertise in which these manufacturing methods have been extensively used, and this knowledge might prove valuable for the construction of vascularized lung scaffolds or, for instance, the development of models of the alveolar barrier, in which endothelial and epithelial cells are in close communication. Electrospun fibers constituted by PCL-gelatin blends were shown to promote iPSC-derived EC attachment, proliferation, and maintenance of the endothelial phenotype. Moreover, hypoxia-induced gene expression of angiogenic and remodeling factors including placental growth factor, epidermal growth factor (EGF) and VEGF was greater in cells seeded onto PCL-gelatin blends than in those cultured on traditional tissue culture plastic.<sup>[354]</sup>

As tissue engineering manufacturing technologies advance, incredible progress is being made toward whole artificial organs. From the collection of human and porcine omental tissue, Noor et al. isolated and reprogrammed the cellular components to generate iPSCs and used the remaining tissue to produce decellularized ECM hydrogels, thereby assembling these components into patient-specific, personalized cardiac patches.<sup>[355]</sup> By mixing iPSC-derived cardiomyocytes (CMs) and ECs with ECM and gelatin hydrogels, respectively, two distinct bioinks were formed and subsequently used for 3D bioprinting of biomimetic cardiac tissue and blood vessels. Ingeniously, gelatin worked as a sacrificial ink, which could be removed after the fabrication of the 3D constructs and result in open vascular-like channels lined by ECs and capable of perfusion. Afterward, using both iPSC-derived CMs and ECs in ECM hydrogel as bioinks, free-form 3D bioprinting was performed into a fluid medium composed of alginate microbeads capable of supporting the printed structures and undergoing a gentle removal procedure after printing. Triaxial and perfusable lumens were successfully obtained using this innovative technique; impressively, small scaled, cellularized whole heart models with major blood vessels were also 3D printed in this work.<sup>[355]</sup>

**Figure 12.** Biofabricated tracheal grafts using electrospinning and 3D (bio)printing. A) Schematic representation of the biofabrication process of electrospun/3D printed hybrid scaffolds. An inner layer of electrospun PCL fibers is then used as substrate for 3D printing. Scanning electron microscopy (SEM) micrographs prove that the two layers are composed of fibers with distinct dimensions and micro/nanoarchitecture. B) Hybrid scaffolds were seeded with human bronchial epithelial cells on the inner layer and iPSC-derived MSCs or chondrocytes embedded in Matrigel on the outer layer. Fluorescence microscopy confirmed the presence of chondrocytes (in red, PKH-26 staining) and bronchial epithelial cells (in blue, DAPI) in the respective layers. Scale bar: 200  $\mu$ m. Adapted with permission<sup>[352]</sup> Copyright 2020, Nature Research. C–F) 3D bioprinting process of HUVEC, human lung microvascular endothelial cell (HLMEC), and iPSC-derived endothelial cell spheroid-based tracheal-like tubular structures. C) Spheroids were first printed onto a needle array, D,E) followed by growth, maturation and fusion on a bioreactor, after which the F) 3D structures were transferred to plastic catheters and maintained in culture. G–I) Macroscopic view of the tracheal-like structures bioprinted from HUVEC, HLMEC, and iPSC-derived endothelial cell (iCell) spheroids. Adapted with permission.<sup>[353]</sup> Copyright 2020, Elsevier Ltd.



In turn, Lewis' group also used free form/embedded 3D printing to print sacrificial gelatin channels within compacted matrices of embryoid bodies and iPSC-derived organoids, termed "organ-building blocks" (OBB), developing a novel technology named sacrificial writing into functional tissue (SWIFT) (Figure 13A).<sup>[356]</sup> The self-healing and viscoelastic properties of the OBB allowed the 3D printing process to occur with no structural defects, and cell viability and organoid integrity were preserved during SWIFT printing. The removal of the gelatin template generates a network of vascular-like channels (resolution of 400  $\mu\text{m}$ ) that can be efficiently perfused, contributing for a more distributed culture media supply throughout the OBB matrix and avoiding the formation of necrotic cores observed in non-perfused models (Figure 13B–E).<sup>[356]</sup> Importantly, using this SWIFT methodology with lung organoids or multicellular spheroids will, in theory, allow for the development of perfusable pulmonary 3D models that may be a valuable asset for in vitro pathophysiological and toxicological studies.

Recently, in a remarkable study by Grigoryan et al., "breathing" poly(ethylene glycol) diacrylate hydrogel-based alveoli compartments enveloped by a perfusable vascular-like network were achieved via stereolithography 3D printing (Figure 14).<sup>[357]</sup> The alveoli compartment of these bioinspired constructs visibly expanded and deflated upon cyclic ventilation, mimicking the behavior of pulmonary alveoli during respiration, and could be seeded with human alveolar epithelial (A549) cells and lung fibroblasts (IMR-90). In addition, perfusion of deoxygenated RBCs through the tubular network during this cyclic ventilation process revealed that gas exchange occurred between the vascular and alveolar mimetic compartments, observed by monitoring oxygen pressure and saturation in RBCs exiting through the outlet channel. Further development of these devices, for example, through seeding with iPSC-derived human endothelial and alveolar cells may generate functional and more physiological representations of the pulmonary respiratory units.

#### 4.3. iPSC-Based Lung Models of Disease

In addition to the application of iPSC-based lung models as test systems for toxicological studies, specific disease models derived from iPSCs can also be developed and used for basic research or pharmacological screening in drug development. Since the publication of the first report in which lung disease patient-derived iPSCs were generated, over a decade ago,<sup>[274]</sup> an increasing number of studies has been focused on the idea of using iPSC technology to develop personalized lung disease models and therapeutic regimes. Relevant progress made in this field is explored and discussed in the next sections.

##### 4.3.1. Pulmonary Fibrotic Diseases

*Idiopathic Pulmonary Fibrosis:* Pulmonary fibrosis typically originates from an exacerbated inflammatory environment that promotes a dysregulated fibrotic response and results in aberrant tissue remodeling and ECM production, culminating in tissue scarring, loss of physiological function, and ultimately respiratory failure.<sup>[358,359]</sup> Fibrotic responses are a common feature of ILDs, a group of parenchymal lung diseases that can arise from exposure to toxicants or allergens, autoimmune diseases, or due to an unknown cause, which is the case of idiopathic interstitial pneumonias. Idiopathic pulmonary fibrosis (IPF) is the most common form of ILD and it represents a particularly aggressive type of idiopathic interstitial pneumonia, characterized by a chronic, progressive fibrotic nature that continuously destroys the pulmonary tissue, compromises lung function, and often leads to pulmonary failure and death.<sup>[360]</sup> IPF affects mainly the older population and is associated with a very poor prognosis, having a median survival of 3.8 years after diagnosis in patients over 65 years of age.<sup>[358,361]</sup> Even though considerable progress has been made in the last few years regarding clinical management of IPF, there is an inherent heterogeneity among different patients in terms of disease manifestation, progression, and therapy response, implying a need for personalized diagnosis and treatment.<sup>[360]</sup>

To this end, patient-derived iPSC-based platforms may be groundbreaking tools to uncover individual features of each IPF case and determine the best therapeutic course to be followed. Accordingly, a few studies have already been directed at fulfilling this goal. In a recent report, a 2D ALI culture method was developed for the culture and differentiation of iPSCs into AT2 cells (Table 2), which were then treated with a profibrotic cytokine cocktail that aimed to mimic the biochemical microenvironment observed in IPF-afflicted lungs.<sup>[362]</sup> This treatment was able to recapitulate some modifications in epithelial gene and protein expression that are also observed in IPF cases, causing an up-regulation of markers associated with ECM remodeling and organization. Interestingly, administration of the cytokine cocktail to iPSC-derived AT2-like cells also increased the expression of proximal airway epithelial genes, such as *FOXJ1*, *MUC5B*, *SCGB1A1*, and *KRT5*, reflecting a particular characteristic observed in IPF-affected alveoli termed "bronchiolization" (loss of proximodistal specification illustrated by the emergence of proximal airway cell markers within the alveoli). This phenomenon was accompanied by a decreased expression of the AT2-specific gene *SFTPC*.<sup>[362]</sup>

A different approach was based on the culture of iPSC-derived mesenchymal-like cells onto stiff polyacrylamide hydrogels, with the objective of emulating the mechanical behavior of fibrotic tissues and, therefore, guide the seeded cells toward

**Figure 13.** Embedded 3D printing (SWIFT) for the generation of biomimetic vascularized cardiac tissue. A) Schematic step-by-step representation of the SWIFT process. B,C) Comparison of tissue viability in matrices with no interior channels (C-i) and perfused OBB matrices following SWIFT printing and culture in both normoxic (21% O<sub>2</sub>; C-ii) and hyperoxic (95 % O<sub>2</sub>; C-iii) medium using live/dead (green/red) fluorescent staining, together with the normalized cell viability values (C-iv). Scale bars: 500  $\mu\text{m}$ . D) Overview of the SWIFT free form 3D printing process originating a network of vascular-like channels embedded into a matrix of embryoid bodies (EBs) connected to inlet and outlet tubes. Scale bar: 10 mm. E) Cross-sections of a perfused OBB matrix stained for live (green) and dead (red) cells 12 h after SWIFT printing. The dashed lines illustrate the typical viability depth observed in controls with no interiorly perfused channels (C-i). Scale bar: 1 mm. Adapted with permission.<sup>[356]</sup> Copyright 2019, American Association for the Advancement of Science.

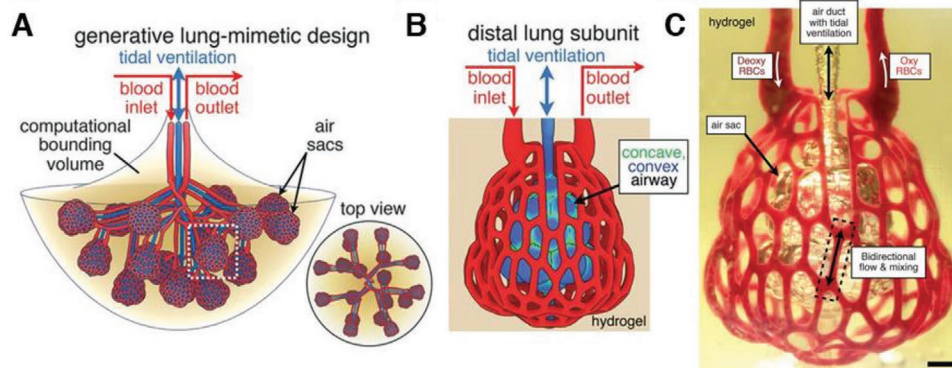


**Figure 14.** 3D-printed bioinspired vascularized alveolar models. A) Schematic representation of the idealized lung biomimetic design, capable of undergoing tidal ventilation and composed of B) several artificial alveolar units surrounded by a functional vasculature. C) Photograph of a 3D-printed hydrogel-based alveolar unit undergoing tidal  $O_2$  ventilation and RBC perfusion through the adjacent tubular network. Scale bar: 1 mm. Adapted with permission.<sup>[357]</sup> Copyright 2019, American Association for the Advancement of Science.

a diseased phenotype.<sup>[363]</sup> Indeed, the obtained mesenchymal-like cells demonstrated a high proliferative capacity and the expression of fibrotic markers, such as  $\alpha$ -SMA, type I collagen, and TGF- $\beta$ . Moreover, rather than growing in a monolayer as primary lung fibroblasts, these cells aggregated into scar-like phenotypes on the hydrogel. Importantly, such activated fibroblastic phenotypes closely resembled those observed in several fibrotic organs regarding gene and protein expression profiles, not limited to the lung, but encompassing liver and kidney tissues. The potential applicability of this 2D model in high-throughput toxicological studies was readily validated, with the identification of a novel small molecule compound (AA5) that demonstrated strong anti-fibrotic action in vitro, ex vivo (using human IPF lung slices) and, subsequently, in murine models of fibrotic ocular and lung disease.<sup>[363]</sup>

Likewise, 3D models of IPF have already been described. Wilkinson and co-workers have generated a 3D self-assembling alveolar model of IPF utilizing collagen-coated alginate beads as templates for cell attachment, growth, and organization into organoids.<sup>[364]</sup> Using a rotating bioreactor apparatus, both fetal human lung fibroblasts and iPSC-derived mesenchymal-like cells were able to adhere to the alginate beads and self-assemble into organoids. Expression of fibrotic markers in fetal human lung fibroblast organoids, namely  $\alpha$ -SMA and type I collagen, was successfully induced by exogenous administration of TGF- $\beta$ 1, and iPSC-derived mesenchymal cells exhibited similar behavior. Interestingly, the introduction of other cell types, including pulmonary fibroblasts, HUVECs, and small airway epithelial cells, to the system resulted in their self-organization into alveolar-like structures, with epithelial cells surrounding the surface of alginate microbeads, mesenchymal cells occupying the interstitial space between adjacent beads, and endothelial cells sparsely distributed without, however, spontaneous formation of vascular-like structures.<sup>[364]</sup>

**Cystic Fibrosis:** CF, an autosomal recessive disorder, is the most frequent monogenetic disease amid the Caucasian population and results from mutations in the gene that codes for CFTR, a chloride and bicarbonate ion transporter, consequently leading to defective CFTR protein production.<sup>[365]</sup> In the lung, CF is associated with faulty mucociliary clearance, repeated infection and exacerbated inflammation, and ultimately,

respiratory failure.<sup>[9,365]</sup> Even though CF affects the epithelial secretory balance of other organs, such as the intestine, liver, pancreas, and gallbladder, its manifestation in the lungs is the principal factor driving high morbidity and mortality rates.<sup>[366]</sup> There is a vast heterogeneity in the disease phenotype manifested among patients carrying similar mutant *CFTR* variants, revealing an ambiguous genotype-phenotype relationship that can be influenced by modifier genes and environmental factors.<sup>[365,367]</sup>

The amenability for genetic manipulation of iPSCs allows, in principle, to isolate and reprogram somatic cells from CF patients back to pluripotency, analyze their respective genotype and identify individual *CFTR* mutant variants, and, applying advanced gene editing technology, correct such mutations, recovering CFTR protein function. The most frequent mutations observed in CF correspond to a deletion of three base pairs (bp) that code for a phenylalanine amino acid in the position 508 ( $\Delta$ F508) of the *CFTR* gene, but numerous mutant alleles carrying distinct missense or nonsense mutations have been described.<sup>[9,365]</sup> Several reports have focused on the development of iPSC-based in vitro models to study CF pathogenesis and evaluate the potential of gene therapy in the treatment of CF. In an earlier study, Mou et al. successfully generated NKX2.1<sup>+</sup> lung progenitors from several CF iPSC lines, one of which was compound heterozygous for *CFTR* mutant alleles  $\Delta$ F508 and G551D ( $\Delta$ F508/G551D) and the remaining lines homozygous for the  $\Delta$ F508 mutation ( $\Delta$ F508/ $\Delta$ F508).<sup>[368]</sup> Later, in 2015, two different research groups reported the generation of gene-corrected CF patient-derived iPSCs using both zinc-finger nuclease<sup>[369]</sup> and CRISPR-Cas9<sup>[370]</sup> gene editing technologies, resulting in the recovery of normal CFTR expression and ion transport function.

More recently, McCauley and colleagues have generated epithelial airway organoids from  $\Delta$ F508/ $\Delta$ F508 patient-derived iPSCs, subsequently using CRISPR-Cas9 technology to correct the *CFTR* mutations and rescue protein function (Figure 15A).<sup>[301]</sup> Expression of functional CFTR channels in gene-corrected iPSC-derived lung epithelial cells was shown by organoid swelling after treatment with forskolin (Figure 15B,C), a cAMP-dependent CFTR agonist, similarly to wild-type *CFTR*-expressing organoids and contrary to those expressing mutated and dysfunctional *CFTR* genes.<sup>[301]</sup>

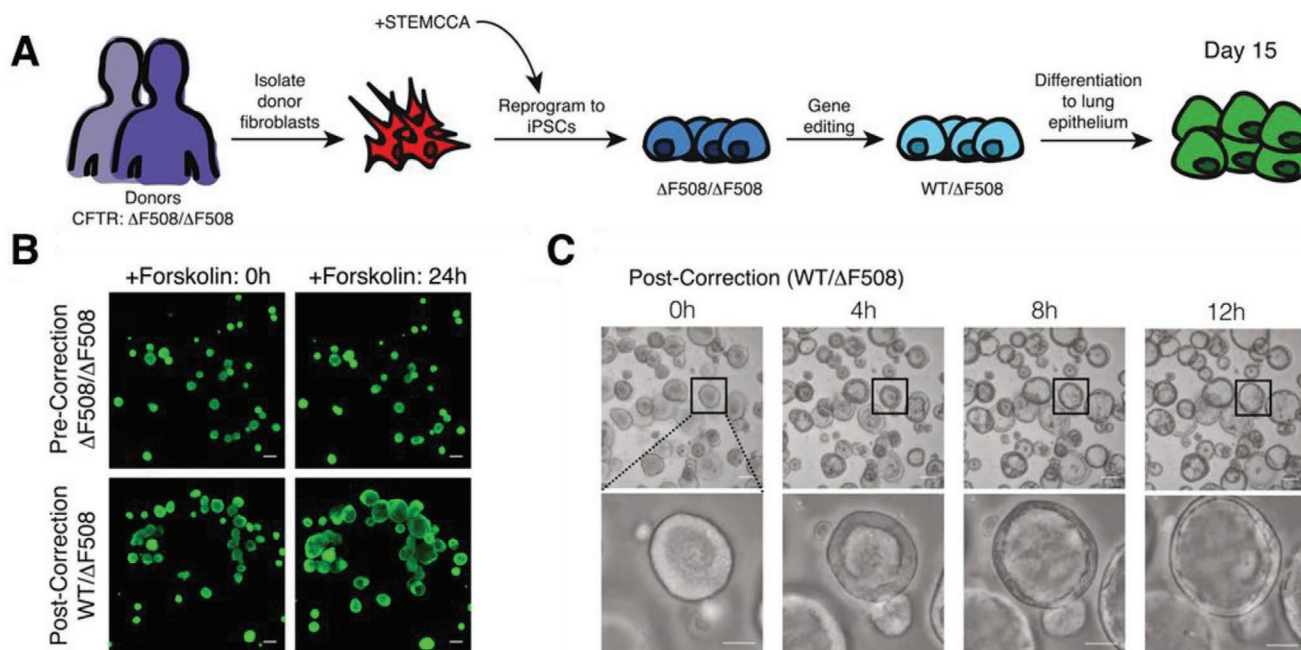


**Figure 15.** Generation of CF patient-derived organoids and CFTR function recovery in gene-corrected cells. A) Protocol overview for the generation of CF patient-derived iPSCs and differentiation into lung epithelium. B) Recovery of forskolin-induced iPSC-derived organoid swelling after *CFTR* gene correction (WT/ΔF508), compared with non-corrected organoids (ΔF508/ΔF508). Living cells were stained with calcein green. Scale bars: 100 μm. C) Time-lapse imaging of gene-corrected organoids demonstrates increasing swelling behavior over 24 h of forskolin treatment. Adapted with permission.<sup>[301]</sup> Copyright 2017, Elsevier Inc.

Importantly, CF patient-derived airway organoids are capable of recapitulating in vivo disease features such as thicker mucus deposition and dysfunctional CFTR activity.<sup>[76,301]</sup> The versatility of iPSCs in generating CF models was further demonstrated by Ruan et al., who made use of CRISPR-Cas9 tools to introduce three different *CFTR* mutant variants (ΔF508, G551D, and G542X, a nonsense mutation) into the genome of wild-type iPSCs.<sup>[371]</sup> In addition, a CF patient-derived iPSC cell line carrying a N1303K *CFTR* mutation has also been recently developed.<sup>[372]</sup> Such a wide portfolio of in vitro iPSC-based CF disease models has an immeasurable potential to investigate genotype-phenotype relationships and disease progression under different *CFTR* mutations, test for individual drug efficacy, and assist gene therapy and precision medicine research.

**Hermansky–Pudlak Syndrome:** Hermansky–Pudlak Syndrome (HPS) is a rare autosomal recessive genetic disease, with a global incidence of 1–9 cases per million individuals that may arise from several disease-causing variants in genes involved in the biogenesis and trafficking of lysosome-related organelles. This hereditary condition is often linked with abnormal pigmentation, resulting in oculocutaneous albinism, and bleeding diathesis. Genetic variants associated with 4 of the 10 HPS types (HPS-1, -2, -4, and -10) cause the manifestation of ILD or pulmonary fibrosis, displaying certain pathological features similar to those observed in IPF.<sup>[373,374]</sup>

Given the genetic nature of this disorder, patient iPSC-derived models may also prove valuable to investigate different disease-causing mechanisms and characterize and replicate the pathophysiology of HPS in vitro. A HPS-1 iPSC line has already been established from the skin fibroblasts of a female patient carrying a mutant variant of *HPS1*, with a homozygous

duplication of 16 bp in exon 15 of this gene.<sup>[375]</sup> In a recent study, HPS-2 patient-derived iPSCs carrying compound heterozygous mutations in exons 15 and 18 of the gene *AP3B1* were genetically corrected using CRISPR-Cas9 technology and subsequently differentiated into AT2 cells to form alveolar organoids.<sup>[195]</sup> While diseased organoids, containing HPS2-iPSCs with no gene editing interventions, demonstrated alterations in AT2 cell physiology, with impaired surfactant secretion and abnormal lamellar body dimensions and cellular distribution, gene-corrected iPSC-derived alveolar organoids had restored AT2 cell function, similar to that of control (non-mutated) iPSC-derived organoids. Patient-derived iPSCs carrying distinct genetic alterations that culminate in HPS can, therefore, be used to model this disease and search for therapeutic solutions.

#### 4.3.2. Infectious Diseases

The use of iPSC-based models to study human lung infectious diseases has been mainly focused on pathogenic agents of viral nature. Two studies from the same research group have identified rare genetic variants underlying severe influenza cases in children, shedding light on the mechanisms leading to such aggravated responses to influenza. In the first report, whole-exome sequencing was performed in a 7-year-old child, whom, following H1N1 (influenza A) infection, suffered ARDS. This genetic analysis revealed the presence of compound heterozygous missense (F410V) and nonsense (Q421X) mutations in the gene coding for interferon regulatory factor 7 (*IRF7*).<sup>[376]</sup> The generation of patient-derived iPSCs carrying these variants and subsequent differentiation into pulmonary epithelial

cells demonstrated that cell-intrinsic innate immune responses related to type I and III interferons (IFNs) were severely impaired, which may explain the patient's ARDS. In the following study, three unrelated children suffering from ARDS caused by influenza A infection were identified as heterozygous carriers of rare missense mutations (P554S and P680L) in the gene coding for Toll-like receptor 3 (*TLR3*), which were shown to cause autosomal dominant *TLR3* dysfunction.<sup>[377]</sup> *TLR3* is a transmembrane receptor involved in the defense against viral pathogens due to its ability to recognize double-stranded RNA, which is commonly originated during viral replication.<sup>[378]</sup> Once again, the generation of patient iPSC-derived *TLR3*-deficient pulmonary epithelial cells demonstrated susceptibility to influenza A viral infection, which was prevented by pre-treatment with exogenous IFN $\alpha$ 2b (type I) and IFN- $\lambda$  (type III).<sup>[377]</sup> As such, both these genetic studies suggest that recombinant IFN-based treatment strategies may help manage severe respiratory disruption caused by influenza A viral infections in children.

In light of the on-going COVID-19 global pandemic, hiPSC-based models have also been developed to explore SARS-CoV-2 infection processes and possible therapeutic routes. Surendran and co-workers (2020) reported the generation of proximal and distal epithelial cells from hiPSCs in 2D monolayers, as well as 2D ALI epithelial airway models containing multi-ciliated and basal cells. However, upon SARS-CoV-2 infection, iPSC-derived cells demonstrated lower infectivity comparing to the Vero and Vero E6 kidney epithelial cell lines, therefore needing further optimization toward a more representative model.<sup>[379]</sup> In turn, Huang et al.<sup>[197]</sup> (2020) differentiated hiPSCs into AT2-like cells (iAT2s), achieving simplified 2D ALI alveolar models to study SARS-CoV-2 cellular entry and replication. In these models, time-dependent SARS-CoV-2 infection and pathology were observed, resulting in vast transcriptional alterations that illustrated a loss of the mature AT2 cell program (that is, diminished expression of mature AT2 markers such as *SFTPC*, *SFTPD*, and *SFTPA1*) and upregulation of the pro-inflammatory NF- $\kappa$ B signaling pathway. Furthermore, this iAT2 cell model was responsive to treatment with two drugs (camostat mesylate, an inhibitor of the pulmonary tissue protease TMPRSS2 (involved in SARS-CoV-2 pathological progression), and remdesivir, a broad-spectrum antiviral drug), resulting in decreased detectable viral transcripts.<sup>[197]</sup> In a parallel report, this hiPSC-based model was used to detect proteomic and phosphoproteomic changes in iAT2 cells upon SARS-CoV-2 infection, helping uncover the pathological mechanisms underlying COVID-19, and to test for new potential antiviral therapies.<sup>[380]</sup> Hence, such human cell-based models of infectious diseases may prove highly valuable for initial research on unknown pathogenic agents or new viral strains and the respective pathogenic programs and drug susceptibilities.

hiPSC-derived lung and intestinal organoids have also been recently developed to study the innate immune response of these mucosal organs to pathogenic threats.<sup>[381]</sup> Expression of PRRs, such as *TLR2* and *TLR4*, was observed in lung organoids, and activation of host defense mechanisms in response to purified microbial ligands or mimetics representing bacteria, fungi, and viruses (including lipopolysaccharide (LPS), poly(I:C), CpG, among others) was detected. Furthermore, it was possible to establish co-cultures of both lung and intestinal organoids with

peripheral blood monocytes, therefore constituting interesting models for the investigation of mucosal tissue infection.<sup>[381]</sup>

#### 4.3.3. Lung Cancer

Lung cancer is the global leading cause of cancer-related death.<sup>[2]</sup> The development of lung malignant tumors is highly dependent on environmental exposure to harmful elements, such as tobacco smoke and pollutants, albeit intrinsic individual characteristics, such as genetic predisposition, may also play an important part in this process.<sup>[382]</sup> Clinically, lung cancer can be divided in two categories: small cell and non-small cell lung cancer (SCLC and NSCLC, respectively). NSCLC corresponds to 85% of all lung cancers, of which lung adenocarcinoma and squamous cell carcinoma are two of the most frequent examples,<sup>[383]</sup> whereas the remaining 15% of cases are linked to SCLC, a neuroendocrine carcinoma with extremely poor prognosis and survival rates.<sup>[384]</sup> Even though considerable progress in the management of lung cancer has been achieved in the last couple of decades, responding to the current demand for specialized, targeted therapies will require, on one hand, access to accurately predictive tools for precise evaluation of the therapeutic effectiveness of new agents and, on the other hand, understanding the mechanisms leading to drug resistance and loss of responsiveness.<sup>[383]</sup> Accordingly, iPSC-based models may prove useful in this context.

Dost et al. reported the use of iPSC-derived organoids to model early-stage lung adenocarcinoma driven by the expression of an oncogenic *KRAS* mutant (G12D).<sup>[385]</sup> Transcriptomic and proteomic analysis revealed that iPSC-derived *KRAS*-mutant AT2 cells displayed profound alterations in gene and protein expression, unravelling a loss of differentiated AT2 phenotype and the emergence of developmental marker expression. In addition, these changes were reflected in murine *KRAS*-mutant cell-derived organoids, primary human early-stage lung adenocarcinoma AT2 cells, and in vivo, using a genetically manipulated mouse model of the disease, implying that iPSC-derived organoids can be used as faithful representations of these malignancies.

As a further example, 3D hydrogel-based models of lymphangioliomyomatosis (LAM), a rare neoplastic and invasive lung disorder, were created for disease modeling and high-throughput screening.<sup>[386]</sup> The biomimetic hydrogel was mainly composed of hyaluronic acid and methylcellulose, displaying several chemical crosslinking peptide motifs, suitable for protease-specific degradation, and physical polymer chain attachments driven by weak (e.g., hydrophobic) interactions, which could be easily disrupted and remodeled by protease-independent mechanisms. This hybrid approach was generated to assess both protease-dependent and protease-independent cell migration and invasion processes, both thought to be involved in LAM and metastatic cancers. LAM patient-derived iPSCs differentiated into SMCs (LAM-SMCs) and cultured on the 3D hydrogels displayed higher migration capability than SMCs derived from healthy individuals, showing that this model can differentiate the behavior of healthy versus malignant cells.<sup>[386]</sup> Moreover, the authors demonstrated the potential of this 3D construct in modeling several types of lung cancer, making use of primary cells or cell lines of both NSCLC and SCLC and proving these also

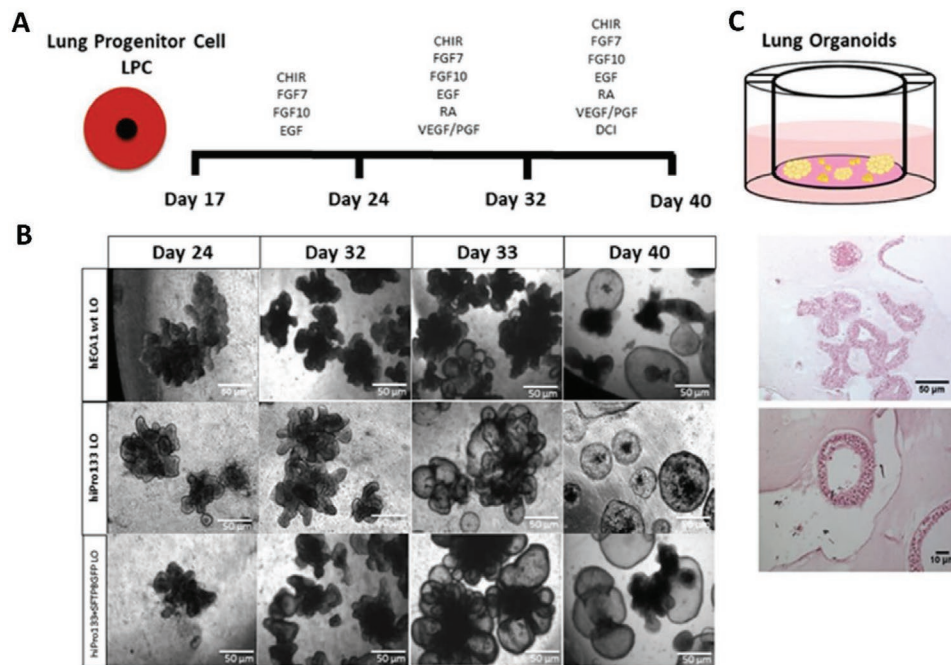


**Figure 16.** Leibel et al. differentiated iPSC-derived lung progenitor cells to 3D lung organoids. A) To form organoids, lung progenitor cells (LPC) were transferred into Matrigel-containing Transwell inserts and underwent directed differentiation. B) Phase contrast images of 3D lung organoids (based on different iPSCs) at different time points during the differentiation process. Scale bars: 50  $\mu$ m. C) Hematoxylin/eosin staining of the organoids at day 40. Scale bar: 50  $\mu$ m. Adapted with permission.<sup>[397]</sup> Copyright 2019, Springer Nature.

behave differently in the established 3D environment, depending on the tumor of origin. The relevance of iPSCs in the field of lung cancer modeling is further accentuated by the common characteristics between these cells and cancer cells, namely the virtually never-ending proliferative capacity, the expression of oncogenic markers, such as Oct-4 and c-Myc, and similar metabolic profiles.<sup>[387,388]</sup> Importantly, the ability for genetic manipulation and editing of iPSCs could also enable the activation or inactivation of oncogenes or tumor suppressing genes and assess the effects of these modifications in tumor development.<sup>[388]</sup>

#### 4.3.4. Others

iPSC technology has equally demonstrated potential for in vitro modeling and therapeutic research of pulmonary arterial hypertension (PAH), a rare chronic and progressive disease in which pulmonary vascular resistance and arterial pressure are increased, eventually resulting in right ventricular failure and, in the absence of proper treatment, death.<sup>[389]</sup> Heterozygous mutations in the gene *BMPR2* (BMP receptor 2) are frequently observed particularly in familial cases of PAH, although this has also been reported in idiopathic PAH. However, the penetrance of these mutations is only about 20%, implying that only this fraction of individuals carrying mutant variants of *BMPR2* will develop symptoms.<sup>[390]</sup> iPSC-derived ECs from familial PAH patients and unaffected individuals carrying *BMPR2* mutations showed distinct functional characteristics, with the former showing decreased survival and migration rates and impaired angiogenic potential, further illustrating how patient-derived

iPSCs are able to preserve specific features from the donor individuals after differentiation.<sup>[391]</sup> These findings are supported by another study from the same research group, in which familial and idiopathic PAH patient-derived iPSC-ECs were compared to primary pulmonary arterial ECs from the same individuals.<sup>[392]</sup> Importantly, this technology also helped uncover compensatory mechanisms in unaffected mutation carriers that protect against disease manifestation, thereby exposing potential therapeutic avenues for PAH.<sup>[391]</sup> Conversely, fibroblasts obtained from non-COPD donor-derived and COPD patient-derived iPSCs showed similar behavior, whereas primary COPD and non-COPD fibroblasts presented distinct functionality and gene expression.<sup>[393]</sup> The elimination of COPD-specific characteristics during iPSC generation and subsequent differentiation is, in this context, associated with the loss of epigenetic signatures during cellular reprogramming.<sup>[393]</sup>

Kunisaki and colleagues have recently developed an iPSC-based organoid model of Bochdalek congenital diaphragmatic hernia, a polygenic disease in which developmental defects in the diaphragm cause herniation of abdominal organs, such as the stomach, intestines, liver, and spleen, into the thoracic cavity, causing severe pulmonary compression and hypoplasia.<sup>[394,395]</sup> Other studies have used iPSC technology to explore gene therapy in SFTPB deficiency, a rare autosomal recessive disorder that results in fatal respiratory failure in infants.<sup>[396]</sup> CRISPR-Cas9-mediated gene editing of patient-derived iAT2 cells carrying an *SFTPB* mutation allowed the successful recovery of a functional AT2 phenotype and rescued surfactant production,<sup>[300]</sup> a result that was also observed after lentiviral delivery of wildtype *SFTPB* to mutant iPSCs

(Figure 16).<sup>[397]</sup> Such an abundance of reports applying iPSC technology to a wide plethora of pulmonary diseases thereby showcases their extensive potential as promising tools for in vitro lung pathophysiological research.

#### 4.4. iPSC-Based OOC Devices

Many commercially available cell types have been used in OOC systems so far. However, since these cells are frequently immortalized or derived from cancer tissue, the next necessary step toward a human tissue-specific model – especially personalized tissue models – is the use of stem cells, such as iPSCs. iPSC-based approaches are very promising because they have the potential to create various types of specialized cells suitable for OOC studies, including, among many others, CMs, kidney podocytes, brain microvascular endothelial cells, and intestinal enterocytes.<sup>[398–401]</sup> As such, there is a clear upward trend in studies that use hiPSCs to develop personalized healthy or diseased tissue and organ models, which could be used for drug and toxicity screening, recapitulating individual patient's physiological characteristics much closer than animal models.<sup>[402,403]</sup> For these reasons, iPSC-based OOC devices could revolutionize preclinical testing, providing an unlimited, patient-specific pluripotent cell source, requiring low cell numbers and reagent volumes, and allowing for tight regulation of the cellular microenvironment and the establishment of biochemical concentration gradients,<sup>[404]</sup> thereby testing multiple drug dosage regimens in a single assay.

So far, there are only a few hiPSC-based OOC devices described, often focused in the generation of specialized human cells that have a very restricted accessibility or limited expansion capabilities in vitro. Accordingly, in 2015, Mathur et al. cultured hiPSC-derived CMs in a biomimetic cardiovascular system to produce a heart-on-chip device in which cellular drug toxicity and efficacy could be tested.<sup>[405]</sup> In the same topic of cardiovascular modeling, hiPSC-CMs and hiPSC-ECs were co-cultured to reproduce cardiac and blood vessel tissues by means of a myocardium-on-chip.<sup>[406]</sup> Hence, hiPSCs can represent an unlimited source for healthy and disease-specific CMs for in vitro cardiac modeling.<sup>[407]</sup>

In the field of neurobiology and neurological disease, Woodruff et al. used a microfluidic system containing hiPSC-derived neurons to investigate early phenotypic changes caused by familial mutations of Alzheimer's disease.<sup>[408]</sup> In a distinct study, culturing iPSC-derived motoneurons and brain microvascular endothelial cells together in an OOC model of the neuromuscular unit significantly enhanced function and in vivo-like maturation of spinal cord neural tissue.<sup>[409]</sup> Several other studies were dedicated to emulate the BBB, since it is still a substantial challenge to artificially reproduce the intricate and highly selective and impermeable structure of this biological barrier. A microfluidic BBB biomimetic platform, in which hiPSC-derived brain microvascular ECs were co-cultured with rat astrocytes, was used to analyze drug permeability.<sup>[398]</sup> Making use of both 3D printing and electrospinning technologies, Qi et al. developed a microchip for the co-culture of hiPSC-derived brain microvascular ECs and astrocytes, subsequently evaluating the permeability of this BBB model to anti-brain tumor drugs and a neurotoxic amyloid peptide.<sup>[349]</sup>

Nevertheless, iPSC-based OOC technology has not been limited to cardiovascular and brain tissue modeling: Workman et al. investigated an intestine chip by converging human iPSC-derived intestinal organoids and microengineering techniques,<sup>[400]</sup> while Musah and colleagues differentiated hiPSCs into podocytes to be used in a human glomerulus-on-chip model.<sup>[144,399]</sup>

Among all applications previously identified in this work, lung-on-chip models have been used to analyze the effects of flow rate,<sup>[410]</sup> air liquid interface (ALI) culture under positive pressure,<sup>[411]</sup> cyclic mechanical stresses,<sup>[148,180]</sup> and air plugs<sup>[412]</sup> on cellular viability, phenotype and response to chemical stimuli/drugs.<sup>[413]</sup> However, all models described so far are mainly based on cell lines and, occasionally, on primary cells rather than iPSCs, presumably owing to the complex, time-consuming, and very demanding differentiation of iPSCs into bronchial and alveolar lung cells, for which standardized protocols are still lacking.

OOC devices and, particularly, hiPSC-based technology can be truly groundbreaking in the context of preclinical and clinical research, enabling extensive in vitro testing and possibly replacing animal experiments entirely, generating more physiologically relevant data and allowing for a tight control of experimental variables and conditions. Importantly, reduction or replacement of animal experimentation is not only ethically and scientifically desirable, but also highly beneficial from an economic and logistic point of view, possibly shortening the duration of preclinical trials and decreasing the exorbitant costs typically associated with in vivo research.

Even though the primary uses for OOC systems have been mainly associated with preclinical drug safety and mechanistic studies,<sup>[414]</sup> additional applications exist, in principle, in virtually every field in which animal testing is currently performed. The potential of OOC systems in personalized medicine should be especially highlighted, since these devices are amenable to the use of patient-derived primary cells or iPSCs (patient-on-a-chip,<sup>[415]</sup> Figure 17). Furthermore, such systems are also suitable for infectious disease research and host-pathogen interaction modeling, being especially valuable for the development of anti-viral therapies such as those newly established for SARS-CoV-2.<sup>[416]</sup> Taking this information into consideration, it is becoming evident that further improvement and streamlined production of personalized OOCs can be an important asset in medical and pharmacological research, possibly decreasing the number of clinical trials required for drug approval through individualizing drug dosage and, thus, avoiding clinical failure and substantial economic loss.<sup>[403,404]</sup> Within REACH, lung-on-chip devices come into play, for instance, to study the effect of inhaled particulate matter and to mimic absorption, distribution, metabolism, and excretion (ADME) stages after inhalation of chemicals or nanomaterials. Besides fundamental and pharmacological research, also encompassing new drug design<sup>[417]</sup> and drug delivery investigation,<sup>[418,419]</sup> OOCs can find a place in cosmetic and chemical industries, where there is a great demand for alternative test methods.<sup>[420,421]</sup>

With further advancements in this technology, it is possible to build multiorgan models that include, for instance, both a pulmonary and a hepatic compartment, which allow the investigation of how inhaled drugs are processed and metabolized by

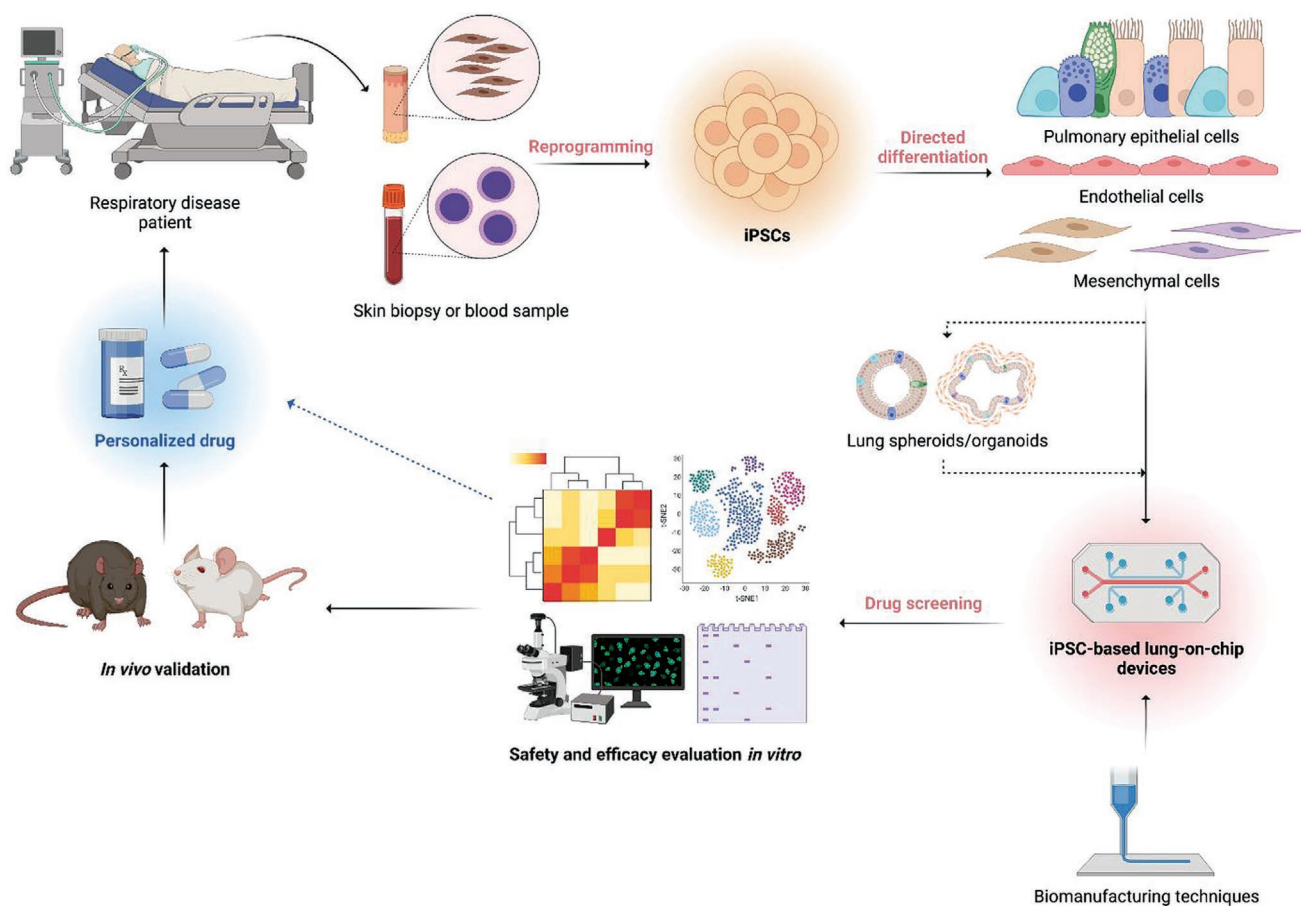


**Figure 17.** Schematics of the cyclic process used for the application of lung-on-chip devices in personalized medicine. Somatic cells are isolated from skin biopsies or blood samples of respiratory disease patients and subsequently cultured and reprogrammed to different cell types of interest. Lung-on-chip devices are generated using various biomufacturing techniques, such as 3D printing, and prepared for iPSCs-derived cell seeding and maintenance. Target drug candidates are tested using the lung-on-chip model, in which extensive safety and efficacy analyses are performed, followed by in vivo testing, after which the final personalized formulation is finally achieved. The main goal of OOC technology is to surpass the need for in vivo validation (dashed blue arrow), therefore allowing the formulation of patient-specific treatments based exclusively on in vitro experimental data. Created with BioRender.com.

the liver and how the resulting byproducts affect the lung.<sup>[422]</sup> Such multiorgan microfluidic platforms<sup>[423–433]</sup> may be greatly advantageous in their suitability for investigating pharmacokinetics (fate of an administered substance during the four stages of ADME) and pharmacodynamics (physiological effect of the substance and its products in the organism). The ultimate goal in this approach would be to attain body-on-chip devices, complex microphysiological systems in which multiple organ compartments are in intricate communication via microfluidic channels and reliable predictions on drug metabolism, efficacy, and off-target interactions and side effects can be performed. Some progress has already been made toward this objective, with body-on-chip devices simultaneously containing three,<sup>[434]</sup> five,<sup>[435]</sup> and six<sup>[436]</sup> different types of tissue being successfully demonstrated. Recently, an eight-organ vascularized OOC device was described by Ingber's group, in which the multiple tissues (liver, gut, lung, heart, skin, blood-brain barrier, kidney, and brain) were connected via a circulatory system and maintained with a universal blood substitute.<sup>[423]</sup> Interestingly, in this device, both lung and skin compartments were maintained

at an ALI, proving once again the suitability of OOC technology to mimic native organ environments and replicating complex human biology.

It should be emphasized, however, that OOC technology is at its inception, with most of the published reports still at a proof-of-concept stage and there is no profound investigation and accumulated knowledge about specific tissue or organ types.<sup>[414]</sup> Most of the OOC devices described to date also lack important biological elements, namely immune cells, which may play a fundamental role on disease modeling and pharmacological response.<sup>[437]</sup> Of note, though the concept of multiorgan and body-on-chip devices is undoubtedly attractive for preclinical research, practical issues arise when emulating diversified tissues with distinct cellular compositions and organization in a single device. First, it is often challenging to find universal cell culture media and environmental conditions capable of sustaining multiple cell types in coexistence; second, while the physiological relevance and representativeness may increase with the inclusion of distinct tissue and organ compartments, this increased complexity may be difficult to achieve and

reproduce on an industrial scale.<sup>[414,415]</sup> Moreover, advancements in biofabrication and device manufacturing tend to occur at faster rates than those on cellular technology, such as iPSCs, and this discrepancy will require close communication and collaboration of stakeholders (academic researchers, clinicians, industrial partners) to ensure smooth integration and mutual adaptation of cellular and bioengineered components and maximize the impact and utility of OOC devices in the laboratory and in the clinic.<sup>[414,437]</sup> As such, generalized incorporation of these devices into the drug development pipeline will first require extensive optimization and upscaling of device manufacturing and cell harvesting and propagation, which should be performed in a high-throughput and affordable fashion.<sup>[437]</sup> In addition, current device manipulation must be performed by specialized personnel that controls all components involved in OOC technology (pumps, actuators, readout equipment);<sup>[414]</sup> further simplification and connection to user-friendly interfaces or process automatization using robotics<sup>[423]</sup> may help improve the accessibility of these systems and facilitate translation from lab-scaled models to the clinic and the pharmaceutical industry.<sup>[437]</sup>

#### 4.5. Limitations of iPSC Technology

The progress made in iPSC technology since its first description and the promise it poses for in vitro research and personalized therapy are undeniable. In fact, this cell reprogramming technology has represented an unrivaled platform to investigate human development and disease pathogenesis, providing a limitless cell supply, suitability for high-throughput studies, and the opportunity to investigate and tackle individual disease characteristics by preserving the genetic signature and antigenic profile from the corresponding donors. However, the widespread use of iPSCs both in the laboratory and in the clinic has been hampered by a number of limitations that are important to bear in mind.

First, it is important to consider the high cost associated with the laborious, time-consuming process for the generation of iPSCs and subsequent differentiation into the cell types of interest, which limits their accessibility and practicality. Additionally, iPSCs are frequently generated and maintained using poorly-defined culture conditions, due to the presence of serum or Matrigel, which may affect the reproducibility among different studies and preclude an eventual clinical translation. Likewise, many of the developed protocols for the generation of iPSCs from somatic cells involve retroviral- or lentiviral-mediated transfection and definitive genomic integration of transgenes coding for the pluripotency transcription factor cocktail (Oct4, Klf4, Sox2, c-Myc), resulting in possible changes on cellular identity and differentiation potential, oncogene activation or tumor suppressor gene inactivation.<sup>[262,387]</sup> Nevertheless, temporary transfection methods have already been developed and applied, most frequently based on Sendai virus, episomal DNA, or synthetic messengerRNA (mRNA).<sup>[387]</sup> Indeed, though these methods may present lower transfection efficiency, the high proliferative capacity of iPSCs enables the selection and subsequent expansion of a small number of successfully transfected colonies.<sup>[262]</sup> In addition, as it was possible to conclude from this review, there are numerous protocols for the generation of the same differentiated cell types from iPSCs,

among which different growth/differentiation factors and time-points are used. It is, therefore, necessary to streamline these different strategies toward simplified, easily reproducible, and more efficient differentiation protocols.<sup>[264]</sup> Another limitation resides in the difficulty in obtaining fully differentiated iPSCs, thereby restricting the use of these tools for developmental or early post-natal biology and disease research.<sup>[264]</sup>

Moreover, in the process of selection and isolation of iPSCs for disease investigation, it should be taken into consideration that cellular behavior can be heavily influenced particularly by individual genetic background, though environmental and lifestyle elements, as well as ethnic characteristics, may also play an important role.<sup>[438]</sup> In fact, inter-donor genetic variability has been repeatedly demonstrated as a preponderate factor in iPSC differentiation, gene expression, and phenotype,<sup>[439–442]</sup> more than any other potentially interfering factor, determining 5–46% of the differences across distinct iPSC phenotypes.<sup>[443]</sup> While it is important to investigate human genetic heterogeneity and its influence on disease pathogenesis and drug response, such an interindividual variability may introduce confounding factors in disease modeling if suitable controls are not included.<sup>[444]</sup> Accordingly, control and diseased iPSC lines should be matched for sex, age, ethnicity, and time in culture.<sup>[445]</sup> Additionally, in disorders caused by known genetic mutant variants, it is possible to use gene editing technology to obtain healthy and diseased isogenic iPSC cell lines from the same donor, thus enabling the use of control and pathological iPSCs with identical genetic backgrounds.<sup>[444,445]</sup> Lastly, iPSC biobanking and the widespread use of well-characterized iPSC lines and common controls across studies, after strict and extensive genomic, transcriptomic, and proteomic profiling, may facilitate reproducibility and comparison of results and help identify sources of inter-study variability.<sup>[445]</sup> For a few years now, the number of iPSC lines available for research purposes has been growing. Several companies (e.g., Thermo Fisher Scientific,<sup>[446]</sup> Takara Bio,<sup>[447]</sup> Tempo Bioscience<sup>[448]</sup>) and certified cell biobanks, like the nonprofit, global biological resource center and leading developer and supplier of authenticated cells lines and microorganisms American type culture collection (ATCC), offer iPSC cell lines for research use. The iPSCs provided by ATCC are derived from primary cardiac fibroblasts obtained from a healthy donor (ACS-1021, ATCC-CYS0105).<sup>[449]</sup> In addition, the European Bank for Induced Pluripotent Stem Cells (EBiSC) collection of human iPSCs is available to academic and commercial researchers for use in disease modeling and other forms of preclinical research.<sup>[450]</sup> It currently includes 896 cell lines, but it is constantly being expanded.<sup>[451]</sup> Furthermore, first good manufacturing practice (GMP)-grade iPSCs suitable for clinical use are commercially available.<sup>[452]</sup> This indicates that the relevance of iPSCs in pharmaceutical research and medical science has been fully recognized and increasing sources of iPSC lines are driving the development of novel in vitro models and therapeutic approaches in the near future.

## 5. Concluding Remarks

The complexity of the pulmonary architecture and microenvironment, the inaccessibility of primary lung cells, and the

difficulty in maintaining cellular identity and specific phenotype in vitro have hindered the development of suitable platforms for basic and developmental lung research, disease modeling, and pharmacological screening. Conversely, the easy accessibility, virtually unlimited proliferation and differentiation potential, and patient-specific nature of iPSCs promise to revolutionize human biology and disease in vitro modeling, effectively counteracting the disadvantages of other commonly used cellular sources. Thus, it is important to consider the significant hurdles that are still associated with iPSC methodologies, in which the time-consuming and expensive protocols, lack of standardization, and the proven inter-individual variability arising from distinct genetic backgrounds may compromise the scalability and reproducibility of these models and, therefore, their clinical translation and industrial production. The combination of iPSCs with OOC systems may provide physiologically relevant and patient-specific models capable of faithfully reproducing the lung microenvironment, where cellular, biochemical, and biomechanical elements come into play and jointly influence cellular behavior and identity. The integration of these models into the pharmaceutical industry and the drug development process will benefit from close interdisciplinary communication of biomedical researchers, engineers, physicians and industrial partners, in order to assist with the translation of these devices from the bench to the clinic.

## Acknowledgements

A.M. and Y.K. contributed equally to this work. This project has received funding from the European Union's HORIZON 2020 MSCA-RISE Marie Skłodowska-Curie Research and Innovation Staff Exchange Research Programme under grant agreement no. 823981. This review was written as thesis for the postgraduate studies program "Toxikologie und Umweltschutz". Y.K. is grateful for the permission by the committee to write this review. The authors thank Julie Earl for proofreading.

Open access funding enabled and organized by Projekt DEAL.

## Conflict of Interest

The authors declare no conflict of interest.

## Keywords

disease models, drug screening, induced pluripotent stem cells, lung cell differentiation, lung-on-chip, organoids models, toxicity screening

Received: August 23, 2021

Revised: November 25, 2021

Published online:

- [1] *Forum of International Respiratory Societies, The Global Impact of Respiratory Disease – Second Edition*, European Respiratory Society, Sheffield 2017.
- [2] F. Bray, J. Ferlay, I. Soerjomataram, R. L. Siegel, L. A. Torre, A. Jemal, *Ca-Cancer J. Clin.* **2018**, *68*, 394.
- [3] P. M. de Groot, C. C. Wu, B. W. Carter, R. F. Munden, *Transl. Lung Cancer Res.* **2018**, *7*, 220.

- [4] J. B. Soriano, P. J. Kendrick, K. R. Paulson, V. Gupta, E. M. Abrams, R. A. Adedoyin, T. B. Adhikari, S. M. Advani, A. Agrawal, E. Ahmadian, F. Alahdab, S. M. Aljunid, K. A. Altirkawi, N. Alvis-Guzman, N. H. Anber, C. L. Andrei, M. Anjomshoa, F. Ansari, J. M. Antó, J. Arabloo, S. M. Athari, S. S. Athari, N. Awoke, A. Badawi, J. A. M. Banoub, D. A. Bennett, I. M. Bensenor, K. S. S. Berfield, R. S. Bernstein, K. Bhattacharyya, et al., *Lancet Respir. Med.* **2020**, *8*, 585.
- [5] M. Xie, X. Liu, X. Cao, M. Guo, X. Li, *Respir. Res.* **2020**, *21*, 49.
- [6] A. Doryab, S. Tas, M. B. Taskin, L. Yang, A. Hilgendorff, J. Groll, D. E. Wagner, O. Schmid, *Adv. Funct. Mater.* **2019**, *29*, 1903114.
- [7] P. Spagnolo, *Orphan Lung Diseases*, Springer, London **2015**, pp. 597–609.
- [8] S. D. Patel, T. R. Bono, S. M. Rowe, G. M. Solomon, *Eur. Respir. Rev.* **2020**, *29*, 190068.
- [9] N. L. Turcios, *Respir. Care* **2020**, *65*, 233.
- [10] K. Gkatzis, S. Taghizadeh, D. Huh, D. Y. R. Stainier, S. Bellusci, *Eur. Respir. J.* **2018**, *52*, 1800876.
- [11] F. Busquet, T. Hartung, G. Pallocca, C. Rovida, M. Leist, *Arch. Toxicol.* **2020**, *94*, 2263.
- [12] D. Movia, A. Prina-Mello, *Animals* **2020**, *10*, 1259.
- [13] A. M. Holmes, R. Solari, S. T. Holgate, *Drug Discov. Today* **2011**, *16*, 659.
- [14] M. Ritskes-Hoitinga, C. Leenaars, W. Beumer, T. C. De Roo, F. Stafleu, F. L. B. Meijboom, *Animals* **2020**, *10*, 1170.
- [15] A. J. Miller, J. R. Spence, *Physiology* **2017**, *32*, 246.
- [16] S. C. Faber, S. D. McCullough, *Appl. Vitro Toxicol.* **2018**, *4*, 115.
- [17] K. Li, X. Yang, C. Xue, L. Zhao, Y. Zhang, X. Gao, *Biomicrofluidics* **2019**, *13*, 031501.
- [18] V. K. Sidhaye, M. Koval, *Lung Epithelial Biology in the Pathogenesis of Pulmonary Disease*, Academic Press, Cambridge, MA **2017**.
- [19] M. Z. Nikolić, D. Sun, E. L. Rawlins, *Development* **2018**, *145*, dev163485.
- [20] K. J. Travaglini, A. N. Nabhan, L. Penland, R. Sinha, A. Gillich, R. V. Sit, S. Chang, S. D. Conley, Y. Mori, J. Seita, G. J. Berry, J. B. Shrager, R. J. Metzger, C. S. Kuo, N. Neff, I. L. Weissman, S. R. Quake, M. A. Krasnow, *Nature* **2020**, *587*, 619.
- [21] M. F. Acosta, P. Muralidharan, S. A. Meenach, D. Hayes, S. M.-Black, H. M. Mansour, *Curr. Pharm. Des.* **2016**, *22*, 2522.
- [22] A. M. Guth, W. J. Janssen, C. M. Bosio, E. C. Crouch, P. M. Henson, S. W. Dow, *Am. J. Physiol.: Lung Cell. Mol. Physiol.* **2009**, *296*, 936.
- [23] L. Barron, S. A. Gharib, J. S. Duffield, *Am. J. Pathol.* **2016**, *186*, 2519.
- [24] O. J. Wouters, M. McKee, J. Luyten, *JAMA, J. Am. Med. Assoc.* **2020**, *323*, 844.
- [25] J. Mestre-Ferrandiz, J. Sussex, A. Towse, *The R&D Cost of a New Medicine*, Office Of Health Economics, London, **2012**.
- [26] P. J. Barnes, S. Bonini, W. Seeger, M. G. Belvisi, B. Ward, A. Holmes, *Eur. Respir. J.* **2015**, *45*, 1197.
- [27] T. Hartung, J. Zurlo, *ALTEX – Altern. to Anim. Exp.* **2012**, *29*, 251.
- [28] D. Movia, S. Bruni-Favier, A. Prina-Mello, *Front. Bioeng. Biotechnol.* **2020**, *0*, 549.
- [29] L. Tanner, A. B. Single, *J. Innate Immun.* **2020**, *12*, 203.
- [30] G. Matute-Bello, C. W. Frevort, T. R. Martin, *Am. J. Physiol.: Lung Cell. Mol. Physiol.* **2008**, *295*, 379.
- [31] J. P. Mizgerd, S. J. Skerrett, *Am. J. Physiol.: Lung Cell. Mol. Physiol.* **2008**, *294*, L387.
- [32] I. W. Y. Mak, N. Evaniew, M. Ghert, *Am. J. Transl. Res.* **2014**, *6*, 114.
- [33] P. Perel, I. Roberts, E. Sena, P. Wheble, C. Briscoe, P. Sandercock, M. Macleod, L. E. Mignini, P. Jayaram, K. S. Khan, *BMJ* **2007**, *334*, 197.
- [34] A. Akhtar, *Camb. Q. Healthc. Ethics* **2015**, *24*, 407.
- [35] W. Rehman, L. M. Arfons, H. M. Lazarus, *Ther. Adv. Hematol.* **2011**, *2*, 291.
- [36] N. Vargesson, *Birth Defects Res. Part C* **2015**, *105*, 140.

- [37] H. Attarwala, *J. Young Pharm.* **2010**, *2*, 332.
- [38] P. Jüni, L. Nartey, S. Reichenbach, R. Sterchi, P. A. Dieppe, P. M. Egger, *Lancet* **2004**, *364*, 2021.
- [39] G. Suntharalingam, M. R. Perry, S. Ward, S. J. Brett, A. Castello-Cortes, M. D. Brunner, N. Panoskaltzis, *N. Engl. J. Med.* **2006**, *355*, 1018.
- [40] E. W. St Clair, *J. Clin. Invest.* **2008**, *118*, 1344.
- [41] A. Dura, L. Gribaldo, P. Deceuninck, I. Campia, EURL ECVAM Review of non-animal models in biomedical research – Respiratory tract diseases, <https://data.jrc.ec.europa.eu/dataset/176d71e6-5082-4b29-8472-b719f6bda323>, **2020** (accessed: November 2021).
- [42] M. I. Hermanns, R. E. Unger, K. Kehe, K. Peters, C. J. Kirkpatrick, *Lab. Investig.* **2004**, *84*, 736.
- [43] K. Luyts, D. Napierska, D. Dinsdale, S. G. Klein, T. Serchi, P. H. M. Hoet, *Toxicol. Vitro* **2015**, *29*, 234.
- [44] P. M. de Jong, M. A. van Sterkenburg, S. C. Hesselting, J. A. Kempenaar, A. A. Mulder, A. M. Mommaas, J. H. Dijkman, M. Ponc, *Am. J. Respir. Cell Mol. Biol.* **1994**, *10*, 271.
- [45] B. J. Gerovac, M. Valencia, N. Baumlin, M. Salathe, G. E. Conner, N. L. Fregien, *Am. J. Respir. Cell Mol. Biol.* **2014**, *51*, 516.
- [46] M. Hittinger, J. Janke, H. Huwer, R. Scherließ, N. Schneider-Daum, C. M. Lehr, *ATLA Altern. Lab. Anim.* **2016**, *44*, 337.
- [47] A. Chandrasekaran, S. Kouthouridis, W. Lee, N. Lin, Z. Ma, M. J. Turner, J. W. Hanrahan, C. Moraes, *Lab Chip* **2019**, *19*, 2786.
- [48] X. Cao, J. P. Coyle, R. Xiong, Y. Wang, R. H. Heflich, B. Ren, W. M. Gwinn, P. Hayden, L. Rojanasakul, *Vitro. Cell. Dev. Biol.: Anim.* **2020**, *57*, 104.
- [49] L. Neilson, C. Mankus, D. Thorne, G. Jackson, J. DeBay, C. Meredith, *Toxicol. Vitro* **2015**, *29*, 1952.
- [50] J. Zavala, B. O'Brien, K. Lichtveld, K. G. Sexton, I. Rusyn, I. Jaspers, W. Vizuete, *Inhal. Toxicol.* **2016**, *28*, 251.
- [51] K. Balogh Sivars, U. Sivars, E. Hornberg, H. Zhang, L. Brändén, R. Bonfante, S. Huang, S. Constant, I. Robinson, C. J. Betts, P. M. Åberg, *Toxicol. Sci.* **2018**, *162*, 301.
- [52] S. Huang, L. Wiszniewski, S. Constant, E. Roggen, *Toxicol. Vitro* **2013**, *27*, 1151.
- [53] D. Jiang, N. Schaefer, H. W. Chu, *Methods in Molecular Biology*, Humana Press Inc., New Jersey **2018**, pp. 91–109.
- [54] S. Chen, J. Schoen, *Reprod. Domest. Anim.* **2019**, *54*, 38.
- [55] C. Jensen, Y. Teng, *Front. Mol. Biosci.* **2020**, *7*, 33.
- [56] M. Mirbagheri, V. Adibnia, B. R. Hughes, S. D. Waldman, X. Banquy, D. K. Hwang, *Mater. Horiz.* **2019**, *6*, 45.
- [57] A. J. Carterson, K. Höner Zu Benstrup, C. M. Ott, M. S. Clarke, D. L. Pierson, C. R. Vanderburg, K. L. Buchanan, C. A. Nickerson, M. J. Schurr, *Infect. Immun.* **2005**, *73*, 1129.
- [58] R. Bhowmick, H. Gappa-Fahlenkamp, *Lung* **2016**, *194*, 419.
- [59] P. Chandorkar, W. Posch, V. Zaderer, M. Blatzer, M. Steger, C. G. Ammann, U. Binder, M. Hermann, P. Hörtnagl, C. Lass-Flörl, D. Wilflingseder, *Sci. Rep.* **2017**, *7*, 11644.
- [60] M. Sacchi, R. Bansal, J. Rouwkema, *Trends Biotechnol.* **2020**, *38*, 623.
- [61] S. G. Klein, T. Serchi, L. Hoffmann, B. Blömeke, A. C. Gutleb, *Part. Fibre Toxicol.* **2013**, *10*, 31
- [62] A. Sharma, S. Sances, M. J. Workman, C. N. Svendsen, *Cell Stem Cell* **2020**, *26*, 309.
- [63] X. Yin, B. E. Mead, H. Safaee, R. Langer, J. M. Karp, O. Levy, *Cell Stem Cell* **2016**, *18*, 25.
- [64] K. Sato, W. Zhang, S. Safarikia, A. Isidan, A. M. Chen, P. Li, H. Francis, L. Kennedy, L. Baiocchi, D. Alvaro, S. Glaser, B. Ekser, G. Alpini, *Hepatology* **2021**, *74*, 491.
- [65] M. Zononi, M. Cortesi, A. Zamagni, C. Arienti, S. Pignatta, A. Tesei, *J. Hematol. Oncol.* **2020**, *13*, 97.
- [66] R. Barrera-Rodríguez, J. M. Fuentes, *Cancer Cell Int.* **2015**, *15*, 47
- [67] L. Hu, S. Sun, T. Wang, Y. Li, K. Jiang, G. Lin, Y. Ma, M. P. Barr, F. Song, G. Zhang, S. Meng, *Am. J. Cancer Res.* **2015**, *5*, 3612.
- [68] S. A. Meenach, A. N. Tsoras, R. C. McGarry, H. M. Mansour, J. Z. Hilt, K. W. Anderson, *Int. J. Oncol.* **2016**, *48*, 1701.
- [69] Z. Zhang, H. Wang, Q. Ding, Y. Xing, Z. Xu, C. Lu, D. Luo, L. Xu, W. Xia, C. Zhou, M. Shi, *PLoS One* **2018**, *13*, e0194016.
- [70] I. Chimenti, F. Pagano, F. Angelini, C. Siciliano, G. Mangino, V. Picchio, E. De Falco, M. Peruzzi, R. Carnevale, M. Ibrahim, G. Biondi-Zoccai, E. Messina, G. Frati, *Stem Cells Transl. Med.* **2017**, *6*, 767.
- [71] M. A. Lancaster, J. A. Knoblich, *Science* **2014**, *345*, 1247125.
- [72] L. Tian, J. Gao, I. M. Garcia, H. J. Chen, A. Castaldi, Y. Chen, *WIREs Dev. Biol.* **2020**, *10*, e399.
- [73] Z. Li, Y. Qian, W. Li, L. Liu, L. Yu, X. Liu, G. Wu, Y. Wang, W. Luo, F. Fang, Y. Liu, F. Song, Z. Cai, W. Chen, W. Huang, *iScience* **2020**, *23*, 101411.
- [74] R. Shi, N. Radulovich, C. Ng, N. Liu, H. Notsuda, M. Cabanero, S. N. Martins-Filho, V. Raghavan, Q. Li, A. S. Mer, J. C. Rosen, M. Li, Yu.-H. Wang, L. Tamblyn, N.-A.n. Pham, B. Haibe-Kains, G. Liu, N. Moghal, M. -. S. Tsao, *Clin. Cancer Res.* **2020**, *26*, 1162.
- [75] M. Kim, H. Mun, C. O. Sung, E. J. Cho, H.-J. Jeon, S.-M. Chun, D. J. Jung, T. H. Shin, G. S. Jeong, D. K. Kim, E. K. Choi, S. -. Yeong, A. M. Taylor, S. Jain, M. Meyerson, S. J. Jang, *Nat. Commun.* **2019**, *10*, 3991.
- [76] N. Sachs, A. Paspaspyropoulos, D. D. Zomer-van Ommen, I. Heo, L. Böttinger, D. Klay, F. Weeber, G. Huelsz-Prince, N. Iakobachvili, G. D. Amatngalim, J. Ligt, A. Hoeck, N. Proost, M. C. Viveen, A. Lyubimova, L. Teeven, S. Derakhshan, J. Korving, H. Begthel, J. F. Dekkers, K. Kumawat, E. Ramos, M. F. Oosterhout, G. J. Offerhaus, D. J. Wiener, E. P. Olimpio, K. K. Dijkstra, E. F. Smit, M. Linden, S. Jaksani, et al., *EMBO J.* **2019**, *38*, 100300.
- [77] I. Heo, D. Dutta, D. A. Schaefer, N. Iakobachvili, B. Artegiani, N. Sachs, K. E. Boonekamp, G. Bowden, A. P. A. Hendrickx, R. J. L. Willems, P. J. Peters, M. W. Riggs, R. O'connor, H. Clevers, *Nat. Microbiol.* **2018**, *3*, 814.
- [78] M. Z. Nikolić, O. Caritg, Q. Jeng, J. A. Johnson, D. Sun, K. J. Howell, J. L. Brady, U. Laresgoiti, G. Allen, R. Butler, M. Zilbauer, A. Giangreco, E. L. Rawlins, *Elife* **2017**, *6*, 26575.
- [79] B. R. Dye, D. R. Hill, M. A. Ferguson, Y. H. Tsai, M. S. Nagy, R. Dyal, J. M. Wells, C. N. Mayhew, R. Nattiv, O. D. Klein, E. S. White, G. H. Deutsch, J. R. Spence, *Elife* **2015**, *4*, e05098.
- [80] Y. Chen, J. Feng, S. Zhao, L. Han, H. Yang, Y. Lin, Z. Rong, *Stem Cells Dev.* **2018**, *27*, 1339.
- [81] H. Meyer-Berg, L. Zhou Yang, M. Pilar de Lucas, A. Zambrano, S. C. Hyde, D. R. Gill, *Stem Cell Res. Ther.* **2020**, *11*, 448.
- [82] T. Takebe, J. M. Wells, *Science* **2019**, *364*, 956.
- [83] F. Schutgens, H. Clevers, *Annu. Rev. Pathol. Mech. Dis.* **2020**, *15*, 211.
- [84] J. Kim, B. K. Koo, J. A. Knoblich, *Nat. Rev. Mol. Cell Biol.* **2020**, *21*, 571.
- [85] C. E. Barkauskas, M. I. Chung, B. Fioret, X. Gao, H. Katsura, B. L. M. Hogan, *Dev.* **2017**, *144*, 986.
- [86] R. J. Jimenez-Valdes, U. I. Can, B. F. Niemeyer, K. H. Benam, *Front. Bioeng. Biotechnol.* **2020**, *8*, 989.
- [87] J. L. Balestrini, A. L. Gard, A. Liu, K. L. Leiby, J. Schwan, B. Kunkemoeller, E. A. Calle, A. Sivarapatna, T. Lin, S. Dimitrievska, S. G. Campbell, L. E. Niklason, *Integr. Biol.* **2015**, *7*, 1598.
- [88] H. Zhou, K. Kitano, X. Ren, T. K. Rajab, M. Wu, S. E. Gilpin, T. Wu, L. Baugh, L. D. Black, D. J. Mathisen, H. C. Ott, *Ann. Surg.* **2018**, *267*, 590.
- [89] O. Rosmark, E. Åhrman, C. Müller, L. Elovsson Rengin, L. Eriksson, A. Malmström, O. Hallgren, A. K. Larsson-Callerfelt, G. Westergren-Thorsson, J. Malmström, *Sci. Rep.* **2018**, *8*, 5409.
- [90] K. Ohata, H. C. Ott, *Surg. Today* **2020**, *50*, 633.
- [91] N. Kawai, Y. Ujii, M. Sakagami, T. Tojo, N. Sawabata, M. Yoshikawa, S. Taniguchi, *Biochem. Biophys. Rep.* **2018**, *15*, 33.
- [92] T. Jensen, B. Roszell, F. Zang, E. Girard, A. Matson, R. Thrall, D. M. Jaworski, C. Hatton, D. J. Weiss, C. Finck, *Tissue Eng. C Methods* **2012**, *18*, 632.

- [93] R. A. Pouliot, B. M. Young, P. A. Link, H. E. Park, A. R. Kahn, K. Shankar, M. B. Schneck, D. J. Weiss, R. L. Heise, *Tissue Eng. C Methods* **2020**, *26*, 332.
- [94] R. H. J. De Hilster, P. K. Sharma, M. R. Jonker, E. S. White, E. A. Gercama, M. Roobeek, W. Timens, M. C. Harmsen, M. N. Hylkema, J. K. Burgess, *Am. J. Physiol.: Lung Cell. Mol. Physiol.* **2020**, *318*, L698.
- [95] D. E. Wagner, N. R. Bonenfant, D. Sokocevic, M. J. DeSarno, Z. D. Borg, C. S. Parsons, E. M. Brooks, J. J. Platz, Z. I. Khalpey, D. M. Hoganson, B. Deng, Y. W. Lam, R. A. Oldinski, T. Ashikaga, D. J. Weiss, *Biomaterials* **2014**, *35*, 2664.
- [96] H. Sun, Y. Zhu, H. Pan, X. Chen, J. L. Balestrini, T. T. Lam, J. E. Kanyo, A. Eichmann, M. Gulati, W. H. Fares, H. Bai, C. A. Feghali-Bostwick, Y. Gan, X. Peng, M. W. Moore, E. S. White, P. Sava, A. L. Gonzalez, Y. Cheng, L. E. Niklason, E. L. Herzog, *Arthritis Rheumatol.* **2016**, *68*, 1251.
- [97] A. J. Booth, R. Hadley, A. M. Cornett, A. A. Dreffs, S. A. Matthes, J. L. Tsui, K. Weiss, J. C. Horowitz, V. F. Fiore, T. H. Barker, B. B. Moore, F. J. Martinez, L. E. Niklason, E. S. White, *Am. J. Respir. Crit. Care Med.* **2012**, *186*, 866.
- [98] D. Sokocevic, N. R. Bonenfant, D. E. Wagner, Z. D. Borg, M. J. Lathrop, Y. W. Lam, B. Deng, M. J. DeSarno, T. Ashikaga, R. Loi, A. M. Hoffman, D. J. Weiss, *Biomaterials* **2013**, *34*, 3256.
- [99] D. E. Wagner, N. R. Bonenfant, C. S. Parsons, D. Sokocevic, E. M. Brooks, Z. D. Borg, M. J. Lathrop, J. D. Wallis, A. B. Daly, Y. W. Lam, B. Deng, M. J. Desarno, T. Ashikaga, R. Loi, D. J. Weiss, *Biomaterials* **2014**, *35*, 3281.
- [100] T. H. Petersen, E. A. Calle, L. Zhao, E. J. Lee, L. Gui, M. S. B. Raredon, K. Gavrilov, T. Yi, Z. W. Zhuang, C. Breuer, E. Herzog, L. E. Niklason, *Science* **2010**, *329*, 538.
- [101] F. E. Uhl, F. Zhang, R. A. Pouliot, J. J. Uriarte, S. Rolandsson Enes, X. Han, Y. Ouyang, K. Xia, G. Westergren-Thorsson, A. Malmström, O. Hallgren, R. J. Linhardt, D. J. Weiss, *Acta Biomater.* **2020**, *102*, 231.
- [102] J. L. Balestrini, A. L. Gard, K. A. Gerhold, E. C. Wilcox, A. Liu, J. Schwan, A. V. Le, P. Baevoova, S. Dimitrievska, L. Zhao, S. Sundaram, H. Sun, L. Rittié, R. Dyal, T. J. Broekelmann, R. P. Mecham, M. A. Schwartz, L. E. Niklason, E. S. White, *Biomaterials* **2016**, *102*, 220.
- [103] S. H. Mahfouzi, S. H. Safiabadi Tali, G. Amoabediny, *Regener. Med.* **2021**, *16*, 757.
- [104] J. D. O'Neill, R. Anfang, A. Anandappa, J. Costa, J. Javidfar, H. M. Wobma, G. Singh, D. O. Freytes, M. D. Bacchetta, J. R. Sonett, G. Vunjak-Novakovic, *Ann. Thorac. Surg.* **2013**, *96*, 1046.
- [105] J. E. Nichols, J. Niles, M. Riddle, G. Vargas, T. Schilagard, L. Ma, K. Edward, S. La Francesca, J. Sakamoto, S. Vega, M. Ogadegbe, R. Mlcak, D. Deyo, L. Woodson, C. Mcquitty, S. Lick, D. Beckles, E. Melo, J. Cortiella, *Tissue Eng., Part A* **2013**, *19*, 2045.
- [106] L. Wang, Y. Zhao, F. Yang, M. Feng, Y. Zhao, X. Chen, J. Mi, Y. Yao, D. Guan, Z. Xiao, B. Chen, J. Dai, *Biomaterials* **2020**, *236*, 119825.
- [107] A. Kosmala, M. Fitzgerald, E. Moore, F. Stam, *Anal. Lett.* **2017**, *50*, 219.
- [108] N. Arya, V. Sardana, M. Saxena, A. Rangarajan, D. S. Katti, *J. R. Soc. Interface* **2012**, *9*, 3288.
- [109] A. E. Kuriakose, W. Hu, K. T. Nguyen, J. U. Menon, *PLoS One* **2019**, *14*, 0217640.
- [110] S. Sohn, M. Van Buskirk, M. J. Buckenmeyer, R. Londono, D. Faulk, *Appl. Sci.* **2020**, *10*, 4277.
- [111] H. Liu, X. Ding, G. Zhou, P. Li, X. Wei, Y. Fan, *J. Nanomater* **2013**, *2013*, 495708.
- [112] A. Moreira, D. Lawson, L. Onyekuru, K. Dziemidowicz, U. Angkawinitwong, P. F. Costa, N. Radacsi, G. R. Williams, *J. Controlled Release* **2021**, *329*, 1172.
- [113] G. E. Morris, J. C. Bridge, L. A. Brace, A. J. Knox, J. W. Aylott, C. E. Brightling, A. M. Ghaemmaghami, F. R. A. J. Rose, *Biofabrication* **2014**, *6*, 035014.
- [114] J. C. Bridge, J. W. Aylott, C. E. Brightling, A. M. Ghaemmaghami, A. J. Knox, M. P. Lewis, F. R. A. J. Rose, G. E. Morris, *J. Vis. Exp.* **2015**, *2015*, 52986.
- [115] P. Azimi, M. S. S. Bafqi, A. Fusco, C. Ricci, G. Gallone, R. Bagherzadeh, G. Donnarumma, M. J. Uddin, M. Latifi, A. Lazzeri, S. Danti, *Tissue Eng. A* **2020**, *26*, 1312.
- [116] B. M. Young, K. Shankar, B. P. Allen, R. A. Pouliot, M. B. Schneck, N. S. Mikhael, R. L. Heise, *ACS Biomater. Sci. Eng.* **2017**, *3*, 3480.
- [117] G. E. Morris, J. C. Bridge, O. M. I. Eltboli, A. J. Knox, J. W. Aylott, C. E. Brightling, A. M. Ghaemmaghami, F. R. A. J. Rose, *Am. J. Physiol.: Lung Cell. Mol. Physiol.* **2014**, *307*, 38.
- [118] D. G. Tamay, T. D. Usal, A. S. Alagoz, D. Yucel, N. Hasirci, V. Hasirci, *Front. Bioeng. Biotechnol.* **2019**, *7*, 164.
- [119] L. Huang, W. Yuan, Y. Hong, S. Fan, X. Yao, T. Ren, L. Song, G. Yang, Y. Zhang, *Cellulose* **2021**, *28*, 241.
- [120] J. Berg, T. Hiller, M. S. Kissner, T. H. Qazi, G. N. Duda, A. C. Hocke, S. Hippenstiel, L. Elomaa, M. Weinhart, C. Fahrenson, J. Kurreck, *Sci. Rep.* **2018**, *8*, 13877.
- [121] A. Mondal, A. Gebeyehu, M. Miranda, D. Bahadur, N. Patel, S. Ramakrishnan, A. K. Rishi, M. Singh, *Sci. Rep.* **2019**, *9*, 19914.
- [122] X. Wang, X. Zhang, X. Dai, X. Wang, X. Li, J. Diao, T. Xu, *3 Biotech* **2018**, *8*, 501.
- [123] P. D. Dalton, C. Vaquette, B. L. Farrugia, T. R. Dargaville, T. D. Brown, D. W. Huttmacher, *Biomater. Sci.* **2013**, *1*, 171.
- [124] S. Bongiovanni Abel, F. Montini Ballarin, G. A. Abraham, *Nanotechnology* **2020**, *31*, 172002.
- [125] N. Radacsi, W. Nuansing, *3D and 4D Printing of Polymer Nanocomposite Materials*, Elsevier, Amsterdam **2019**, p. 191.
- [126] L. Zheng, K. Kurselis, A. El-Tamer, N. Hinze, C. Reinhardt, L. Overmeyer, K. Chichkov, *Nanoscale Res. Lett.* **2019**, *14*, 134.
- [127] D. Tan, Y. Li, F. Qi, H. Yang, Q. Gong, X. Dong, X. Duan, *Appl. Phys. Lett.* **2007**, *90*, 071106.
- [128] M. M. De Santis, D. A. Bölükbas, S. Lindstedt, D. E. Wagner, *Eur. Respir. J.* **2018**, *52*, 1601355.
- [129] U. Marx, T. Akabane, T. B. Andersson, E. Baker, M. Beilmann, S. Beken, S. Brendler-Schwaab, M. Cirit, R. David, E. M. Dehne, I. Durieux, L. Ewart, S. C. Fitzpatrick, O. Frey, F. Fuchs, L. G. Griffith, G. A. Hamilton, T. Hartung, J. Hoeng, H. Hogberg, D. J. Hughes, D. E. Ingber, A. Iskandar, T. Kanamori, H. Kojima, J. Kuehnl, M. Leist, B. Li, P. Loskill, et al., *ALTEX* **2020**, *37*, 364.
- [130] U. Marx, T. B. Andersson, A. Bahinski, M. Beilmann, S. Beken, F. R. Cassee, M. Cirit, M. Daneshian, S. Fitzpatrick, O. Frey, C. Gaertner, C. Giese, L. Griffith, T. Hartung, M. B. Heringa, J. Hoeng, W. H. De Jong, H. Kojima, J. Kuehnl, M. Leist, *ALTEX* **2016**, *33*, 272.
- [131] Y. Cong, X. Han, Y. Wang, Z. Chen, Y. Lu, T. Liu, Z. Wu, Y. Jin, Y. Luo, X. Zhang, *Micromachines* **2020**, *11*, 381.
- [132] H. Kimura, T. Yamamoto, H. Sakai, Y. Sakai, T. Fujii, *Lab Chip* **2008**, *8*, 741.
- [133] H. J. Kim, D. Huh, G. Hamilton, D. E. Ingber, *Lab Chip* **2012**, *12*, 2165.
- [134] P. M. Van Midwoud, M. T. Merema, E. Verpoorte, G. M. M. Groothuis, *Lab Chip* **2010**, *10*, 2778.
- [135] K. J. Jang, M. A. Otieno, J. Ronxhi, H. K. Lim, L. Ewart, K. R. Kodella, D. B. Petropolis, G. Kulkarni, J. E. Rubins, D. Conegliano, J. Nawroth, D. Simic, W. Lam, M. Singer, E. Barale, B. Singh, M. Sonee, A. J. Streeter, C. Manthey, B. Jones, A. Srivastava, L. C. Andersson, D. Williams, H. Park, R. Barrile, J. Sliz, A. Herland, S. Haney, K. Karalis, D. E. Ingber, et al., *Sci. Transl. Med.* **2019**, *11*, 5516.
- [136] D. Bavli, S. Prill, E. Ezra, G. Levy, M. Cohen, M. Vinken, J. Vanfleteren, M. Jaeger, Y. Nahmias, *Proc. Natl. Acad. Sci. USA* **2016**, *113*, 2231.
- [137] N. S. Bhise, V. Manoharan, S. Massa, A. Tamayol, M. Ghaderi, M. Miscuglio, Q. Lang, Y. S. Zhang, S. R. Shin, G. Calzone, N. Annabi, T. D. Shupe, C. E. Bishop, A. Atala, M. R. Dokmeci, A. Khademhosseini, *Biofabrication* **2016**, *8*, 014101.

- [138] H. Kaji, T. Ishibashi, K. Nagamine, M. Kanzaki, M. Nishizawa, *Bio-materials* **2010**, *31*, 6981.
- [139] J. Saliba, A. Daou, S. Damiaty, J. Saliba, M. El-Sabban, R. Mhanna, *Genes* **2018**, *9*, 285.
- [140] M. W. van der Helm, A. D. van der Meer, J. C. T. Eijkel, A. van den Berg, L. I. Segerink, *Tissue Barriers* **2016**, *4*, 1142493.
- [141] M. J. Wilmer, C. P. Ng, H. L. Lanz, P. Vulto, L. Suter-Dick, R. Masereeuw, *Trends Biotechnol.* **2016**, *34*, 156.
- [142] L. C. Snouber, F. Letourneur, P. Chafey, C. Broussard, M. Monge, C. Legallais, E. Leclerc, *Biotechnol. Prog.* **2012**, *28*, 474.
- [143] N. Ashammakhi, K. Wesseling-Perry, A. Hasan, E. Elkhammas, Y. S. Zhang, *Kidney Int.* **2018**, *94*, 1073.
- [144] S. Musah, N. Dimitrakakis, D. M. Camacho, G. M. Church, D. E. Ingber, *Nat. Protoc.* **2018**, *13*, 1662.
- [145] K. Schimek, H. H. Hsu, M. Boehme, J. J. Kornet, U. Marx, R. Lauster, R. Pörtner, G. Lindner, *Bioengineering* **2018**, *5*, 43.
- [146] F. Akther, S. B. Yakob, N.-T. Nguyen, H. T. Ta, *Biosensors* **2020**, *10*, 182.
- [147] R. Nossa, J. Costa, L. Cacopardo, A. Ahluwalia, *J. Tissue Eng.* **2021**, *12*, 20417314211008696.
- [148] D. Huh, B. D. Matthews, A. Mammoto, M. Montoya-Zavala, H. Y. Hsin, D. E. Ingber, *Science* **2010**, *328*, 1662 LP.
- [149] M. Ochs, J. R. Nyengaard, A. Jung, L. Knudsen, M. Voigt, T. Wahlers, J. Richter, H. J. G. Gundersen, *Am. J. Respir. Crit. Care Med.* **2004**, *169*, 120.
- [150] D. Huh, *Ann. Am. Thorac. Soc.* **2015**, *12*, S42.
- [151] D. Huh, D. C. Leslie, B. D. Matthews, J. P. Fraser, S. Jurek, G. A. Hamilton, K. S. Thorneloe, M. A. McAlexander, D. E. Ingber, *Sci. Transl. Med.* **2012**, *4*, 159ra147.
- [152] M. W. Toepke, D. J. Beebe, *Lab Chip* **2006**, *6*, 1484.
- [153] N. Siddiqui, S. Asawa, B. Birru, R. Baadhe, S. Rao, *Mol. Biotechnol.* **2018**, *60*, 506.
- [154] S. Gautam, A. K. Dinda, N. C. Mishra, *Mater. Sci. Eng. C* **2013**, *33*, 1228.
- [155] C. Vaquette, C. Frochot, R. Rahouadj, S. Muller, X. Wang, *Soft Mater* **2008**, *6*, 25.
- [156] T. Li, L. Tian, S. Liao, X. Ding, S. A. Irvine, S. Ramakrishna, *J. Mech. Behav. Biomed. Mater.* **2019**, *98*, 48.
- [157] Q. Yao, W. Zhang, Y. Hu, J. Chen, C. Shao, X. Fan, Y. Fu, *Exp. Ther. Med.* **2017**, *14*, 4141.
- [158] I. V. Gilevich, I. S. Polyakov, V. A. Porkhanov, V. P. Chekhonin, *Bull. Exp. Biol. Med.* **2017**, *163*, 400.
- [159] X. Chen, Y. Y. Qi, L. L. Wang, Z. Yin, G. L. Yin, X. H. Zou, H. W. Ouyang, *Biomaterials* **2008**, *29*, 3683.
- [160] C. Dong, Y. Lv, *Polymers* **2016**, *8*, 42.
- [161] M. P. Linnes, B. D. Ratner, C. M. Giachelli, *Biomaterials* **2007**, *28*, 5298.
- [162] L. Almany, D. Seliktar, *Biomaterials* **2005**, *26*, 2467.
- [163] H. G. Şenel Ayaz, A. Perets, H. Ayaz, K. D. Gilroy, M. Govindaraj, D. Brookstein, P. I. Lelkes, *Biomaterials* **2014**, *35*, 8540.
- [164] B. Zhang, M. Montgomery, M. D. Chamberlain, S. Ogawa, A. Korolj, A. Pahnke, L. A. Wells, S. Masse, J. Kim, L. Reis, A. Momen, S. S. Nunes, A. R. Wheeler, K. Nanthakumar, G. Keller, M. V. Sefton, M. Radisic, *Nat. Mater.* **2016**, *15*, 669.
- [165] K. A. Homan, D. B. Kolesky, M. A. Skylar-Scott, J. Herrmann, H. Obuobi, A. Moisan, J. A. Lewis, *Sci. Rep.* **2016**, *6*, 34845.
- [166] E. J. Weber, A. Chapron, B. D. Chapron, J. L. Voellinger, K. A. Lidberg, C. K. Yeung, Z. Wang, Y. Yamaura, D. W. Hailey, T. Neumann, D. D. Shen, K. E. Thummel, K. A. Muczynski, J. Himmelfarb, E. J. Kelly, *Kidney Int.* **2016**, *90*, 627.
- [167] S. J. Trietsch, E. Naumovska, D. Kurek, M. C. Setyawati, M. K. Vormann, K. J. Wilschut, H. L. Lanz, A. Nicolas, C. P. Ng, J. Joore, S. Kustermann, A. Roth, T. Hankemeier, A. Moisan, P. Vulto, *Nat. Commun.* **2017**, *8*, 262.
- [168] G. Adriani, D. Ma, A. Pavesi, R. D. Kamm, E. L. K. Goh, *Lab Chip* **2017**, *17*, 448.
- [169] D. T. T. Phan, X. Wang, B. M. Craver, A. Sobrino, D. Zhao, J. C. Chen, L. Y. N. Lee, S. C. George, A. P. Lee, C. C. W. Hughes, *Lab Chip* **2017**, *17*, 511.
- [170] X. Yang, K. Li, X. Zhang, C. Liu, B. Guo, W. Wen, X. Gao, *Lab Chip* **2018**, *18*, 486.
- [171] M. J. Mondrinos, Y. S. Yi, N. K. Wu, X. Ding, D. Huh, *Lab Chip* **2017**, *17*, 3146.
- [172] K. L. Sellgren, E. J. Butala, B. P. Gilmour, S. H. Randell, S. Grego, *Lab Chip* **2014**, *14*, 3349.
- [173] C. C. Peng, W. H. Liao, Y. H. Chen, C. Y. Wu, Y. C. Tung, *Lab Chip* **2013**, *13*, 3239.
- [174] D. D. Nalayanda, Q. Wang, W. B. Fulton, T. H. Wang, F. Abdullah, *J. Pediatr. Surg.* **2010**, *45*, 45.
- [175] S. Lee, J. Ko, D. Park, S. R. Lee, M. Chung, Y. Lee, N. L. Jeon, *Lab Chip* **2018**, *18*, 2686.
- [176] P. Zamprogno, S. Wüthrich, S. Achenbach, G. Thoma, J. D. Stucki, N. Hobi, N. Schneider-Daum, C. M. Lehr, H. Huwer, T. Geiser, R. A. Schmid, O. T. Guenat, *Commun. Biol.* **2021**, *4*, 168.
- [177] M. Humayun, C. W. Chow, E. W. K. Young, *Lab Chip* **2018**, *18*, 1298.
- [178] P. Zamprogno, S. Wüthrich, S. Achenbach, G. Thoma, J. D. Stucki, N. Hobi, N. Schneider-Daum, C. M. Lehr, H. Huwer, T. Geiser, R. A. Schmid, O. T. Guenat, *Commun. Biol.* **2021**, *4*, 168.
- [179] J. D. Stucki, N. Hobi, A. Galimov, A. O. Stucki, N. Schneider-Daum, C.-M. Lehr, H. Huwer, M. Frick, M. Funke-Chambour, T. Geiser, O. T. Guenat, *Sci. Rep.* **2018**, *8*, 14359.
- [180] A. O. Stucki, J. D. Stucki, S. R. R. Hall, M. Felder, Y. Mermoud, R. A. Schmid, T. Geiser, O. T. Guenat, *Lab Chip* **2015**, *15*, 1302.
- [181] D. Huh, H. J. Kim, J. P. Fraser, D. E. Shea, M. Khan, A. Bahinski, G. A. Hamilton, D. E. Ingber, *Nat. Protoc.* **2013**, *8*, 2135.
- [182] Y. Mermoud, M. Felder, J. D. Stucki, A. O. Stucki, O. T. Guenat, *Sensors Actuators, B Chem* **2018**, *255*, 3647.
- [183] S. C. Faber, S. D. McCullough, *Appl. Vitro. Toxicol.* **2018**, *4*, 115.
- [184] J. C. Nawroth, R. Barrile, D. Conegliano, S. van Riet, P. S. Hiemstra, R. Villenave, *Adv. Drug Delivery Rev.* **2019**, *140*, 12.
- [185] H. W. Snoeck, *Development* **2015**, *142*, 13.
- [186] R. F. Conway, T. Frum, A. S. Conchola, J. R. Spence, *BioEssays* **2020**, *42*, 2000006.
- [187] M. Hagiwara, N. Maruta, M. Marumoto, *Tissue Eng., Part C* **2017**, *23*, 323.
- [188] S. E. Gilpin, D. E. Wagner, *Eur. Respir. Rev.* **2018**, *27*, 180021.
- [189] Y. S. Prakash, D. J. Tschumperlin, K. R. Stenmark, *Am. J. Physiol.: Lung Cell. Mol. Physiol.* **2015**, *309*, L625.
- [190] Y.-W. Chen, S. X. Huang, A. L. R. T. de Carvalho, S.-H. Ho, M. N. Islam, S. Volpi, L. D. Notarangelo, M. Ciancanelli, J.-L. Casanova, J. Bhattacharya, A. F. Liang, L. M. Palermo, M. Porotto, A. Moscona, H. - W. Snoeck, *Nat. Cell Biol.* **2017**, *19*, 542.
- [191] A. I. Vazquez-Armendariz, M. Heiner, E. El Agha, I. Salwig, A. Hoek, M. C. Hessler, I. Shalashova, A. Shrestha, G. Carraro, J. P. Mengel, A. Günther, R. E. Morty, I. Vadász, M. Schwemmler, W. Kummer, T. Hain, A. Goesmann, S. Bellusci, W. Seeger, T. Braun, S. Herold, *EMBO J.* **2020**, *39*, 103476.
- [192] A. Jain, R. Barrile, A. van der Meer, A. Mammoto, T. Mammoto, K. De Ceunynck, O. Aisiku, M. Otieno, C. Loudon, G. Hamilton, R. Flaumenhaft, D. Ingber, *Clin. Pharmacol. Ther.* **2018**, *103*, 332.
- [193] K. Han, S. E. Pierce, A. Li, K. Spees, G. R. Anderson, J. A. Seoane, Y. H. Lo, M. Dubreuil, M. Olivas, R. A. Kamber, M. Wainberg, K. Kostyrko, M. R. Kelly, M. Yousefi, S. W. Simpkins, D. Yao, K. Lee, C. J. Kuo, P. K. Jackson, A. Sweet-Cordero, A. Kundaje, A. J. Gentles, C. Curtis, M. M. Winslow, M. C. Bassik, *Nature* **2020**, *580*, 136.
- [194] V. Kilin, C. Mas, S. Constant, J.-P. Wolf, L. Bonacina, *Sci. Rep.* **2017**, *7*, 16233.
- [195] Y. Korogi, S. Gotoh, S. Ikeo, Y. Yamamoto, N. Sone, K. Tamai, S. Konishi, T. Nagasaki, H. Matsumoto, I. Ito,

- T. F. Chen-Yoshikawa, H. Date, M. Hagiwara, I. Asaka, A. Hotta, M. Mishima, T. Hirai, *Stem Cell Rep.* **2019**, *12*, 431.
- [196] M. Porotto, M. Ferren, Y. W. Chen, Y. Siu, N. Makhsous, B. Rima, T. Briese, A. L. Greninger, H. W. Snoeck, A. Moscona, *MBio* **2019**, *10*, e00723.
- [197] J. Huang, A. J. Hume, K. M. Abo, R. B. Werder, C. Villacorta-Martin, K. D. Alysandratos, M. Lou Beermann, C. Simone-Roach, J. Lindstrom-Vautrin, J. Olejnik, E. L. Suder, E. Bullitt, A. Hinds, A. Sharma, M. Bosmann, R. Wang, F. Hawkins, E. J. Burks, M. Saeed, A. A. Wilson, E. Mühlberger, D. N. Kotton, *Cell Stem Cell* **2020**, *27*, 962.
- [198] M. Zhang, P. Wang, R. Luo, Y. Wang, Z. Li, Y. Guo, Y. Yao, M. Li, T. Tao, W. Chen, J. Han, H. Liu, K. Cui, X. Zhang, Y. Zheng, J. Qin, *Adv. Sci.* **2021**, *8*, 2002928.
- [199] H. Katsura, V. Sontake, A. Tata, Y. Kobayashi, C. E. Edwards, B. E. Heaton, A. Konkimalla, T. Asakura, Y. Mikami, E. J. Fritch, P. J. Lee, N. S. Heaton, R. C. Boucher, S. H. Randell, R. S. Baric, P. R. Tata, *Cell Stem Cell* **2020**, *27*, 890.
- [200] R. Novak, M. Didier, E. Calamari, C. F. Ng, Y. Choe, S. L. Clauson, B. A. Nestor, J. Puerta, R. Fleming, S. J. Firoozinezhad, D. E. Ingber, *J. Vis. Exp.* **2018**, *140*, 58151.
- [201] M. Felder, B. Trueeb, A. O. Stucki, S. Borcard, J. D. Stucki, B. Schnyder, T. Geiser, O. T. Guenat, *Front. Bioeng. Biotechnol.* **2019**, *7*, 1.
- [202] S. Wang, E. Li, Y. Gao, Y. Wang, Z. Guo, J. He, J. Zhang, Z. Gao, Q. Wang, *PLoS One* **2013**, *8*, 56448.
- [203] T. Yu, Z. Guo, H. Fan, J. Song, Y. Liu, Z. Gao, Q. Wang, *Oncotarget* **2016**, *7*, 25593.
- [204] L. Zhao, Z. Wang, S. Fan, Q. Meng, B. Li, S. Shao, Q. Wang, *Biomed. Microdevices* **2010**, *12*, 325.
- [205] B. A. Hassell, G. Goyal, E. Lee, A. Sontheimer-Phelps, O. Levy, C. S. Chen, D. E. Ingber, *Cell Rep.* **2017**, *21*, 508.
- [206] S. H. Kim, J. H. Kang, I. Y. Chung, B. G. Chung, *Electrophoresis* **2011**, *32*, 254.
- [207] S. Han, J. J. Yan, Y. Shin, J. J. Jeon, J. Won, H. E. Jeong, R. D. Kamm, Y. J. Kim, S. Chung, *Lab Chip* **2012**, *12*, 3861.
- [208] K. H. Benam, R. Villenave, C. Lucchesi, A. Varone, C. Hubeau, H. H. Lee, S. E. Alves, M. Salmon, T. C. Ferrante, J. C. Weaver, A. Bahinski, G. A. Hamilton, D. E. Ingber, *Nat. Methods* **2016**, *13*, 151.
- [209] K. H. Benam, M. Mazur, Y. Choe, T. C. Ferrante, R. Novak, D. E. Ingber, *Methods in Molecular Biology*, Humana Press Inc., New Jersey **2017**, pp. 345–365.
- [210] A. P. Nesmith, A. Agarwal, M. L. McCain, K. K. Parker, *Lab Chip* **2014**, *14*, 3925.
- [211] M. Asmani, S. Velumani, Y. Li, N. Wawrzyniak, I. Hsia, Z. Chen, B. Hinz, R. Zhao, *Nat. Commun.* **2018**, *9*, 2066.
- [212] T. H. Punde, W.-H. Wu, P.-C. Lien, Y.-L. Chang, P.-H. Kuo, M. D.-T. Chang, K.-Y. Lee, C.-D. Huang, H.-P. Kuo, Y.-F. Chan, P.-C. Shih, C.-H. Liu, *Integr. Biol.* **2015**, *7*, 162.
- [213] L. J. Barkal, C. L. Procknow, Y. R. Álvarez-García, M. Niu, J. A. Jiménez-Torres, R. A. Brockman-Schneider, J. E. Gern, L. C. Denlinger, A. B. Theberge, N. P. Keller, E. Berthier, D. J. Beebe, *Nat. Commun.* **2017**, *8*, 1770.
- [214] A. Artzy-Schnirman, H. Zidan, S. Elias-Kirma, L. Ben-Porat, J. Tenenbaum-Katan, P. Carius, R. Fishler, N. Schneider-Daum, C. Lehr, J. Sznitman, *Adv. Biosyst.* **2019**, *3*, 1900026.
- [215] H. Tavana, P. Zamankhan, P. J. Christensen, J. B. Grotberg, S. Takayama, *Biomed. Microdevices* **2011**, *13*, 731.
- [216] S. K. Gupta, E. A. Torrico Guzmán, S. A. Meenach, *Int. J. Cancer* **2017**, *141*, 2143.
- [217] L. Wallstabe, C. Göttlich, L. C. Nelke, J. Kühnemundt, T. Schwarz, T. Nerreter, H. Einsele, H. Walles, G. Dandekar, S. L. Nietzer, M. Hudecek, *JCI Insight* **2019**, *4*, 126345.
- [218] J. Chen, X. Chu, J. Zhang, Q. Nie, W. Tang, J. Su, H. Yan, H. Zheng, Z. Chen, X. Chen, M.-M. Song, X. Yi, P.-S. Li, Y.-F. Guan, G. Li, C.-X. Deng, R. Rosell, Y.-L. Wu, W.-Z. Zhong, *Thorac. Cancer* **2020**, *11*, 2279.
- [219] D. J. Jung, T. H. Shin, M. Kim, C. O. Sung, S. J. Jang, G. S. Jeong, *Lab Chip* **2019**, *19*, 2854.
- [220] Z. Xu, Y. Gao, Y. Hao, E. Li, Y. Wang, J. Zhang, W. Wang, Z. Gao, Q. Wang, *Biomaterials* **2013**, *34*, 4109.
- [221] F. J. Kelly, J. C. Fussell, *Philos. Trans. R. Soc. A Math. Phys. Eng. Sci.* **2020**, *378*, 20190322.
- [222] M. S. Peixoto, M. F. de Oliveira Galvão, S. R. Batistuzzo de Medeiros, *Chemosphere* **2017**, *188*, 32.
- [223] C. F. Vogelmeier, G. J. Criner, F. J. Martinez, A. Anzueto, P. J. Barnes, J. Bourbeau, B. R. Celli, R. Chen, M. Decramer, L. M. Fabbri, P. Frith, D. M. G. Halpin, M. V. López Varela, M. Nishimura, N. Roche, R. Rodriguez-Roisin, D. D. Sin, D. Singh, R. Stockley, J. Vestbo, J. A. Wedzicha, A. Agustí, *Am. J. Respir. Crit. Care Med.* **2017**, *195*, 557.
- [224] K. Ganguly, B. Levänen, L. Palmberg, A. Åkesson, A. Lindén, *Eur. Respir. Rev.* **2018**, *27*, 170122.
- [225] R. Xiong, Q. Wu, R. Trbojevich, L. Muskhelishvili, K. Davis, M. Bryant, P. Richter, X. Cao, *Toxicol. Lett.* **2019**, *303*, 16.
- [226] J. A. Gindele, T. Kiechle, K. Benediktus, G. Birk, M. Brendel, F. Heinemann, C. T. Wohnhaas, M. LeBlanc, H. Zhang, Y. Strulovici-Barel, R. G. Crystal, M. J. Thomas, B. Stierstorfer, K. Quast, J. Schymeinsky, *Sci. Rep.* **2020**, *10*, 6257.
- [227] A. R. Iskandar, Y. Martinez, F. Martin, W. K. Schlage, P. Leroy, A. Sewer, L. O. Torres, S. Majeed, C. Merg, K. Trivedi, E. Guedj, S. Frentzel, C. Mathis, N. V. Ivanov, M. C. Peitsch, J. Hoeng, *Toxicol. Res.* **2017**, *6*, 930.
- [228] K. H. Benam, R. Novak, J. Nawroth, M. Hirano-Kobayashi, T. C. Ferrante, Y. Choe, R. Prantil-Baun, J. C. Weaver, A. Bahinski, K. K. Parker, D. E. Ingber, *Cell Syst* **2016**, *3*, 456.
- [229] C. Herr, K. Tsitouras, J. Niederstraßer, C. Backes, C. Beisswenger, L. Dong, L. Guillot, A. Keller, R. Bals, *Respir. Res.* **2020**, *21*, 67.
- [230] H. M. Braakhuis, S. K. Kloet, S. Kezic, F. Kuper, M. V. D. Z. Park, S. Bellmann, M. van der Zande, S. Le Gac, P. Krystek, R. J. B. Peters, I. M. C. M. Rietjens, H. Bouwmeester, *Arch. Toxicol.* **2015**, *89*, 1469.
- [231] J. Ji, A. Hedelin, M. Malmlöf, V. Kessler, G. Seisenbaeva, P. Gerde, L. Palmberg, *PLoS One* **2017**, *12*, 0170428.
- [232] J. Li, H. Yang, S. Sha, J. Li, Z. Zhou, Y. Cao, *Ecotoxicol. Environ. Saf.* **2019**, *186*, 109770.
- [233] F. Zhang, G. V. Aquino, A. Dabi, E. D. Bruce, *Toxicol. Vitro.* **2019**, *56*, 1.
- [234] D. Ritter, J. Knebel, M. Niehof, I. Loiaz, M. Marradi, R. Gracia, Y. te Welscher, C. F. van Nostrum, C. Falciani, A. Pini, M. Strandh, T. Hansen, *Toxicol. Vitro.* **2020**, *63*, 104714.
- [235] S. Elias-Kirma, A. Artzy-Schnirman, P. Das, M. Heller-Algazi, N. Korin, J. Sznitman, *Front. Bioeng. Biotechnol.* **2020**, *8*, 91.
- [236] F. Blank, B. M. Rothen-Rutishauser, S. Schurch, P. Gehr, *J. Aerosol Med. Depos. Clear. Eff. Lung* **2006**, *19*, 392.
- [237] A. G. Lenz, T. Stoeger, D. Cej, M. Schmidmeir, N. Semren, G. Burgstaller, B. Lentner, O. Eickelberg, S. Meiners, O. Schmid, *Am. J. Respir. Cell Mol. Biol.* **2014**, *51*, 526.
- [238] M. Röhm, S. Carle, F. Maigler, J. Flamm, V. Kramer, C. Mavoungou, O. Schmid, K. Schindowski, *Int. J. Pharm.* **2017**, *532*, 537.
- [239] D. Cej, A. Doryab, A. Lenz, A. Schröppel, P. Mayer, G. Burgstaller, R. Nossa, A. Ahluwalia, O. Schmid, *Biotechnol. Bioeng.* **2021**, *118*, 690.
- [240] D. Mazzei, M. A. Guzzardi, S. Giusti, A. Ahluwalia, *Biotechnol. Bioeng.* **2010**, *106*, 127.
- [241] S. Giusti, F. Pagliari, F. Vozzi, A. Tirella, D. Mazzei, M. Cabiati, S. Del Ry, A. Ahluwalia, *Procedia Eng.* **2013**, *59*, 219.
- [242] M. Zhang, C. Xu, L. Jiang, J. Qin, *Toxicol. Res.* **2018**, *7*, 1048.
- [243] R. Fishler, P. Hofemeier, Y. Etzion, Y. Dubowski, J. Sznitman, *Sci. Rep.* **2015**, *5*, 14071.
- [244] C. Méausoone, R. El Khawaja, G. Tremolet, S. Siffert, R. Cousin, F. Cazier, S. Billet, D. Courcot, Y. Landkocz, *Toxicol. Vitro.* **2019**, *58*, 110.

- [245] C. Bisig, P. Comte, M. Güdel, J. Czerwinski, A. Mayer, L. Müller, A. Petri-Fink, B. Rothen-Rutishauser, *Environ. Pollut.* **2018**, 235, 263.
- [246] P. S. Hiemstra, G. Grootaers, A. M. van der Does, C. A. M. Krul, I. M. Kooter, *Toxicol. Vitro* **2018**, 47, 137.
- [247] S. Upadhyay, L. Palmberg, *Toxicol. Sci.* **2018**, 164, 21.
- [248] J. Fogh, J. M. Fogh, T. Orfeo, *J. Natl. Cancer Inst.* **1977**, 59, 221.
- [249] B. Q. Shen, W. E. Finkbeiner, J. J. Wine, R. J. Msrny, J. H. Widdicombe, *Am. J. Physiol.: Lung Cell. Mol. Physiol.* **1994**, 266, L493.
- [250] M. Brower, D. N. Carney, H. K. Oie, A. F. Gazdar, J. D. Minna, *Cancer Res.* **1986**, 46, 798.
- [251] D. Giard, S. Aaronson, G. Todaro, P. Arnstein, J. Kersey, H. Dosik, W. Parks, *J. Natl. Cancer Inst.* **1973**, 51, 1417.
- [252] A. L. Cozens, M. J. Yezzi, K. Kunzelmann, T. Ohrui, L. Chin, K. Eng, W. E. Finkbeiner, J. H. Widdicombe, D. C. Gruenert, *Am. J. Respir. Cell Mol. Biol.* **1994**, 10, 38.
- [253] C. D. Albright, R. T. Jones, E. A. Hudson, J. A. Fontana, B. F. Trump, J. H. Resau, *Cell Biol. Toxicol.* **1990**, 6, 379.
- [254] A. Kuehn, S. Kletting, C. De Souza Carvalho-Wodarz, U. Repnik, G. Griffiths, U. Fischer, E. Meese, H. Huwer, D. Wirth, T. May, N. Schneider-Daum, C.-M. Lehr, *ALTEX* **2016**, 33, 251.
- [255] P. K. Mehta, R. K. Karls, E. H. White, E. W. Ades, F. D. Quinn, *Microb. Pathog.* **2006**, 41, 119.
- [256] H. Zeng, C. Pappas, J. A. Belser, K. V. Houser, W. Zhong, D. A. Wadford, T. Stevens, R. Balczon, J. M. Katz, T. M. Tumpey, *J. Virol.* **2012**, 86, 667.
- [257] W. Suh, *Arch. Pharm. Res.* **2017**, 40, 1.
- [258] B. A. Calvert, A. L. Ryan, in *Advances in Experimental Medicine and Biology*, Springer, Berlin **2020**, pp. 1–16.
- [259] P. F. Mercer, K. Abbott-Banner, I. M. Adcock, R. G. Knowles, *Clin. Sci.* **2015**, 128, 235.
- [260] Q. Wang, S. Bhattacharya, J. A. Mereness, C. Anderson, J. A. Lillis, R. S. Misra, S. Romas, H. Huyck, A. Howell, G. Bandyopadhyay, K. Donlon, J. R. Myers, J. Ashton, G. S. Pryhuber, T. J. Mariani, *Pediatr. Res.* **2019**, 87, 511.
- [261] A. L. Gard, R. J. Luu, C. R. Miller, R. Maloney, B. P. Cain, E. E. Marr, D. M. Burns, R. Gaibler, T. J. Mulhern, C. A. Wong, J. Alladina, J. R. Coppeta, P. Liu, J. P. Wang, H. Azizgolshani, R. F. Fezzie, J. L. Balestrini, B. C. Isenberg, B. D. Medoff, R. W. Finberg, J. T. Borenstein, *Sci. Rep.* **2021**, 11, 14961.
- [262] S. Moradi, H. Mahdizadeh, T. Šarić, J. Kim, J. Harati, H. Shahsavarani, B. Greber, J. B. Moore, *Stem Cell Res. Ther.* **2019**, 10, 341.
- [263] E. Ahmed, C. Sansac, S. Assou, D. Gras, A. Petit, I. Vachier, P. Chanez, J. De Vos, A. Bourdin, *Pharmacol. Ther.* **2018**, 183, 58.
- [264] R. Wang, K. B. McCauley, D. N. Kotton, F. Hawkins, in *Methods in Cell Biology*, Academic Press Inc., Cambridge, MA **2020**, pp. 95–114.
- [265] K. Takahashi, S. Yamanaka, *Cell* **2006**, 126, 663.
- [266] L. Cong, F. A. Ran, D. Cox, S. Lin, R. Barretto, N. Habib, P. D. Hsu, X. Wu, W. Jiang, L. A. Marraffini, F. Zhang, *Science* **2013**, 339, 819.
- [267] P. Mali, L. Yang, K. M. Esvelt, J. Aach, M. Guell, J. E. DiCarlo, J. E. Norville, G. M. Church, *Science* **2013**, 339, 823.
- [268] P. Karagiannis, K. Takahashi, M. Saito, Y. Yoshida, K. Okita, A. Watanabe, H. Inoue, J. K. Yamashita, M. Todani, M. Nakagawa, M. Osawa, Y. Yashiro, S. Yamanaka, K. Osafune, *Physiol. Rev.* **2019**, 99, 79.
- [269] A. Berical, R. E. Lee, S. H. Randell, F. Hawkins, *Front. Pharmacol.* **2019**, 10, 74.
- [270] M. A. Glicksman, *Clin. Ther.* **2018**, 40, 1060.
- [271] Y. Shi, H. Inoue, J. C. Wu, S. Yamanaka, *Nat. Rev. Drug Discovery* **2017**, 16, 115.
- [272] M. Grskovic, A. Javaherian, B. Strulovici, G. Q. Daley, *Nat. Rev. Drug Discovery* **2011**, 10, 915.
- [273] F. Hawkins, D. N. Kotton, *Ann. Am. Thorac. Soc.* **2015**, 12, S50.
- [274] A. Somers, J.-C. Jean, C. A. Sommer, A. Omari, C. C. Ford, J. A. Mills, L. Ying, A. G. Sommer, J. M. Jean, B. W. Smith, R. Lafyatis, M. - F. Demierre, D. J. Weiss, D. L. French, P. Gadue, G. J. Murphy, G. Mostoslavsky, D. N. Kotton, *Stem Cells* **2010**, 28, 1728.
- [275] A. P. Wong, S. Chin, S. Xia, J. Garner, C. E. Bear, J. Rossant, *Nat. Protoc.* **2015**, 10, 363.
- [276] S. T. Rashid, S. Corbiveau, N. Hannan, S. J. Marciniak, E. Miranda, G. Alexander, I. Huang-Doran, J. Griffin, L. Ahrlund-Richter, J. Skepper, R. Semple, A. Weber, D. A. Lomas, L. Vallier, *J. Clin. Invest.* **2010**, 120, 3127.
- [277] N. Lachmann, C. Happle, M. Ackermann, D. Lüttge, M. Wetzke, S. Merkert, M. Hetzel, G. Kensah, M. Jara-Avaca, A. Mucci, J. Skuljec, A. M. Dittrich, N. Pfaff, S. Brenning, A. Schambach, D. Steinemann, G. Göhring, T. Cantz, U. Martin, N. Schwerk, G. Hansen, T. Moritz, *Am. J. Respir. Crit. Care Med.* **2014**, 189, 167.
- [278] B. R. Dye, A. J. Miller, J. R. Spence, *Curr. Pathobiol. Rep.* **2016**, 4, 47.
- [279] M. Ghaedi, L. E. Niklason, J. C. Williams, *Curr. Transplant. Rep.* **2015**, 2, 81.
- [280] C. T. Stabler, E. E. Morrissey, *Cell Tissue Res.* **2017**, 367, 677.
- [281] M. L. Litvack, T. J. Wagle, J. Lee, J. Wang, C. Ackerley, E. Grunebaum, M. Post, *Am. J. Respir. Crit. Care Med.* **2016**, 193, 1219.
- [282] K. Takata, T. Kozaki, C. Z. W. Lee, M. S. Thion, M. Otsuka, S. Lim, K. H. Utami, K. Fidan, D. S. Park, B. Malleret, S. Chakarov, P. See, D. Low, G. Low, M. Garcia-Miralles, R. Zeng, J. Zhang, C. C. Goh, A. Gul, S. Hubert, B. Lee, J. Chen, I. Low, N. B. Shadan, J. Lum, T. S. Wei, E. Mok, S. Kawanishi, Y. Kitamura, A. Larbi, et al., *Immunity* **2017**, 47, 183.
- [283] X. Yu, A. Buttgerit, I. Lelios, S. G. Utz, D. Cansever, B. Becher, M. Greter, *Immunity* **2017**, 47, 903.
- [284] E. G. Perdiguerro, F. Geissmann, *Cold Spring Harb. Symp. Quant. Biol.* **2013**, 78, 91.
- [285] J. Buchrieser, W. James, M. D. Moore, *Stem Cell Rep.* **2017**, 8, 334.
- [286] A. Kubo, K. Shinozaki, J. M. Shannon, V. Kouskoff, M. Kennedy, S. Woo, H. J. Fehling, G. Keller, *Development* **2004**, 131, 1651.
- [287] K. A. D'Amour, A. D. Agulnick, S. Eliazar, O. G. Kelly, E. Kroon, E. E. Baetge, *Nat. Biotechnol.* **2005**, 23, 1534.
- [288] A. Korostylev, P. U. Mahaddalkar, O. Keminer, K. Hadian, K. Schorpp, P. Gribbon, H. Lickert, *Mol. Metab.* **2017**, 6, 640.
- [289] J. R. Spence, C. N. Mayhew, S. A. Rankin, M. F. Kuhar, J. E. Vallance, K. Tolle, E. E. Hoskins, V. V. Kalinichenko, S. I. Wells, A. M. Zorn, N. F. Shroyer, J. M. Wells, *Nature* **2011**, 470, 105.
- [290] K. Cameron, R. Tan, W. Schmidt-Heck, G. Campos, M. J. Lyall, Y. Wang, B. Lucendo-Villarin, D. Szkolnicka, N. Bates, S. J. Kimber, J. G. Hengstler, P. Godoy, S. J. Forbes, D. C. Hay, *Stem Cell Rep.* **2015**, 5, 1250.
- [291] K. A. D'Amour, A. G. Bang, S. Eliazar, O. G. Kelly, A. D. Agulnick, N. G. Smart, M. A. Moorman, E. Kroon, M. K. Carpenter, E. E. Baetge, *Nat. Biotechnol.* **2006**, 24, 1392.
- [292] T. A. Longmire, L. Ikonomou, F. Hawkins, C. Christodoulou, Y. Cao, J. C. Jean, L. W. Kwok, H. Mou, J. Rajagopal, S. S. Shen, A. A. Dowton, M. Serra, D. J. Weiss, M. D. Green, H. - W. Snoeck, M. I. Ramirez, D. N. Kotton, *Cell Stem Cell* **2012**, 10, 398.
- [293] M. S. Bogacheva, S. Khan, L. K. Kanninen, M. Yliperttula, A. W. Leung, Y. R. Lou, *J. Cell. Physiol.* **2018**, 233, 3578.
- [294] M. D. Green, A. Chen, M. C. Nostro, S. L. D'Souza, C. Schaniel, I. R. Lemischka, V. Gouon-Evans, G. Keller, H. W. Snoeck, *Nat. Biotechnol.* **2011**, 29, 267.
- [295] A. P. Wong, C. E. Bear, S. Chin, P. Pasceri, T. O. Thompson, L. J. Huan, F. Ratjen, J. Ellis, J. Rossant, *Nat. Biotechnol.* **2012**, 30, 876.
- [296] A. L. Firth, C. T. Dargitz, S. J. Qualls, T. Menon, R. Wright, O. Singer, F. H. Gage, A. Khanna, I. M. Verma, *Proc. Natl. Acad. Sci. USA* **2014**, 111, 1723.

- [297] F. Hawkins, P. Kramer, A. Jacob, I. Driver, D. C. Thomas, K. B. McCauley, N. Skvir, A. M. Crane, A. A. Kurmann, A. N. Hollenberg, S. Nguyen, B. G. Wong, A. S. Khalil, S. X. L. Huang, S. Guttentag, J. R. Rock, J. M. Shannon, B. R. Davis, D. N. Kotton, *J. Clin. Invest.* **2017**, *127*, 2277.
- [298] S. X. L. Huang, M. N. Islam, J. O'Neill, Z. Hu, Y. G. Yang, Y. W. Chen, M. Mumau, M. D. Green, G. Vunjak-Novakovic, J. Bhattacharya, H. - W. Snoeck, *Nat. Biotechnol.* **2014**, *32*, 84.
- [299] S. Gotoh, I. Ito, T. Nagasaki, Y. Yamamoto, S. Konishi, Y. Korogi, H. Matsumoto, S. Muro, T. Hirai, M. Funato, S. - I. Mae, T. Toyoda, A. Sato-Otsubo, S. Ogawa, K. Osafune, M. Mishima, *Stem Cell Rep.* **2014**, *3*, 394.
- [300] A. Jacob, M. Morley, F. Hawkins, K. B. McCauley, J. C. Jean, H. Heins, C. L. Na, T. E. Weaver, M. Vedaie, K. Hurley, A. Hinds, S. J. Russo, S. Kook, W. Zacharias, M. Ochs, K. Traber, L. J. Quinton, A. Crane, B. R. Davis, F. V. White, J. Wambach, J. A. Whitsett, F. S. Cole, E. E. Morrissey, S. H. Guttentag, M. F. Beers, D. N. Kotton, *Cell Stem Cell* **2017**, *21*, 472.
- [301] K. B. McCauley, F. Hawkins, M. Serra, D. C. Thomas, A. Jacob, D. N. Kotton, *Cell Stem Cell* **2017**, *20*, 844.
- [302] S. Konishi, S. Gotoh, K. Tateishi, Y. Yamamoto, Y. Korogi, T. Nagasaki, H. Matsumoto, S. Muro, T. Hirai, I. Ito, S. Tsukita, M. Mishima, *Stem Cell Rep.* **2016**, *6*, 18.
- [303] S. Yoshie, K. Omori, A. Hazama, *Channels* **2019**, *13*, 227.
- [304] Y. Yamamoto, S. Gotoh, Y. Korogi, M. Seki, S. Konishi, S. Ikeo, N. Sone, T. Nagasaki, H. Matsumoto, S. Muro, I. Ito, T. Hirai, T. Kohno, Y. Suzuki, M. Mishima, *Nat. Methods* **2017**, *14*, 1097.
- [305] A. Jacob, M. Vedaie, D. A. Roberts, D. C. Thomas, C. Villacorta-Martin, K. D. Alysandratos, F. Hawkins, D. N. Kotton, *Nat. Protoc.* **2019**, *14*, 3303.
- [306] M. Ghaedi, E. S. White, L. E. Niklason, M. Ghaedi, E. A. Calle, J. J. Mendez, A. L. Gard, J. Balestrini, A. Booth, P. F. Bove, L. Gui, *J. Clin. Invest.* **2013**, *123*, 4950.
- [307] W. J. Zacharias, D. B. Frank, J. A. Zepp, M. P. Morley, F. A. Alkhaleel, J. Kong, S. Zhou, E. Cantu, E. E. Morrissey, *Nature* **2018**, *555*, 251.
- [308] S. Kanagaki, S. Ikeo, T. Suezawa, Y. Yamamoto, M. Seki, T. Hirai, M. Hagiwara, Y. Suzuki, S. Gotoh, *Stem Cells* **2021**, *39*, 156.
- [309] M. Ghaedi, J. J. Mendez, P. F. Bove, A. Sivarapatna, M. S. B. Raredon, L. E. Niklason, *Biomaterials* **2014**, *35*, 699.
- [310] I. I. Slukvin, A. Kumar, *Cell. Mol. Life Sci.* **2018**, *75*, 3507.
- [311] M. A. Vodyanik, J. Yu, X. Zhang, S. Tian, R. Stewart, J. A. Thomson, I. I. Slukvin, *Cell Stem Cell* **2010**, *7*, 718.
- [312] R. A. Wimmer, A. Leopoldi, M. Aichinger, D. Kerjaschki, J. M. Penninger, *Nat. Protoc.* **2019**, *14*, 3082.
- [313] C. Patsch, L. Challet-Meylan, E. C. Thoma, E. Urich, T. Heckel, J. F. O'Sullivan, S. J. Grainger, F. G. Kapp, L. Sun, K. Christensen, Y. Xia, M. H. C. Florido, W. He, W. Pan, M. Prummer, C. R. Warren, R. Jakob-Roetne, U. Certa, R. Jagasia, P. - O. Freskgård, I. Adatto, D. Kling, P. Huang, L. I. Zon, E. L. Chaikof, R. E. Gerszten, M. Graf, R. Iacone, C. A. Cowan, *Nat. Cell Biol.* **2015**, *17*, 994.
- [314] A. Harding, E. Cortez-Toledo, N. L. Magner, J. R. Beegle, D. P. Coleal-Bergum, D. Hao, A. Wang, J. A. Nolte, P. Zhou, *Stem Cells* **2017**, *35*, 909.
- [315] T. Ikuno, H. Masumoto, K. Yamamizu, M. Yoshioka, K. Minakata, T. Ikeda, R. Sakata, J. K. Yamashita, *PLoS One* **2017**, *12*, 0173271.
- [316] R. Ohtani-Kaneko, K. Sato, A. Tsutiya, Y. Nakagawa, K. Hashizume, H. Tazawa, *Biomed. Microdevices* **2017**, *19*, 91.
- [317] R. A. Wimmer, A. Leopoldi, M. Aichinger, N. Wick, B. Hantusch, M. Novatchkova, J. Taubenschmid, M. Hämmerle, C. Esk, J. A. Bagley, D. Lindenhofer, G. Chen, M. Boehm, C. A. Agu, F. Yang, B. Fu, J. Zuber, J. A. Knoblich, D. Kerjaschki, J. M. Penninger, *Nature* **2019**, *565*, 505.
- [318] V. V. Orlova, F. E. Van Den Hil, S. Petrus-Reurer, Y. Drabsch, P. Ten Dijke, C. L. Mummery, *Nat. Protoc.* **2014**, *9*, 1514.
- [319] S. Kusuma, Y. I. Shen, D. Hanjaya-Putra, P. Mali, L. Cheng, S. Gerech, *Proc. Natl. Acad. Sci. USA* **2013**, *110*, 12601.
- [320] C. Happle, N. Lachmann, J. Škuljec, M. Wetzke, M. Ackermann, S. Brenning, A. Mucci, A. C. Jirno, S. Groos, A. Mirenska, C. Hennig, T. Rodt, J. P. Bankstahl, N. Schwerk, T. Moritz, G. Hansen, *Sci. Transl. Med.* **2014**, *6*, 250ra113.
- [321] T. Suzuki, P. Arumugam, T. Sakagami, N. Lachmann, C. Chalk, A. Sallese, S. Abe, C. Trapnell, B. Carey, T. Moritz, P. Malik, C. Lutzko, R. E. Wood, B. C. Trapnell, *Nature* **2014**, *514*, 450.
- [322] N. Lachmann, M. Ackermann, E. Frenzel, S. Liebhaber, S. Brenning, C. Happle, D. Hoffmann, O. Klimentkova, D. Lüttge, T. Buchegger, M. P. Kühnel, A. Schambach, S. Janciauskiene, C. Figueiredo, G. Hansen, J. Skokowa, T. Moritz, *Stem Cell Rep.* **2015**, *4*, 282.
- [323] F. Tasnim, J. Xing, X. Huang, S. Mo, X. Wei, M. H. Tan, H. Yu, *Biomaterials* **2019**, *192*, 377.
- [324] C. Z. W. Lee, T. Kozaki, F. Ginhoux, *Nat. Rev. Immunol.* **2018**, *18*, 716.
- [325] S. X. L. Huang, M. D. Green, A. T. De Carvalho, M. Mumau, Y. W. Chen, S. L. D'souza, H. W. Snoeck, *Nat. Protoc.* **2015**, *10*, 413.
- [326] F. J. Hawkins, S. Suzuki, M. Lou Beermann, C. Barilla, R. Wang, C. Villacorta-Martin, A. Bercal, J. C. Jean, J. Le Suer, T. Matte, C. Simone-Roach, Y. Tang, T. M. Schlaeger, A. M. Crane, N. Matthias, S. X. L. Huang, S. H. Randell, J. Wu, J. R. Spence, G. Carraro, B. R. Stripp, A. Rab, E. J. Sorsher, A. Horani, S. L. Brody, B. R. Davis, D. N. Kotton, *Cell Stem Cell* **2020**, *28*, 79.
- [327] P. Hor, V. Punj, B. A. Calvert, A. Castaldi, A. J. Miller, G. Carraro, B. R. Stripp, S. L. Brody, J. R. Spence, J. K. Ichida, A. L. Ryan, Z. Borok, *iScience* **2020**, *23*, 101083.
- [328] H. R. Heo, J. Kim, W. J. Kim, S. R. Yang, S. S. Han, S. J. Lee, Y. Hong, S. H. Hong, *Sci. Rep.* **2019**, *9*, 505.
- [329] L. Tamò, Y. Hibaoui, S. Kallol, M. P. Alves, C. Albrecht, K. E. Hostettler, A. Feki, J.-S. Rougier, H. Abriel, L. Knudsen, A. Gazdhar, T. Geiser, *Am. J. Physiol. Cell. Mol. Physiol.* **2018**, *315*, L921.
- [330] S. van Riet, D. K. Ninaber, H. M. M. Mikkers, T. D. Tetley, C. R. Jost, A. A. Mulder, T. Pasman, D. Baptista, A. A. Poot, R. Truckenmüller, C. L. Mummery, C. Freund, R. J. Rottier, P. S. Hiemstra, *Sci. Rep.* **2020**, *10*, 5499.
- [331] B. R. Dye, P. H. Dedhia, A. J. Miller, M. S. Nagy, E. S. White, L. D. Shea, J. R. Spence, *Elife* **2016**, *5*, <https://doi.org/10.7554/eLife.19732>.
- [332] A. J. Miller, D. R. Hill, M. S. Nagy, Y. Aoki, B. R. Dye, A. M. Chin, S. Huang, F. Zhu, E. S. White, V. Lama, J. R. Spence, *Stem Cell Rep.* **2018**, *10*, 101.
- [333] A. J. Miller, B. R. Dye, D. Ferrer-Torres, D. R. Hill, A. W. Overeem, L. D. Shea, J. R. Spence, *Nat. Protoc.* **2019**, *14*, 518.
- [334] G. Paolicelli, A. De Luca, S. S. Jose, M. Antonini, I. Teloni, J. Fric, T. Zelante, *Front. Immunol.* **2019**, *10*, 323.
- [335] J. Kong, S. Wen, W. Cao, P. Yue, X. Xu, Y. Zhang, L. Luo, T. Chen, L. Li, F. Wang, et al., *Stem Cell Res. Ther.* **2021**, *12*, 95.
- [336] B. R. Dye, R. L. Youngblood, R. S. Oakes, T. Kasputis, D. W. Clough, J. R. Spence, L. D. Shea, *Biomaterials* **2020**, *234*, 119757.
- [337] J. van der Vaart, H. Clevers, *J. Intern. Med.* **2021**, *289*, 604.
- [338] M. M. Lamers, J. van der Vaart, K. evin Knoops, S. Riesebosch, T. I. Breugem, A. Z. Mykytyn, J. Beumer, D. Schipper, K. Bezstarosti, C. D. Koopman, N. Groen, R. B. G. Ravelli, H. Q. Duimel, J. A. A. Demmers, G. M. G. M. Verjans, M. P. G. Koopmans, M. J. Muraro, P. J. Peters, H. Clevers, B. L. Haagmans, *EMBO J.* **2021**, *40*, 105912.
- [339] S. E. Gilpin, X. Ren, T. Okamoto, J. P. Guyette, H. Mou, J. Rajagopal, D. J. Mathisen, J. P. Vacanti, H. C. Ott, *Ann. Thorac. Surg.* **2014**, *98*, 1721.
- [340] M. Ghaedi, A. V. Le, G. Hatachi, A. Beloiartsev, K. Rocco, A. Sivarapatna, J. J. Mendez, P. Baevova, R. N. Dyal, K. L. Leiby,

- E. S. White, L. E. Niklason, *J. Tissue Eng. Regen. Med.* **2018**, *12*, 1623.
- [341] X. Ren, P. T. Moser, S. E. Gilpin, T. Okamoto, T. Wu, L. F. Tapias, F. E. Mercier, L. Xiong, R. Ghawi, D. T. Scadden, D. J. Mathisen, H. C. Ott, *Nat. Biotechnol.* **2015**, *33*, 1097.
- [342] N. V. Dorrello, B. A. Guenthart, J. D. O'Neill, J. Kim, K. Cunningham, Y. W. Chen, M. Biscotti, T. Swayne, H. M. Wobma, S. X. L. Huang, H. -. W. Snoeck, M. Bacchetta, G. Vunjak-Novakovic, *Sci. Adv.* **2017**, *3*, 1700521.
- [343] N. V. Dorrello, G. Vunjak-Novakovic, *Front. Bioeng. Biotechnol.* **2020**, *8*, 269.
- [344] H. C. Ott, B. Clippinger, C. Conrad, C. Schuetz, I. Pomerantseva, L. Ikononou, D. Kotton, J. P. Vacanti, *Nat. Med.* **2010**, *16*, 927.
- [345] Y. Yuan, A. J. Engler, M. S. Raredon, A. Le, P. Baevova, M. C. Yoder, L. E. Niklason, *Biomaterials* **2019**, *200*, 25.
- [346] D. Sridharan, A. Palaniappan, B. N. Blackstone, J. A. Dougherty, N. Kumar, P. B. Seshagiri, N. Sayed, H. M. Powell, M. Khan, *Mater. Sci. Eng. C* **2021**, *118*, 111354.
- [347] N. Kumar, D. Sridharan, A. Palaniappan, J. A. Dougherty, A. Czirok, D. G. Isai, M. Mergaye, M. G. Angelos, H. M. Powell, M. Khan, *Front. Bioeng. Biotechnol.* **2020**, *8*, 567842.
- [348] F. Maiullari, M. Costantini, M. Milan, V. Pace, M. Chirivi, S. Maiullari, A. Rainer, D. Baci, H. E. S. Marei, D. Seliktar, C. Gargioli, C. Bearzi, R. Rizzi, *Sci. Rep.* **2018**, *8*, 13532.
- [349] D. Qi, S. Wu, H. Lin, M. A. Kuss, Y. Lei, A. Krasnoslobodtsev, S. Ahmed, C. Zhang, H. J. Kim, P. Jiang, B. Duan, *ACS Appl. Mater. Interfaces* **2018**, *10*, 21825.
- [350] C. Lin, C. Liu, L. Zhang, Z. Huang, P. Zhao, R. Chen, M. Pang, Z. Chen, L. He, C. Luo, L. Rong, B. Liu, *Int. J. Mol. Med.* **2018**, *41*, 697.
- [351] E. Hoveizi, M. Nabiuni, K. Parivar, J. Ai, M. Massumi, *J. Biomed. Mater. Res. A* **2014**, *102*, 4027.
- [352] I. G. Kim, S. A. Park, S. H. Lee, J. S. Choi, H. Cho, S. J. Lee, Y. W. Kwon, S. K. Kwon, *Sci. Rep.* **2020**, *10*, 4326.
- [353] D. Taniguchi, K. Matsumoto, R. Machino, Y. Takeoka, A. Elgalad, Y. Taura, S. Oyama, T. Tetsuo, M. Moriyama, K. Takagi, M. Kunizaki, T. Tsuchiya, T. Miyazaki, G. Hatachi, N. Matsuo, K. Nakayama, T. Nagayasu, *Tissue Cell* **2020**, *63*, 101321.
- [354] R. P. Tan, A. H. P. Chan, K. Lennartsson, M. M. Miravet, B. S. L. Lee, J. Rnjak-Kovacina, Z. E. Clayton, J. P. Cooke, M. K. C. Ng, S. Patel, S. G. Wise, *Stem Cell Res. Ther.* **2018**, *9*, 70.
- [355] N. Noor, A. Shapira, R. Edri, I. Gal, L. Wertheim, T. Dvir, *Adv. Sci.* **2019**, *6*, 1900344.
- [356] M. A. Skylar-Scott, S. G. M. Uzel, L. L. Nam, J. H. Ahrens, R. L. Truby, S. Damaraju, J. A. Lewis, *Sci. Adv.* **2019**, *5*, aaw2459.
- [357] B. Grigoryan, S. J. Paulsen, D. C. Corbett, D. W. Sazer, C. L. Fortin, A. J. Zaita, P. T. Greenfield, N. J. Calafat, J. P. Gounley, A. H. Ta, F. Johansson, A. Randles, J. E. Rosenkrantz, J. D. Louis-Rosenberg, P. A. Galie, K. R. Stevens, J. S. Miller, *Science* **2019**, *364*, 458.
- [358] M. Wijnsbeek, V. Cottin, *N. Engl. J. Med.* **2020**, *383*, 958.
- [359] A. Sundararayanan, Y. Chen, L. D. Black, B. B. Aldridge, D. L. Kaplan, *Adv. Drug Delivery Rev.* **2018**, *129*, 78.
- [360] S. Barratt, A. Creamer, C. Hayton, N. Chaudhuri, *J. Clin. Med.* **2018**, *7*, 201.
- [361] D. J. Lederer, F. J. Martinez, *N. Engl. J. Med.* **2018**, *378*, 1811.
- [362] E. Schruf, V. Schroeder, H. Q. Le, T. Schönberger, D. Raedel, E. L. Stewart, K. Fundel-Clemens, T. Bluhmki, S. Weigle, M. Schuler, M. J. Thomas, R. Heilker, M. J. Webster, M. Dass, M. Frick, B. Stierstorfer, K. Quast, J. P. Garnett, *FASEB J.* **2020**, *34*, 7825.
- [363] P. Vijayaraj, A. Minasyan, A. Durra, S. Karumbayaram, M. Mehrabi, C. J. Aros, S. D. Ahadome, D. W. Shia, K. Chung, J. M. Sandlin, K. F. Darmawan, K. V. Bhatt, C. C. Manze, M. K. Paul, D. C. Wilkinson, W. Yan, A. T. Clark, T. M. Rickabaugh, W. D. Wallace, T. G. Graeber, R. Damoiseaux, B. N. Gomperts, *Cell Rep.* **2019**, *29*, 3488.
- [364] D. C. Wilkinson, J. A. Alva-Ornelas, J. M. S. Sucre, P. Vijayaraj, A. Durra, W. Richardson, S. J. Jonas, M. K. Paul, S. Karumbayaram, B. Dunn, B. N. Gomperts, *Stem Cells Transl. Med.* **2017**, *6*, 622.
- [365] S. D. Patel, T. R. Bono, S. M. Rowe, G. M. Solomon, *Eur. Respir. Rev.* **2020**, *29*, 190068.
- [366] P. Duchesneau, T. K. Waddell, G. Karoubi, *Int. J. Mol. Sci.* **2020**, *21*, 5219.
- [367] G. R. Cutting, *Nat. Rev. Genet.* **2015**, *16*, 45.
- [368] H. Mou, R. Zhao, R. Sherwood, T. Ahfeldt, A. Lapey, J. Wain, L. Sicilian, K. Izvolosky, F. H. Lau, K. Musunuru, C. Cowan, J. Rajagopal, *Cell Stem Cell* **2012**, *10*, 385.
- [369] A. M. Crane, P. Kramer, J. H. Bui, W. J. Chung, X. S. Li, M. L. Gonzalez-Garay, F. Hawkins, W. Liao, D. Mora, S. Choi, J. Wang, H. C. Sun, D. E. Paschon, D. Y. Guschin, P. D. Gregory, D. N. Kotton, M. C. Holmes, E. J. Sorscher, B. R. Davis, *Stem Cell Rep.* **2015**, *4*, 569.
- [370] A. L. Firth, T. Menon, G. S. Parker, S. J. Qualls, B. M. Lewis, E. Ke, C. T. Dargitz, R. Wright, A. Khanna, F. H. Gage, I. M. Verma, *Cell Rep.* **2015**, *12*, 1385.
- [371] J. Ruan, H. Hirai, D. Yang, L. Ma, X. Hou, H. Jiang, H. Wei, C. Rajagopalan, H. Mou, G. Wang, J. Zhang, K. Li, Y. E. Chen, F. Sun, J. Xu, *Mol. Ther. Nucleic Acids.* **2019**, *16*, 73.
- [372] S. Merkert, M. Schubert, A. Haase, H. M. Janssens, B. Scholte, N. Lachmann, G. Göhring, U. Martin, *Stem Cell Res.* **2020**, *44*, 101744.
- [373] T. Yokoyama, B. R. Gochuico, *Eur. Respir. Rev.* **2021**, *30*, 200193.
- [374] A. Strikoudis, A. Cieślak, L. Loffredo, Y. W. Chen, N. Patel, A. Saqi, D. J. Lederer, H. W. Snoeck, *Cell Rep.* **2019**, *27*, 3709.
- [375] J. A. Maguire, L. Lu, J. A. Mills, L. M. Sullivan, A. Gagne, P. Gadue, D. L. French, *Stem Cell Res.* **2016**, *16*, 233.
- [376] M. J. Ciancanelli, S. X. L. Huang, P. Luthra, H. Garner, Y. Itan, S. Volpi, F. G. Lafaille, C. Trouillet, M. Schmolke, R. A. Albrecht, E. Israelsson, H. K. Lim, M. Casadio, T. Hermesh, L. Lorenzo, L. W. Leung, V. Pedergrana, B. Boisson, S. Okada, C. Picard, B. Ringuier, F. Troussier, D. Chaussabel, L. Abel, I. Pellier, L. D. Notarangelo, A. Garcia-Sastre, C. F. Basler, F. Geissmann, S. -. Y. Zhang, et al., *Science* **2015**, *348*, 448.
- [377] H. K. Lim, S. X. L. Huang, J. Chen, G. Kerner, O. Gilliaux, P. Bastard, K. Dobbs, N. Hernandez, N. Goudin, M. L. Hasek, E. J. Garcia Reino, F. G. Lafaille, L. Lorenzo, P. Luthra, T. Kochetkov, B. Bigio, S. Boucherit, F. Rozenberg, C. Vedrinne, M. D. Keller, Y. Itan, A. Garcia-Sastre, M. Celard, J. S. Orange, M. J. Ciancanelli, I. Meyts, Q. Zhang, L. Abel, L. D. Notarangelo, H.-W. Snoeck, J.-L. Casanova, S.-Y. Zhang, *J. Exp. Med.* **2019**, *216*, 2038.
- [378] R. Perales-Linares, S. Navas-Martin, *Immunology* **2013**, *140*, 153.
- [379] H. Surendran, S. Nandakumar, R. Pal, *Stem Cells Dev.* **2020**, *29*, 1365.
- [380] R. M. Hekman, A. J. Hume, R. K. Goel, K. M. Abo, J. Huang, B. C. Blum, R. B. Werder, E. L. Suder, I. Paul, S. Phanse, A. Youssef, K. D. Alysandratos, D. Padhorny, S. Ojha, A. Mora-Martin, D. Kretov, P. E. A. Ash, M. Verma, J. Zhao, J. J. Patten, C. Villacorta-Martin, D. Bolzan, C. Perea-Resa, E. Bullitt, A. Hinds, A. Tilston-Lunel, X. Varelas, S. Farhangmehr, U. Braunschweig, J. H. Kwan, et al., *Mol. Cell* **2020**, *80*, 1104.
- [381] S. S. Jose, M. De Zuani, F. Tidu, M. Hortová Kohoutková, L. Pazzagli, G. Forte, R. Spaccapelo, T. Zelante, J. Frič, *Clin. Transl. Immunol.* **2020**, *9*, 1131.
- [382] K. M. Latimer, T. F. Mott, *Am. Fam. Physician.* **2015**, *91*.
- [383] R. S. Herbst, D. Morgensztern, C. Boshoff, *Nature* **2018**, *553*, 446.
- [384] C. M. Rudin, E. Brambilla, C. Faivre-Finn, J. Sage, *Nat. Rev. Dis. Prim.* **2021**, *7*, 3.
- [385] A. F. M. Dost, A. L. Moye, M. Vedaie, L. M. Tran, E. Fung, D. Heinze, C. Villacorta-Martin, J. Huang, R. Hekman,

- J. H. Kwan, B. C. Blum, S. M. Louie, S. P. Rowbotham, J. Sainz De Aja, M. E. Piper, P. J. Bhetariya, R. T. Bronson, A. Emili, G. Mostoslavsky, G. A. Fishbein, W. D. Wallace, K. Krysan, S. M. Dubinett, J. Yanagawa, D. N. Kotton, C. F. Kim, *Cell Stem Cell* **2020**, *27*, 663.
- [386] R. Y. Tam, J. Yockell-Lelièvre, L. J. Smith, L. M. Julian, A. E. G. Baker, C. Choey, M. S. Hasim, J. Dimitroulakos, W. L. Stanford, M. S. Shoichet, *Adv. Mater.* **2019**, *31*, 1806214.
- [387] M. X. Doss, A. Sachinidis, *Cells* **2019**, *8*, 403.
- [388] E. L. Curry, M. Moad, C. N. Robson, R. Heer, *World J. Stem Cells* **2015**, *7*, 461.
- [389] N. Lan, B. Massam, S. Kulkarni, C. Lang, *Diseases* **2018**, *6*, 38.
- [390] A. Andruska, E. Spiekerkoetter, *Int. J. Mol. Sci.* **2018**, *19*, 2499.
- [391] M. Gu, N. Y. Shao, S. Sa, D. Li, V. Termglinchan, M. Ameen, I. Karakikes, G. Sosa, F. Grubert, J. Lee, A. Cao, S. Taylor, Y. Ma, Z. Zhao, J. Chappell, R. Hamid, E. D. Austin, J. D. Gold, J. C. Wu, M. P. Snyder, M. Rabinovitch, *Cell Stem Cell* **2017**, *20*, 490.
- [392] S. Sa, M. Gu, J. Chappell, N. Y. Shao, M. Ameen, K. A. T. Elliott, D. Li, F. Grubert, C. G. Li, S. Taylor, A. Cao, Y. Ma, R. Fong, L. Nguyen, J. C. Wu, M. P. Snyder, M. Rabinovitch, *Am. J. Respir. Crit. Care Med.* **2017**, *195*, 930.
- [393] H. Basma, Y. Gunji, S. Iwasawa, A. Nelson, M. Farid, J. Ikari, X. Liu, X. Wang, J. Michalski, L. Smith, J. Iqbal, R. El Behery, W. West, S. Yelamanchili, D. Rennard, O. Holz, K.-C. Mueller, H. Magnussen, K. Rabe, P. J. Castaldi, S. I. Rennard, *Am. J. Physiol. – Lung Cell. Mol. Physiol.* **2014**, *306*, 552.
- [394] S. M. Kunisaki, G. Jiang, J. C. Biancotti, K. K. Y. Ho, B. R. Dye, A. P. Liu, J. R. Spence, *Stem Cells Transl. Med.* **2021**, *10*, 98.
- [395] M. Longoni, B. R. Pober, F. A. High, Congenital Diaphragmatic Hernia Overview, <https://www.ncbi.nlm.nih.gov/books/NBK1359/> **2006** (accessed: November 2021).
- [396] M. A. Wilder, *J. Perinat. Neonatal Nurs.* **2004**, *18*, 61.
- [397] S. L. Leibel, A. Winquist, I. Tseu, J. Wang, D. Luo, S. Shojaie, N. Nathan, E. Snyder, M. Post, *Sci. Rep.* **2019**, *9*, 13450.
- [398] Y. I. Wang, H. E. Abaci, M. L. Shuler, *Biotechnol. Bioeng.* **2017**, *114*, 184.
- [399] S. Musah, A. Mammoto, T. C. Ferrante, S. S. F. Jeanty, M. Hirano-Kobayashi, T. Mammoto, K. Roberts, S. Chung, R. Novak, M. Ingram, T. Fatanat-Didar, S. Koshy, J. C. Weaver, G. M. Church, D. E. Ingber, *Nat. Biomed. Eng.* **2017**, *1*, 69.
- [400] M. J. Workman, J. P. Gleeson, E. J. Troisi, H. Q. Estrada, S. J. Kerns, C. D. Hinojosa, G. A. Hamilton, S. R. Targan, C. N. Svendsen, R. J. Barrett, *CMGH* **2018**, *5*, 669.
- [401] D. E. Ingber, *Dev* **2018**, *145*, dev156125.
- [402] T. Zhao, Z. N. Zhang, Z. Rong, Y. Xu, *Nature* **2011**, *474*, 212.
- [403] E. W. Esch, A. Bahinski, D. Huh, *Nat. Rev. Drug Discovery* **2015**, *14*, 248.
- [404] Y. A. Jodat, M. G. Kang, K. Kiaee, G. J. Kim, A. F. H. Martinez, A. Rosenkranz, H. Bae, S. R. Shin, *Curr. Pharm. Des.* **2019**, *24*, 5471.
- [405] A. Mathur, P. Loskill, K. Shao, N. Huebsch, S. G. Hong, S. G. Marcus, N. Marks, M. Mandegar, B. R. Conklin, L. P. Lee, K. E. Healy, *Sci. Rep.* **2015**, *5*, 8883.
- [406] B. W. Ellis, A. Acun, U. Isik Can, P. Zorlutuna, *Biomicrofluidics* **2017**, *11*, 024105.
- [407] E. Tzatzalos, O. J. Abilez, P. Shukla, J. C. Wu, *Adv. Drug Delivery Rev.* **2016**, *96*, 234.
- [408] G. Woodruff, S. M. Reyna, M. Dunlap, R. Van Der Kant, J. A. Callender, J. E. Young, E. A. Roberts, L. S. B. Goldstein, *Cell Rep.* **2016**, *17*, 759.
- [409] S. Sances, R. Ho, G. Vatine, D. West, A. Laperle, A. Meyer, M. Godoy, P. S. Kay, B. Mandefro, S. Hatata, C. Hinojosa, N. Wen, D. Sareen, G. A. Hamilton, C. N. Svendsen, *Stem Cell Rep.* **2018**, *10*, 1222.
- [410] D. D. Nalayanda, C. M. Puleo, W. B. Fulton, T. H. Wang, F. Abdullah, *Exp. Lung Res.* **2007**, *33*, 321.
- [411] D. D. Nalayanda, W. B. Fulton, P. M. Colombani, T. H. Wang, F. Abdullah, *J. Pediatr. Surg.* **2014**, *49*, 61.
- [412] D. Huh, H. Fujioka, Y. C. Tung, N. Futai, R. Paine, J. B. Grotberg, S. Takayama, *Proc. Natl. Acad. Sci. USA* **2007**, *104*, 18886.
- [413] D. Ritter, J. Knebel, *Adv. Toxicol.* **2014**, *2014*, 185201.
- [414] Q. Ramadan, M. Zourob, *Biomicrofluidics* **2020**, *14*, 041501.
- [415] S. Ahadian, R. Civitarese, D. Bannerman, M. H. Mohammadi, R. Lu, E. Wang, L. Davenport-Huyer, B. Lai, B. Zhang, Y. Zhao, S. Mandla, A. Korolj, M. Radisic, *Adv. Healthcare Mater.* **2018**, *7*, <https://doi.org/10.1002/adhm.201800734>.
- [416] H. Tang, Y. Abouleila, L. Si, A. M. Ortega-Prieto, C. L. Mummery, D. E. Ingber, A. Mashaghi, *Trends Microbiol.* **2020**, *28*, 934.
- [417] A. A. Kizilkurtlu, T. Polat, G. B. Aydin, A. Akpek, *Curr. Pharm. Des.* **2019**, *24*, 5386.
- [418] S. Ehrmann, O. Schmid, C. Darquenne, B. Rothen-Rutishauser, J. Sznitman, L. Yang, H. Barosova, L. Vecellio, J. Mitchell, N. Heuzé-Vourc'h, *Expert Opin. Drug Deliv.* **2020**, *17*, 463.
- [419] H. Moghadas, M. S. Saidi, N. Kashaninejad, N. T. Nguyen, *Drug Deliv. Transl. Res.* **2018**, *8*, 830.
- [420] S. Adler, D. Basketter, S. Creton, O. Pelkonen, J. Van Benthem, V. Zuang, K. E. Andersen, A. Angers-Loustau, A. Aptula, A. Bal-Price, E. Benfenati, U. Bernauer, J. Bessems, F. Y. Bois, A. Boobis, E. Brandon, S. Bremer, T. Broschard, S. Casati, S. Coecke, R. Corvi, M. Cronin, G. Daston, W. Dekant, S. Felter, E. Grignard, U. Gundert-Remy, T. Heinonen, I. Kimber, J. Kleinjans, et al., *Arch. Toxicol.* **2011**, *85*, 367.
- [421] K. Taylor, L. R. Alvarez, *Comput. Toxicol.* **2020**, *13*, 100112.
- [422] D. Bovard, A. Sandoz, K. Luetlich, S. Frentzel, A. Iskandar, D. Marescotti, K. Trivedi, E. Guedj, Q. Dutertre, M. C. Peitsch, J. Hoeng, *Lab Chip* **2018**, *18*, 3814.
- [423] R. Novak, M. Ingram, S. Marquez, D. Das, A. Delahanty, A. Herland, B. M. Maoz, S. S. F. Jeanty, M. R. Somayaji, M. Burt, E. Calamari, A. Chalkiadaki, A. Cho, Y. Choe, D. B. Chou, M. Fronce, S. Dauth, T. Divic, J. Fernandez-Alcon, T. Ferrante, J. Ferrier, E. A. Fitzgerald, R. Fleming, S. Jalili-Firoozinezhad, T. Grevesse, J. A. Goss, T. Hamkins-Indik, O. Henry, C. Hinojosa, T. Huffstater, et al., *Nat. Biomed. Eng.* **2020**, *4*, 407.
- [424] J. R. Coppeta, M. J. Mescher, B. C. Isenberg, A. J. Spencer, E. S. Kim, A. R. Lever, T. J. Mulhern, R. Prantil-Baun, J. C. Comolli, J. T. Borenstein, *Lab Chip* **2017**, *17*, 134.
- [425] J. H. Sung, M. L. Shuler, *Lab Chip* **2009**, *9*, 1385.
- [426] A. M. Ghaemmaghami, M. J. Hancock, H. Harrington, H. Kaji, A. Khademhosseini, *Drug Discov. Today* **2012**, *17*, 173.
- [427] I. Maschmeyer, A. K. Lorenz, K. Schimek, T. Hasenberg, A. P. Ramme, J. Hübner, M. Lindner, C. Drewell, S. Bauer, A. Thomas, N. S. Sambo, F. Sonntag, R. Lauster, U. Marx, *Lab Chip* **2015**, *15*, 2688.
- [428] D. Huh, G. A. Hamilton, D. E. Ingber, *Trends Cell Biol.* **2011**, *21*, 745.
- [429] D. Pamies, A. Bal-Price, C. Chesné, S. Coecke, A. Dinnyes, C. Eskes, R. Grillari, G. Gstraunthaler, T. Hartung, P. Jennings, M. Leist, U. Martin, R. Passier, J. C. Schwaborn, G. N. Stacey, H. Ellinger-Ziegelbauer, M. Daneshian, *ALTEX* **2018**, *35*, 353.
- [430] S. Ishida, *Drug Metab. Pharmacokin.* **2018**, *33*, 49.
- [431] C. W. McAleer, A. Poinçon, C. J. Long, R. L. Brighton, B. D. Wilkin, L. R. Bridges, N. Narasimhan Sriram, K. Fabre, R. McDougall, V. P. Muse, J. T. Mettetal, A. Srivastava, D. Williams, M. T. Schnepfer, J. L. Roles, M. L. Shuler, J. J. Hickman, L. Ewart, *Sci. Rep.* **2019**, *9*, 9619.
- [432] Z. Li, Y. Guo, Y. Yu, C. Xu, H. Xu, J. Qin, *Integr. Biol.* **2016**, *8*, 1022.
- [433] C. Oleaga, C. Bernabini, A. S. T. Smith, B. Srinivasan, M. Jackson, W. McLamb, V. Platt, R. Bridges, Y. Cai, N. Santhanam, B. Berry, S. Najjar, N. Akanda, X. Guo, C. Martin, G. Ekman, M. B. Esch, J. Langer, G. Ouedraogo, J. Cotovio, L. Breton, M. L. Shuler, J. J. Hickman, *Sci. Rep.* **2016**, *6*, 20030.

- [434] A. Skardal, S. V. Murphy, M. Devarasetty, I. Mead, H. W. Kang, Y. J. Seol, Y. S. Zhang, S. R. Shin, L. Zhao, J. Aleman, A. R. Hall, T. D. Shupe, A. Kleensang, M. R. Dokmeci, S. Jin Lee, J. D. Jackson, J. J. Yoo, T. Hartung, A. Khademhosseini, S. Soker, C. E. Bishop, A. Atala, *Sci. Rep.* **2017**, *7*, 8837.
- [435] P. G. Miller, M. L. Shuler, *Biotechnol. Bioeng.* **2016**, *113*, 2213.
- [436] A. Skardal, J. Aleman, S. Forsythe, S. Rajan, S. Murphy, M. Devarasetty, N. Pourhabibi Zarandi, G. Nzou, R. Wicks, H. Sadri-Ardekani, C. Bishop, S. Soker, A. Hall, T. Shupe, A. Atala, *Biofabrication* **2020**, *12*, 025017.
- [437] C. Ma, Y. Peng, H. Li, W. Chen, *Trends Pharmacol. Sci.* **2021**, *42*, 119.
- [438] A. Cochrane, H. J. Albers, R. Passier, C. L. Mummery, A. van den Berg, V. V. Orlova, A. D. van der Meer, *Adv. Drug Delivery Rev.* **2019**, *140*, 68.
- [439] C. K. Burrows, N. E. Banovich, B. J. Pavlovic, K. Patterson, I. Gallego Romero, J. K. Pritchard, Y. Gilad, *PLoS Genet.* **2016**, *12*, 1005793.
- [440] M. Kajiwara, T. Aoi, K. Okita, R. Takahashi, H. Inoue, N. Takayama, H. Endo, K. Eto, J. Toguchida, S. Uemoto, S. Yamanaka, *Proc. Natl. Acad. Sci. USA* **2012**, *109*, 12538.
- [441] A. Kyttälä, R. Moraghebi, C. Valensisi, J. Kettunen, C. Andrus, K. K. Pasumarthy, M. Nakanishi, K. Nishimura, M. Ohtaka, J. Weltner, B. Van Handel, O. Parkkonen, J. Sinisalo, A. Jalanko, R. D. Hawkins, N. - B. Woods, T. Otonkoski, R. Trokovic, *Stem Cell Rep.* **2016**, *6*, 200.
- [442] C. DeBoever, H. Li, D. Jakubosky, P. Benaglio, J. Reyna, K. M. Olson, H. Huang, W. Biggs, E. Sandoval, M. D'Antonio, K. Jepsen, H. Matsui, A. Arias, B. Ren, N. Nariai, E. N. Smith, A. D'antonio-Chronowska, E. K. Farley, K. A. Frazer, *Cell Stem Cell* **2017**, *20*, 533.
- [443] H. Kilpinen, A. Goncalves, A. Leha, V. Afzal, K. Alasoo, S. Ashford, S. Bala, D. Bensaddek, F. P. Casale, O. J. Culley, P. Danecek, A. Faulconbridge, P. W. Harrison, A. Kathuria, D. McCarthy, S. A. McCarthy, R. Meleckyte, Y. Memari, N. Moens, F. Soares, A. Mann, I. Streeter, C. A. Agu, A. Alderton, R. Nelson, S. Harper, M. Patel, A. White, S. R. Patel, L. Clarke, et al., *Nature* **2017**, *546*, 370.
- [444] R. G. Rowe, G. Q. Daley, *Nat. Rev. Genet.* **2019**, *20*, 377.
- [445] V. Volpato, C. Webber, *DMM Dis. Model. Mech.* **2020**, *13*, dmm042317.
- [446] Human Episomal iPSC Line, <https://www.thermofisher.com/order/catalog/product/A18945?SID=srch-srp-A18945>, (accessed: November 2021).
- [447] Human induced pluripotent stem cells, <https://www.takarabio.com/products/stem-cell-research/stem-cells-and-stem-cell-derived-cells/human-induced-pluripotent-stem-cells>, (accessed: November 2021).
- [448] Tempo Bioscience TempoStemBank™-iPSC: Human iPSC Stem Cell Lines, <https://www.tempobioscience.com/products/custom-cell-types/ipsc-lines.html>, (accessed: November 2021).
- [449] ATCC-CYS0105 Human Induced Pluripotent Stem (IPS) Cells | ATCC, <https://www.atcc.org/products/acs-1021#>, (accessed: November 2021).
- [450] P. A. De Sousa, R. Steeg, E. Wachter, K. Bruce, J. King, M. Hoeve, S. Khadun, G. McConnachie, J. Holder, A. Kurtz, S. Seltmann, J. Dewender, S. Reimann, G. Stacey, O. O'shea, C. Chapman, L. Healy, H. Zimmermann, B. Bolton, T. Rawat, I. Atkin, A. Veiga, B. Kuebler, B. M. Serano, T. Saric, J. Hescheler, O. Brüstle, M. Peitz, C. Thiele, N. Geijsen, et al., *Stem Cell Res.* **2017**, *20*, 105.
- [451] EBiSC Cell Line Search, <https://cells.ebisc.org/search>, (accessed: November 2021).
- [452] Rheincell, <https://www.rheincell.de/products.html>, (accessed: November 2021).



**Anabela Moreira** is a Junior Researcher at BIOFABICS (Portugal). She holds a M.Sc. degree in Bioengineering and is specialized in Molecular Biotechnology. Currently, her projects are related to the fields of tissue engineering and regenerative medicine, involving research on biofabrication, drug delivery, and in vitro organotypic models for pharmacological and toxicological screening.



**Michelle Müller** studied Applied Life Sciences at the University of Applied Sciences Kaiserslautern (Germany) and holds a M.Sc. degree in Applied Life Sciences. Since 2016 she is working in the group "Cell Models and Toxicology" at Fraunhofer IBMT, currently working on her doctoral thesis (Saarland University, Germany) with the research focus on hiPSC differentiation to generate reliable lung cells for medical, pharmaceutical and toxicological research applications.



**Pedro Costa** is the founder, CEO and CTO of the company BIOFABICS, which is specialized in the creation of 3D biotissue analogues. Before that, he was coordinator of the world's first M.Sc. Programme in Biofabrication (Utrecht University), manager of the Utrecht Biofabrication Facility, postdoctoral researcher at University Medical Center Utrecht (Netherlands), and postdoctoral researcher at Technical University of Munich (Germany). He received a B.Sc. in applied biology and a Ph.D. in biomedical engineering, both from University of Minho (Portugal). His current research focuses on the combination of organ-on-chip, biofabrication and bioreactor technologies for tissue engineering and regenerative medicine applications.



**Yvonne Kohl** is a senior researcher at the Fraunhofer IBMT specialized in toxicology. She studied at the Technical University of Kaiserslautern in the Department of Food Chemistry and Environmental Toxicology (Germany). Afterwards she did her Ph.D. thesis in the field of nanotoxicology and obtained her PhD at the Saarland University (Faculty of Science and Technology Chemistry, Pharmacy, Bio- and Materials Sciences, Germany) in 2011. At the Fraunhofer IBMT she is working on the development of novel toxicological screening technologies and in vitro methods according to the 3R principle to study human impacts of nanoscale materials.